AN ABSTRACT OF THE DISSERTATION OF

Sumitra Sengupta for the degree of Doctor in Philosophy in Toxicology presented on June 4, 2010.
Title: Chemical and Biological Approaches to Identify Vertebrate Tissue Regeneration Pathways

Abstract approved:

_____

Robert L. Tanguay

Abstract

Numerous human conditions would be improved if therapies to encourage tissue regeneration were available. The goal of regenerative medicine is to encourage the body`s intrinsic ability to repair and restore tissues lost by disease, injury or aging. While certain vertebrates have the inherent capacity to regenerate, mammals do not. To study tissue regeneration we developed an early life stage zebrafish model. Through comparative global mRNA expression analysis in regenerating tissues isolated from adult caudal fins, hearts and larval fins, we discovered that *raldh2* is induced across all regenerating platforms and its *expression* is critical during early stages of regeneration. Our studies determined the role of *Wnt* and *Fgf* in larval regenerating tissue, establishing the early life stage model as a powerful platform to study regeneration. Utilizing this model we developed a rapid *in vivo* larval regeneration assay to identify small molecule modulators of regeneration. Our initial screening of a 2000 member FDA approved drug library identified eight glucocorticoids (GCs) that inhibited regeneration. We chose beclomethasone dipropionate (BDP) as a representative glucocorticoid receptor (GR) ligand and performed mRNA expression analysis in BDP exposed fin regenerates to identify downstream effectors of GR that are required to block tissue regeneration. Bioinformatic analysis revealed that *Cripto-1* mRNA expression increased significantly

following BDP exposure. We hypothesized that misexpression of *Cripto-1, an* Activin inhibitor, was necessary for GR ligands to block tissue regeneration. Suppression of *Cripto-1* by morpholino or retinoic acid exposure restored regeneration in the presence of BDP supporting our hypothesis. Our chemical biological screen also identified 21 glucocorticoids that activated GR but did not impact regeneration. We hypothesized that differences in ligand structure induced alternate GR conformational changes and these structural differences resulted in distinct regenerative activity. Docking studies identified that ligands with large substitutions at position17 induce an energetically stable active GR confirmation that correlates with the blocking of tissue regeneration. Our research identified novel GR ligands with cortisol backbones and bulky C17 substitutions that confirmed our hypothesis. Collectively, our results demonstrate the power of the larval zebrafish regeneration model to understand the pathways that permit tissue regeneration.

.

Chemical and Biological Approaches to Identify Vertebrate Tissue Regeneration Pathways

by
Sumitra Sengupta

A DISSERTATION

submitted to

Oregon State University

in partial fulfillment of
the requirements for the
degree of

Doctor of Philosophy

Presented June 4, 2010
Commencement June 2011

Doctor of Philosophy dissertation of Sumitra Sengupta presented on June 4, 2010.

APPROVED:

Major Professor, representing Toxicology

Head of the Department of Environmental and Molecular Toxicology

---

Dean of the Graduate School

I understand that my dissertation will become part of the permanent collection of Oregon State University libraries. My signature below authorizes release of my dissertation to any reader upon request.

Sumitra Sengupta, Author

ACKNOWLEDGEMENTS

I would like to thank Environmental and Molecular Toxicology department for giving me this opportunity to obtain an excellent training. My deepest gratitude to Dr. Robert Tanguay for being such an excellent mentor. I would like to thank him for being patient, guiding me and supporting me as and when required. I will always look up to him as a great source of inspiration. I also want to thank Dr. Lijoy K. Mathew who has guided me throughout my graduate school career by being my second mentor. I will always be thankful to Jane La Du for all her guidance intellectually and spiritually and for being my home away from home. Lisa Truong and Hao Truong has to be thanked for being such an excellent technical support. I would like to thank the entire Tanguay lab and my friends here at OSU who have always supported me and encouraged me throughout my training. I want to thank all my committee members, namely, Dr. Mark Leid, Dr. Siva Kolluri, Dr. Andrew Buermeyer and Dr. Emily Ho for serving in my graduate committee, helping me with the fellowship grants and guiding me throughout my graduate studies. I also want to thank Partiban Jesudason and Jessica Perry for helping me with various experiments. Most importantly, I want to thank my parents, my family members, friends, and Miss Debi Mukherjee who has been a great support for me all through my studies. Finally, I want to dedicate my thesis to Dr. Sukta Das, who has been an excellent teacher and source of inspiration and courage.

CONTRIBUTION OF AUTHORS

This dissertation is a collective effort of many collaborators from different universities and all Tanguay lab members. In Chapter 1, Dr. Lijoy K Mathew primarily prepared the manuscript. Jill A Franzosa helped with the retinoic acid exposure experiments. In Chapter 2, Dr. Lijoy K Mathew assisted me with the microarray analysis and quantitative-PCR experiments. Jane LaDu provided technical support for this project including assistance with morpholinos microinjections and animal care. Lisa Truong provided assistance with processing of the microarray data. Hao Truong provided technical assistance in the preparation of the manuscript. In Chapter3, William Bisson conducted the docking studies. Dr. Randall Peterson provided us with the 2000-member small molecule library for rapid throughput regeneration assay.

TABLE OF CONTENTS

TABLE OF CONTENTS (Continued)

LIST OF FIGURES

LIST OF FIGURES (Continued)

LIST OF TABLES

Chemical and Biological Approaches to Identify Vertebrate Tissue Regeneration Pathways

CHAPTER 1 - INTRODUCTION

Tissue Regeneration

The process of tissue regeneration replaces tissues and organs lost by amputation, disease, injury or aging. The concept of tissue regeneration dates back to Greek mythology such as that of Prometheus. Observed in few members of the animal kingdom such as hydra, planaria and starfish, the capacity to regenerate becomes restricted as we go higher in the evolutionary tree. In most cases humans mostly demonstrate inflammation and scarring in response to injury or loss of tissue or organ [1, 2]. The field of regenerative medicine aims to revitalize tissues and organs damaged by disease, injury, or even the normal aging process. Today doctors use regenerative medicine to speed up healing or to assist injuries that cannot heal or repair on their own. The ultimate goal of the field is to encourage the body`s natural healing process by activating the inherent ability to repair and regenerate. This multidisciplinary field involves biology, medicine and engineering, and the combination has devised innovative therapies aiming to heal or reconstruct diseased tissue and support the regeneration of diseased or injured organs.

In the last few years stem cells have become a possible source to replace damaged tissues [3]. The most investigated cell types are neurons and myocytes due to their lack of native regenerative potential [4, 5]. To date stem cell therapy can replace specific cell

types but not recreate a functional organ or an appendage as these requires reconstitution of numerous cells types and establishment of interactions between them. This process is known as epimorphic tissue regeneration originating from the term “epimorphosis” which Thomas Hunt Morgan used to define regenerative processes involving proliferation [6]. Epimorphic regeneration requires the formation of a special structure called the blastema followed by the reconstitution of a complex tissue with multiple cell types. Typically, a blastema is a mass of proliferative, pluripotent progenitor cells. Progress in the study of epimorphic tissue regeneration has been very slow. Vertebrates such as salamander, newt and zebrafish that demonstrate epimorphic tissue regeneration can provide us a better understanding of the biology of regeneration. Since the fundamental processes and mechanisms are conserved between vertebrates, studies performed in these regenerative models will reveal why some vertebrates can regenerate and others cannot. These studies will provide us with opportunities to manipulate the genome and promote regeneration in mammals. Thus, regeneration can be envisioned using ‘pharmacological’ agents, genes, or stem cells

Zebrafish Regeneration

There are several vertebrate regeneration models such as salamanders and newts to evaluate tissue regeneration. Zebrafish, a member of the teleost family, has emerged as a powerful regenerative model. They have the remarkable ability to regenerate numerous organs and appendages including fins, optic nerves, scales, heart and spinal cord. The organization of the genome and the genetic pathways involved with signal transduction and embryonic development are highly conserved between zebrafish and humans [7, 8]. The zebrafish genome is sequenced and multiple genetic

markers and gene array chips are available commercially (http:// www.sanger.ac.uk/Projects/D_rerio/) [9].

Studies using adult heart and caudal fin tissue regeneration models have revealed important molecular signaling pathways implicated in regenerative growth and angiogenesis. The ability of several teleost fish to regenerate their fins after injury has been documented in species such as *Salaria pavo* [10], *Tilapia melanopleura, Cyprinus carpio, Carassius auratus* [11, 12, 13], *Fundulus heteroclitus* [14] and the zebrafish, *Danio rerio* [14, 15]. This diversity indicates that regeneration is functionally conserved in members of the teleost family. Due to advances in zebrafish genetics, rapid regeneration time and the ability to obtain vast quantities of externally fertilized embryos, the zebrafish has emerged as a prevailing vertebrate regeneration model. Currently regeneration of heart and caudal fin are being extensively studied to dissect the molecular signaling pathways involved in regeneration.

Coronary heart diseases such as myocardial infarction (MI) are the biggest healthcare concern in the US today. Therefore, therapeutic approaches allowing the regenerative replacement of damaged tissues is essential for the treatment of cardiovascular diseases. However, heart is the least regenerating organ of the body in mammals. Therefore, zebrafish have been utilized to identify signaling molecules that permit heart regeneration [16]. Current, literature indicates that heart regeneration in both newt and zebrafish models proceed through wound formation proliferation and wound healing or complete outgrowth [17]. The use of zebrafish genetic mutants such as *nbl* and *nighcap* accompanied by gene expression analysis studies have revealed genes important for regeneration such as *mps1*, *hsp40*, *mxsb*, *msxc*, *notch1b* and *deltaC* [18]. Recent reports suggest that zebrafish heart regeneration is driven primarily

by pre-existing cardiomyocytes, rather than by progenitor cells as suggested previously [20].

The heart regeneration model in zebrafish has proved to be successful in identifying genes critical for cardiac regeneration. Low survival rate after surgery, difficulty in performing genetic and chemical screens and the long regeneration time brings to question the ease of performing successful experiments in this model. Adult caudal fin regeneration in zebrafish is also an established model to study epimorphic tissue regeneration. There is evidence that caudal fin regeneration has a high degree of similarity with heart regeneration suggested by the expression of regeneration specific genes such as *mxsb, msxc, notch1b and deltaC*. The genetic mutants' *nbl* and *nighcap* characterized by the loss of heart regeneration, fail to regenerate their caudal fin as well. This evidence suggests that caudal fin model is a more efficient model to study tissue regeneration.

The adult caudal fin consists of 18 bony rays (lepidotrichia) attached to the skeleton by ligaments. Each lepidotrichia is comprised of two hemirays. Blood vessels, nerves, and mesenchymal cells are all present in the region between two hemirays. The fin grows by successive addition of new hemirays to the distal most segments. The adult caudal fin regenerates by three distinct stages (1) wound healing, (2) blastema formation, (3) regenerative outgrowth. Following partial amputation, the local non-proliferating epithelial cells migrate to form the apical epithelial wound cap (AEC) [21, 22, 23] within 12 hours post amputation (hpa). Following wound closure, the underlying mesenchymal cells become disorganized, forming the blastema beneath the amputation plane within 48hpa [21, 22]. Next, cells of the blastema compartmentalize the distal most regions into a non-proliferative, *msxb*-positive population and the more proximal

region into a region of highly proliferative (*msxb*-negative) cells [26]. The regenerative outgrowth replaces the lost tissues within two weeks.

Molecular Signaling During Zebrafish Caudal Fin Regeneration

Regenerative medicine, aims to elucidate the signaling molecules essential for a regenerative outcome. Reports indicate that fin regeneration like other biological processes such as embryonic development, is governed by multiple signaling events. However, this process involves the implementation of novel genetic programs rather than the reiteration of developmental programs. Mutagenesis screens, antisense RNA knockdown, chemical genetics and gene expression studies have identified key players of the regenerative process.

Wnt Signaling

Multiple studies have emphasized the role of Wnt signaling in tissue regeneration. The first evidence of the role of Wnt signaling in fin regeneration was the expression of *Lef1,* a Wnt pathway target gene expression in wound epithelium distal to amputation plane at 12 hpa suggesting its role on blastema formation [27]. SU5402, a Fgfr 1 inhibitor and Retinoic acid (RA) did not prevent *Lef1* expression suggesting that both Fgf and RA signaling were downstream of Wnt signaling. Overexpression of *Dikkopf1(Dkk)* using a heatshock inducible transgenic line also inhibits fin regeneration [28]. Further chemical genetic approaches recognized Wnt inhibitors that block regeneration [29-31]. Comparative toxicogenomic analysis identified alterations in the Wnt signaling pathway in TCDD exposed fin regenerates. Molecular analysis revealed

induced Rspondin1 expression by TCDD exposure interferes with *Dkk* mediated internalization of the frizzled coreceptor LRP5/6 resulting in increased LRP5/6 density [32]. This leads to overactivation of the Wnt signaling pathway and hence impaired regeneration.

Fgf Signaling

One of the most studied pathways involved in zebrafish regeneration is fibroblast growth factor (Fgf) signaling. Fgf receptor 1 (Fgfr1) is expressed in mesenchymal cells located proximal to the wound epidermis [33]. The role of Fgf signaling has been demonstrated using a Fgfr1 inhibitor (SU5402) as well as a transgenic line (*hsp70:dn-fgfr1*) that expresses a dominant negative Fgfr1 protein upon heat shock [19, 34, 35]. A genetic mutant study revealed the requirement of *fgf20a*, an Fgfr1 ligand, in the initiation of regeneration and the formation of blastema [36]. Fgf signaling has also been implicated in patterning as treatment with SU5402 following blastema formation caused impaired regeneration.[33]. Recent reports indicate that Fgf signaling impacts multiple cell types during regeneration. It helps establish expression of *lef1* and *shh* in proximal regions of the basal epidermal layer, supporting morphogenesis in this area. At the same time, Fgfs function in an inhibitory manner within the distal epidermal cells, by interacting with Ras signaling to maintain inhibitory signals like *Wnt5b* [37].

Retinoic Acid Signaling

Retinoic acid (RA) signaling was the first signaling pathway reported to be involved in tissue regeneration [38]. Expression of retinoic acid receptor-gamma (RAR-gamma) in the blastema and morphological changes in the RA exposed fin regenerates implicated the role of retinoic acid signaling as well [39-41]. This signaling pathway

impacts the size of the wound epidermis impinging on patterning within blastema [39] in addition to inducing apoptosis in the AEC [42]

Activin β Signaling

A chemical genetics approach utilizing SB431542 (a specific inhibitor of ALK4) has demonstrated that *activinβA* expression is induced in regenerating fin tissue as early as 6hpa [43]. Further studies suggested that the lack of regenerative outgrowth in fins exposed to an activin signaling inhibitors was due to impaired mesenchymal disorganization and proliferation suggesting the role of *activinβA* in maintaining the proliferative potential of the blastema.

Sonic Hedgehog Signaling

Members of the sonic hedgehog signaling pathway identified by marker analysis, have been localized to distinct regions of a regenerating fin tissue. Sonic hedgehog (*shh*), its membrane-bound receptor patched1 (ptc1) and bone morphogenic protein 2b (*bmp2b*) [44] play a role in patterning of developing and regenerating adult teleost fins. Administration of all-trans-retinoic acid treatment transiently decreased the expression of *shh, ptc1 and bmp2* suggesting direct regulation of *shh* by retinoic acid [45]. Recently identified *fam53b/smp* demonstrated its role in cell cycle regulation and patterning during regeneration by modulating a host of genes that include *shh* [46].

Identification of the above pathways essential for regeneration shows progress in the field of regeneration biology [47]. With the advancement of technology, recently identified role of microRNA [48], telomerase activity [49] and histone demethylase [50] in tissue regeneration indicate we are still at the early stages of gene discovery and rapid progress is essential for advancement in the field.

Early Life Stage Fin Regneration Model

The adult zebrafish regeneration model has made significant contribution to the field of regenerative medicine. However, technical barriers such as lengthy regeneration time, requirement to attain adulthood as well as lack of many molecular and genetic tools such as transient repression technique and genetic tractability [51] restrict both adult heart and caudal fin regenerative models. An early life stage model of tissue regeneration would overcome these technical barriers, allowing the field to progress at a faster pace. Larval zebrafish is widely utilized to study biological processes and offers numerous advantages including ease of genetic and molecular tractability, rapid *ex* utero development into transparent embryos, direct observation of organ function and fully functional organ system within 3-5 days post fertilization [52, 53]. Even though the adult heart regeneration model has made significant contributions to the field of regenerative medicine the recent development of targeted cell ablation techniques [54] allowed experiments in two day old larvae. This model indicates a growing interest in larval heart regeneration model. This move recognizes the advantages associated with early life stage zebrafish models. The potential of larval zebrafish in the field of regenerative medicine came to the forefront with the identification of regenerative properties of two day old zebrafish. Two-day-old larvae completely regenerate their fin tissue [55-57] within the three days following amputation. The larval model has unique advantages including rapid regeneration time, experimentally tractable life stage and the ease of chemical and molecular manipulations. Although the physical structures of the adult and larval fins differ significantly, increasing evidence suggests remarkable similarities at the cellular and molecular level [55, 57]. Larval fin regeneration processes also involve the

formation of a wound epithelium on amputation followed by blastema formation and regenerative progression [55]. Inhibition of this process by chemical inhibitors, such as SU5402 [55, 56], further adds to the evidence of conserved regnertaive processes in the two models. The advantages associated with the early life stage model indicate the potential to offer a dynamic contribution to identify novel regulators of regeneration.

Chemical Genetics and Regeneration

Understanding a biological phenomenon often begins by perturbing it. Over the past century genetic manipulations have played a crucial role in elucidating correlation between genes and their function. Large-scale genetic screens have revealed the mechanisms underlying many aspects of complex biological processes including tissue regeneration. Genetic screens used to identify fin regeneration mutants have revealed the role of Fgf signaling in tissue regeneration [36, 58]. Mutagenesis studies can be either forward or reverse in design depending on the question asked [59]. However, mutagenesis studies are often associated with lethality. Chemical genetics has emerged in the last five to ten years as a complimentary approach to elucidate biological functions. Chemical genetics approaches offers distinct advantage over mutagenesis. Chemical exposures provide temporal control over protein functions and their effects are often reversible. This temporal control provides insight into the timing of events and the nature of the modulated process. Chemical effects can also be modulated by varying the concentrations of exposures. A single small molecule can simultaneously target multiple specific targets within a family or across different protein families [60] or focus on a specific member of the family as well [61]. Small molecules targeting specific developmental pathways [62] have identified novel genes involved in vertebrate

development. Identification of probes that dictate stem cell fate has revolutionized the field of stem cell therapy [63]. Use of chemical inhibitors of signaling pathways such as SU5402 (Fgfr1 inhibitor) [31], BIO (GSK3β inhibitor) [29], LY294002 (PI3kinase inhibitor) [64] and SB431542 (ALK4 inhibitor) [43] have corroborated mutagenesis.

Currently the major limitation in the field of chemical genetics is the limited number of small molecules available that alter specific protein function. One way to address this issue is by performing reverse genetic screens using chemicals such as toxins and drugs that have a known molecular target. The underlying premise is that if a chemical inhibits a molecular target critical for regenerative progression, the result will impact the process. The identification of the affected target will help us a to understand regenerative biology [30]. Following this argument we demonstrated that aryl hydrocarbon receptor (AHR) activation by TCDD impaired caudal fin regeneration in zebrafish [65]. Further molecular studies revealed that inappropriate activation of Wnt signaling by AhR perturbed tissue regeneration [32, 56]. Studying inhibition of fin regeneration by TCDD led to a better understanding of tissue regeneration as well as revealed molecular mechanisms of AHR biology.

Rapid i*n vivo* Larval Regeneration Assay

Despite the potential of chemical genetics approaches to understand biology, the spectrum of compounds that can be used to study and therapeutically manipulate regeneration is limited. This lack of mechanistic breadth limits the opportunities to study tissue regeneration. It is likely that expansion of the repertoire of chemical probes is necessary in order to fully utilize the zebrafish regenerative model. We adopted a chemical genetic approach to study tissue regeneration in early life stage larval

regeneration model [66] and developed a larval regeneration assay to screen for modulators of tissue regeneration [30]. The unique advantages of the larval model is that it is adaptable to high throughput screening and therefore used in multiwell plate screening technologies. They aslo display an easily distinguishable phenotype demonstrating unsuccessful regenerative progression. These allowed the development of a rapid phenotypic screening protocol. The idea of this assay was to generate a repertoire of chemicals of diverse background that impair regeneration. Identification of such probes will lead to elucidation of their molecular targets culminating in rapid identification of molecules critical for regeneration.

We initially screened a 2000 member library consisting of FDA approved drugs. Classification of the chemicals that impaired regeneration based on their function led to identification of glucocorticoids (GCs) as modulators of tissue regeneration. Understanding how glucocorticoids modulate tissue regeneration will help us not only to identify novel members of the regenerative pathway but also contribute towards knowledge aboutglucocorticoid receptor (GR) biology.

Glucocorticoids

GCs are important regulators of homeostasis. The adrenal corticosteroid hormones cortisol and corticosterone are the endogenous GCs. Physiological effects of the endogenous GCs involve a dampening of the stress response mediated by their anti-inflammatory properties [69]. The successful administration of cortisone in rheumatoid arthritis led to the recognition of the anti-inflammatory property of the cortisol backbone. An entire class of steroidal drugs was developed by structural modification of this

backbone. Their strong anti-inflammatory properties have made synthetic GCs such as dexamethasone and prednisolone among the most successful synthetic drugs in history.

GCs act via binding to the GR, a member of the nuclear receptor super family of ligand activated transcription factors. [70, 71] In the absence of ligands, the GR is sequestered in the cytoplasm by HSP90 and HSP70. Upon ligand binding, the receptors dissociate from their chaperones and translocate to the nucleus. Inside the nucleus, the ligand-bound GR can bind to other transcription factors such as AP-1 or NFκB preventing them from binding to their target sites (transrepression) or form a dimer to bind to glucocorticoid response elements (GREs) and modulate transcription (transactivation). The pharmacology of GCs largely depends on ligand concentration and receptor expression levels in the target tissue. The response generated by a ligand bound GR is tissue specific and is speculated to depend on a large number of factors including coactivators and the co repressors.

Our in vivo larval regeneration assay identified GCs as modulators of tissue regeneration. Further studies with beclomethasone dipropionate (BDP), a GR ligand from the screened library revealed that inapproprtiate activation of GR mediates inhibition of regeneration. During the regeneration assay the amputated larvae was exposed to BDP continuously for three days. Time course analysis revealed that exposure during initial four hours after amputation is sufficient for inhibition, suggesting that GCs target the early stages of regeneration. Since GCs are well known for their anti-inflammatory properties, a phenomenon that has been known to play important role in wound healing [72], we assessed the role of neutrophil and macrophages in the larval regenerating system. There was no difference in response to regeneration when Pu1, a transcription factor required for neutrophil and macrophage development was repressed.

This observation was consistent with reports from studies with the Pu.1 null mice that demonstrate proper healing [73] corroborating that wound healing is not dependent on inflammatory cells. Humans, however are believed to respond to injury by scarring caused by hyper inflammation, which does not permit regeneration. In summary, this study identified glucocorticoids as novel modulators of the early stages of regeneration. Further studies are necessary to reveal the downstream targets of GCs that play key role during regeneration.

Structure Activity Relationship and Regenerative Medicine

While the goal in academia is to elucidate biological pathways, the industry aims to develop drugs using chemical genetics [74]. The cortisol backbone has undergone significant manipulations since its discovery as the endogenous ligand of GR. Despite the well known anti-inflammatory effects of GCs the current focus of the pharmaceutical industry is to overcome the side effects on metabolism, bone and central nervous system associated with prolonged use of the drugs [75]. The idea is to discover GR ligands that reduce the incidence or severity of side effects while maintaining potent anti-inflammatory activity [76]. In addition, better understanding of GC pharmacology is necessary for optimization of currently available drugs.

To date there are few reports of GCs modulating tissue regeneration. These reports involve both promotion [77] as well as inhibition of regeneration [30] in different cell types emphasizing its tissue specific action. The newly identified role of GCs in regenerative medicine needs to be explored to understand regenerative biology as well as develop drugs that encourage tissue regeneration in mammals. Currently there is a gap in terms of drug development in the field of regenerative medicine. This gap can be

bridged using forward chemical genetic studies. The larval zebrafish has emerged as a widely used model, allowing rapid screening of libraries for defined targets which includes cardiovascular [79] and neurobehavioral effects [80, 81]. Our larval regeneration assay enabled us to develop an easy phenotypic screen for GR ligands based on the characteristic “v” shaped pattern in the non regenerating caudal fin [30]. Further use of this regeneration assay has the potential to identify GR ligands in an *in vivo* model using a basic phenotypic screen. GR ligands that fail to impact regeneration in the assay will reveal structural preference that dictate a regenerative response. This is will provide directionality to the field of regenerative medicine, focusing on drug development. A better understanding of the pharmacological effects of glucocorticoids will have tremendous value for discovering new drugs and for finding new applications of known drugs. Approaches such as this one will open new avenues in the field of GR biology and allow an understanding of the global effect of these ligands in biologically relevant regenerative system.

We approached the current gaps in our understanding of the complex regenerative pathways and their interactions that are influenced by GCs in three steps

1. Establish an early stage model of regeneration utilizing global genomic analysis to identify common molecular signaling between different regeneration platforms (Chapter2)
2. Elucidate the molecular mechanisms by which GCs modulate tissue regeneration (Chapter3)
3. Adopt a structure activity replationship (SAR) approach to identify structural preference critical for impact on regeneration (Chapter4)

References

1. Metcalfe, A.D. and M.W. Ferguson, Bioengineering skin using mechanisms of regeneration and repair. Biomaterials, 2007. 28(34): p. 5100-13.

2. Metcalfe, A.D. and M.W. Ferguson, Tissue engineering of replacement skin: the crossroads of biomaterials, wound healing, embryonic development, stem cells and regeneration. J R Soc Interface, 2007. 4(14): p. 413-37.

3. Springer, M.L., T.R. Brazelton, and H.M. Blau, Not the usual suspects: the unexpected sources of tissue regeneration. J Clin Invest, 2001. 107(11): p. 1355-6.

4. Bjorklund, A. and O. Lindvall, Cell replacement therapies for central nervous system disorders. Nat Neurosci, 2000. 3(6): p. 537-44.

5. Chien, K.R. and E.N. Olson, Converging pathways and principles in heart development and disease: CV@CSH. Cell, 2002. 110(2): p. 153-62.

6. Morgan, T.H., Regeneration and Liability to Injury. Science, 1901. 14(346): p. 235-248.

7. Woods, I.G., et al., A comparative map of the zebrafish genome. Genome Res, 2000. 10(12): p. 1903-14.

8. Postlethwait, J.H., et al., Zebrafish comparative genomics and the origins of vertebrate chromosomes. Genome Res, 2000. 10(12): p. 1890-902.

9. Kelly, P.D., et al., Genetic linkage mapping of zebrafish genes and ESTs. Genome Res, 2000. 10(4): p. 558-67.

10. Misof, B.Y. and G.P. Wagner, Regeneration in Salaria pavo (Blenniidae, Teleostei). Histogenesis of the regenerating pectoral fin suggests different mechanisms for morphogenesis and structural maintenance. Anat Embryol (Berl), 1992. 186(2): p. 153-65.

11. Becerra, J., et al., Regeneration of fin rays in teleosts: a histochemical, radioautographic, and ultrastructural study. Arch Histol Cytol, 1996. 59(1): p. 15-35.

12. Mari-Beffa, M., et al., Cell to cell interactions during teleosts fin regeneration. Int J Dev Biol, 1996. Suppl 1: p. 179S-180S.

13. Santos Ruiz, L., J.A. Santamaria, and J. Becerra, Cell proliferation in fin fish regeneration. Int J Dev Biol, 1996. Suppl 1: p. 183S-184S.

14. Geraudie, J. and M. Singer, The fish fin regenerate. Monogr Dev Biol, 1992. 23: p. 62-72.

15. Akimenko, M.A., et al., Differential induction of four msx homeobox genes during fin development and regeneration in zebrafish. Development, 1995. 121(2): p. 347-57.

16. Poss, K.D., L.G. Wilson, and M.T. Keating, Heart regeneration in zebrafish. Science, 2002. 298(5601): p. 2188-90.

17. Scott, I.C. and D.Y. Stainier, Development. Fishing out a new heart. Science, 2002. 298(5601): p. 2141-2.

18. Jopling, C., et al., Zebrafish heart regeneration occurs by cardiomyocyte dedifferentiation and proliferation. Nature. 464(7288): p. 606-9.

19. Lepilina, A., et al., A dynamic epicardial injury response supports progenitor cell activity during zebrafish heart regeneration. Cell, 2006. 127(3): p. 607-19.

20. Kikuchi, K., et al., Primary contribution to zebrafish heart regeneration by gata4(+) cardiomyocytes. Nature. 464(7288): p. 601-5.

21. Poleo, G., et al., Cell proliferation and movement during early fin regeneration in zebrafish. Dev Dyn, 2001. 221(4): p. 380-90.

22. Santos-Ruiz, L., et al., Cell proliferation during blastema formation in the regenerating teleost fin. Dev Dyn, 2002. 223(2): p. 262-72.

23. Nechiporuk, A. and M.T. Keating, A proliferation gradient between proximal and msxb-expressing distal blastema directs zebrafish fin regeneration. Development, 2002. 129(11): p. 2607-17.

24. Poss, K.D., M.T. Keating, and A. Nechiporuk, Tales of regeneration in zebrafish. Dev Dyn, 2003. 226(2): p. 202-10.

25. Akimenko, M.A., et al., Old questions, new tools, and some answers to the mystery of fin regeneration. Dev Dyn, 2003. 226(2): p. 190-201.

26. Nechiporuk, A., et al., Positional cloning of a temperature-sensitive mutant emmental reveals a role for sly1 during cell proliferation in zebrafish fin regeneration. Dev Biol, 2003. 258(2): p. 291-306.

27. Kawakami, Y., et al., Wnt/beta-catenin signaling regulates vertebrate limb regeneration. Genes Dev, 2006. 20(23): p. 3232-7.

28. Stoick-Cooper, C.L., et al., Distinct Wnt signaling pathways have opposing roles in appendage regeneration. Development, 2007. 134(3): p. 479-89.

29. Chen, B., et al., Small molecule-mediated disruption of Wnt-dependent signaling in tissue regeneration and cancer. Nat Chem Biol, 2009. 5(2): p. 100-7.

30. Mathew, L.K., et al., Unraveling tissue regeneration pathways using chemical genetics. J Biol Chem, 2007. 282(48): p. 35202-10.

31. Zodrow, J.M. and R.L. Tanguay, 2,3,7,8-tetrachlorodibenzo-p-dioxin inhibits zebrafish caudal fin regeneration. Toxicol Sci, 2003. 76(1): p. 151-61.

32. Mathew, L.K., et al., Crosstalk between AHR and Wnt signaling through R-Spondin1 impairs tissue regeneration in zebrafish. FASEB J, 2008. 22(8): p. 3087-96.

33. Poss, K.D., et al., Roles for Fgf signaling during zebrafish fin regeneration. Dev Biol, 2000. 222(2): p. 347-58.

34. Lee, Y., et al., Fgf signaling instructs position-dependent growth rate during zebrafish fin regeneration. Development, 2005. 132(23): p. 5173-83.

35. Poss, K.D., J. Shen, and M.T. Keating, Induction of lef1 during zebrafish fin regeneration. Dev Dyn, 2000. 219(2): p. 282-6.

36. Whitehead, G.G., et al., fgf20 is essential for initiating zebrafish fin regeneration. Science, 2005. 310(5756): p. 1957-60.

37. Lee, Y., et al., Maintenance of blastemal proliferation by functionally diverse epidermis in regenerating zebrafish fins. Dev Biol, 2009. 331(2): p. 270-80.

38. Geraudie, J., et al., Is exogenous retinoic acid necessary to alter positional information during regeneration of the fin in zebrafish? Prog Clin Biol Res, 1993. 383B: p. 803-14.

39. Ferretti, P. and J. Geraudie, Retinoic acid-induced cell death in the wound epidermis of regenerating zebrafish fins. Dev Dyn, 1995. 202(3): p. 271-83.

40. Geraudie, J., et al., Caudal fin regeneration in wild type and long-fin mutant zebrafish is affected by retinoic acid. Int J Dev Biol, 1995. 39(2): p. 373-81.

41. White, J.A., et al., A zebrafish retinoic acid receptor expressed in the regenerating caudal fin. Development, 1994. 120(7): p. 1861-72.

42. Ferretti, P. and S. Ghosh, Expression of regeneration-associated cytoskeletal proteins reveals differences and similarities between regenerating organs. Dev Dyn, 1997. 210(3): p. 288-304.

43. Jazwinska, A., R. Badakov, and M.T. Keating, Activin-betaA signaling is required for zebrafish fin regeneration. Curr Biol, 2007. 17(16): p. 1390-5.

44. Quint, E., et al., Bone patterning is altered in the regenerating zebrafish caudal fin after ectopic expression of sonic hedgehog and bmp2b or exposure to cyclopamine. Proc Natl Acad Sci U S A, 2002. 99(13): p. 8713-8.

45. Laforest, L., et al., Involvement of the sonic hedgehog, patched 1 and bmp2 genes in patterning of the zebrafish dermal fin rays. Development, 1998. 125(21): p. 4175-84.

46. Kizil, C., et al., Simplet controls cell proliferation and gene transcription during zebrafish caudal fin regeneration. Dev Biol, 2009. 325(2): p. 329-40.

47. Tal, T.L., J.A. Franzosa, and R.L. Tanguay, Molecular signaling networks that choreograph epimorphic fin regeneration in zebrafish - a mini-review. Gerontology. 56(2): p. 231-40.

48. Thatcher, E.J., et al., Regulation of zebrafish fin regeneration by microRNAs. Proc Natl Acad Sci U S A, 2008. 105(47): p. 18384-9.

49. Lund, T.C., et al., Expression of telomerase and telomere length are unaffected by either age or limb regeneration in Danio rerio. PLoS One, 2009. 4(11): p. e7688.

50. Stewart, S., Z.Y. Tsun, and J.C. Izpisua Belmonte, A histone demethylase is necessary for regeneration in zebrafish. Proc Natl Acad Sci U S A, 2009. 106(47): p. 19889-94.

51. Barros, T.P., et al., Zebrafish: an emerging technology for in vivo pharmacological assessment to identify potential safety liabilities in early drug discovery. Br J Pharmacol, 2008. 154(7): p. 1400-13.

52. Westerfield, M., The zebrafish book a guide for the laboratory use of zebrafish Danio (Brachydanio) rerio. 1993, Institute of Neuroscience, University of Oregon: [Eugene, OR.

53. Westerfield, M., The zebrafish book : a guide for the laboratory use of zebrafish (Danio rerio). Ed. 4. ed. 2000, [Eugene, Or.]: M. Westerfield. 1 v. (unpaged).

54. Curado, S., et al., Conditional targeted cell ablation in zebrafish: a new tool for regeneration studies. Dev Dyn, 2007. 236(4): p. 1025-35.

55. Kawakami, A., T. Fukazawa, and H. Takeda, Early fin primordia of zebrafish larvae regenerate by a similar growth control mechanism with adult regeneration. Dev Dyn, 2004. 231(4): p. 693-9.

56. Mathew, L.K., E.A. Andreasen, and R.L. Tanguay, Aryl hydrocarbon receptor activation inhibits regenerative growth. Mol Pharmacol, 2006. 69(1): p. 257-65.

57. Nakatani, Y., A. Kawakami, and A. Kudo, Cellular and molecular processes of regeneration, with special emphasis on fish fins. Dev Growth Differ, 2007. 49(2): p. 145-54.

58. Poss, K.D., et al., Mps1 defines a proximal blastemal proliferative compartment essential for zebrafish fin regeneration. Development, 2002. 129(22): p. 5141-9.

59. Stockwell, B.R., Exploring biology with small organic molecules. Nature, 2004. 432(7019): p. 846-54.

60. Xu, Y., Y. Shi, and S. Ding, A chemical approach to stem-cell biology and regenerative medicine. Nature, 2008. 453(7193): p. 338-44.

61. Knight, Z.A., et al., A pharmacological map of the PI3-K family defines a role for p110alpha in insulin signaling. Cell, 2006. 125(4): p. 733-47.

62. Peterson, R.T., et al., Small molecule developmental screens reveal the logic and timing of vertebrate development. Proc Natl Acad Sci U S A, 2000. 97(24): p. 12965-9.

63. Firestone, A.J. and J.K. Chen, Controlling destiny through chemistry: small-molecule regulators of cell fate. ACS Chem Biol. 5(1): p. 15-34.

64. Alvarez, Y., et al., Selective inhibition of retinal angiogenesis by targeting PI3 kinase. PLoS One, 2009. 4(11): p. e7867.

65. Andreasen, E.A., L.K. Mathew, and R.L. Tanguay, Regenerative growth is impacted by TCDD: gene expression analysis reveals extracellular matrix modulation. Toxicol Sci, 2006. 92(1): p. 254-69.

66. Mathew, L.K., et al., Comparative expression profiling reveals an essential role for raldh2 in epimorphic regeneration. J Biol Chem, 2009. 284(48): p. 33642-53.

67. Oppedal, D. and M.I. Goldsmith, A chemical screen to identify novel inhibitors of fin regeneration in zebrafish. Zebrafish. 7(1): p. 53-60.

68. Rombough, P., Gills are needed for ionoregulation before they are needed for O(2) uptake in developing zebrafish, Danio rerio. J Exp Biol, 2002. 205(Pt 12): p. 1787-94.

69. Munck, A., P.M. Guyre, and N.J. Holbrook, Physiological functions of glucocorticoids in stress and their relation to pharmacological actions. Endocr Rev, 1984. 5(1): p. 25-44.

70. Yamamoto, K.R., Steroid receptor regulated transcription of specific genes and gene networks. Annu Rev Genet, 1985. 19: p. 209-52.

71. Beato, M., P. Herrlich, and G. Schutz, Steroid hormone receptors: many actors in search of a plot. Cell, 1995. 83(6): p. 851-7.

72. Grose, R., et al., A role for endogenous glucocorticoids in wound repair. EMBO Rep, 2002. 3(6): p. 575-82.

73. Martin, P., et al., Wound healing in the PU.1 null mouse--tissue repair is not dependent on inflammatory cells. Curr Biol, 2003. 13(13): p. 1122-8.

74. Kawasumi, M. and P. Nghiem, Chemical genetics: elucidating biological systems with small-molecule compounds. J Invest Dermatol, 2007. 127(7): p. 1577-84.

75. Hillier, S.G., Diamonds are forever: the cortisone legacy. J Endocrinol, 2007. 195(1): p. 1-6.

76. Rosen, J., K. Marschke, and D. Rungta, Nuclear hormone receptor assays for drug discovery. Curr Opin Drug Discov Devel, 2003. 6(2): p. 224-30.

77. Wang, J., et al., Identification of select glucocorticoids as Smoothened agonists: Potential utility for regenerative medicine. Proc Natl Acad Sci U S A.

78. Cai, S.X., J. Drewe, and S. Kasibhatla, A chemical genetics approach for the discovery of apoptosis inducers: from phenotypic cell based HTS assay and structure-activity relationship studies, to identification of potential anticancer agents and molecular targets. Curr Med Chem, 2006. 13(22): p. 2627-44.

79. Das, B.C., et al., A forward chemical screen in zebrafish identifies a retinoic acid derivative with receptor specificity. PLoS One. 5(4): p. e10004.

80. Kokel, D., et al., Rapid behavior-based identification of neuroactive small molecules in the zebrafish. Nat Chem Biol. 6(3): p. 231-237.

81. Rihel, J., et al., Zebrafish behavioral profiling links drugs to biological targets and rest/wake regulation. Science. 327(5963): p. 348-51.

CHAPTER 2 – Comparative Expression Profiling Reveals an Essential Role for Raldh2 in Epimorphic Regeneration

*Sumitra Sengupta, *Lijoy K Mathew, Jill A Franzosa, Jessica Perry, Jane La Du, Eric A Andreasen, and Robert L Tanguay.

Department of Environmental and Molecular Toxicology, Environmental Health Sciences Center, Oregon State University, Corvallis, OR, 97331.

*Authors contributed equally to this manuscript.

Published in Journal of Biological Chemistry (2009)

Abstract

Zebrafish have the remarkable ability to regenerate body parts including the heart and fins by a process referred to as epimorphic regeneration. Recent studies have illustrated that similar to adult zebrafish, early life stage-larvae also possess the ability to regenerate the caudal fin. A comparative microarray analysis was used to determine the degree of conservation in gene expression among the regenerating adult caudal fin, adult heart and larval fin. Results indicate that these tissues respond to amputation/injury with strikingly similar genomic responses. Comparative analysis revealed *raldh2*, a rate-limiting enzyme for the synthesis of Retinoic acid (RA), as one of the most highly induced genes across the three regeneration platforms. *In situ* localization and functional studies indicate that *raldh2* expression is critical for the formation of wound epithelium and blastema. Patterning during regenerative outgrowth was considered to be the primary function of RA signaling; however our results suggest that it is also required for early stages of tissue regeneration. Expression of *raldh2* is regulated by Wnt and FGF/ERK signaling.

Introduction

Injury, disease and aging all result in a loss of tissue and reduced quality of life. Numerous human conditions could be significantly improved if therapies that encourage tissue regeneration were available. Most adult tissues and organs, especially in humans and other mammals, have lost their regenerative potential. As a result, injury to a tissue or organ usually results in permanent damage from scarring to disability. The field of regenerative medicine is aimed at developing strategies to restore individual cell types, complex tissues, or structures that are lost or damaged. Currently, one of the main approaches in the field of regenerative medicine is to guide the process of differentiation of stem cells into specific cell types and then into complex structures [1]. Alternatively, another strategy is to determine how certain organisms have retained the ability to regenerate their tissues, organs and appendages [2, 3]. By understanding the molecular pathways that differentially function in these “lower” animals, we will be in a stronger position to uncover why mammals fail to react to injury with a regenerative response.

Lower vertebrate model systems such as urodele amphibians and teleost fish have the remarkable ability to regenerate organs such as the heart, spinal cord, retina and limbs/fins [2, 3]. In recent years, zebrafish has been established as a research model for the identification of molecular signaling pathways that govern the process of regeneration. Adult zebrafish caudal fin regeneration occurs by epimorphic regeneration, which involves reprogramming and differentiation of blastema cells to different cell types to restore the tissue to its original form [2, 4-6]. A genetic zebrafish mutant study revealed that Fgf20a is absolutely required for the initiation and formation of blastema,

whereas recent reports suggest that Wnt/β-catenin signaling seems to act upstream of FGF signaling [7, 8]. Even though major progress has been made in the identification of some of the essential pathways for regeneration such as FGF, Wnt and Activin-βA (actβA) signaling, most would agree that we are still at the early stages of gene discovery [5, 7-10].

Similar to adult zebrafish, early life stage larvae have the ability to regenerate amputated caudal fins through the formation of the wound epithelium and blastema [7, 11-16]. Also, similar to the adult zebrafish, chemical inhibition of FGFR1 by SU5402, aryl hydrocarbon receptor (AHR) activation by TCDD and Glucocorticoid receptor (GR) activation by Beclomethasone abrogated larval fin regeneration [13-15, 17], suggesting that there are similarities at the cellular and molecular level between adult and larval regeneration. Since many of the experimental advantages of zebrafish lie at the earliest life stages, the study of fin regeneration during this experimentally tractable life stage is enticing.

A comprehensive microarray analysis of adult zebrafish fin and adult heart regeneration identified some conserved genomic responses to amputation in these distinct regeneration models [18, 19]. This suggests that the pathways essential for the initiation of regeneration may be conserved. To identify whether there are corresponding similarities in the regenerative gene expression response in the early life stage model, we conducted broad-based microarray analysis of larval and adult fin regeneration and compared the gene expression changes. Comparative analysis between larval and the adult fin regeneration systems indicated a high degree of similarity between the two gene expression profiles. When the larval gene list was compared with the published zebrafish heart regeneration gene list, similar pattern of

gene expression changes were revealed. Since the tissue architecture of larval fin, adult fin and heart are very different; the significant commonality in the gene expression changes must be reflective of conserved molecular signaling. To demonstrate the power of the larval fin regeneration model, we analyzed the role of a candidate gene and performed functional studies.

Materials and Methods

Zebrafish lines and care

For the larval fin regeneration studies, fertilized eggs were obtained from AB strain zebrafish (University of Oregon, Eugene, OR). For the adult *in situ* hybridization study, 2 month old AB strain zebrafish were used. The fin amputations were performed as previously described [15, 16, 20, 21]. The *Tg(hsp70l:tcf3-GFP)* line was obtained from ZIRC.

Chemicals

The RA synthesis inhibitors DEAB and Citral were purchased from Sigma Aldrich (St. Louis, MO). The amputated larvae were exposed to DEAB and Citral at a final concentration of 250 and 25μM, respectively, and the solutions were changed daily until 3 dpa. The ERK1/2 inhibitor U0126 was purchased from EMD Biosciences (San Diego, CA). U0126 and SU5402 were continuously exposed at a final concentration of 100μM. The inhibitory effect on regeneration by the various chemicals used was quantified with the images using ImagePro Plus software program (Media Cybernetics, Inc., Silver Spring, MD).

Fin Development

The development of the fin vasculature was analyzed using a transgenic fish (Tg-fli-GFP) that expresses green fluorescent protein in the vasculature under the control of the fli promoter. Periodically, bright field pictures were taken to analyze the development of the fin rays and overall structural changes. Simultaneously, fluorescent pictures at 488nM were taken to reveal vasculature development.

Isolation of RNA

The caudal fin tissues of 2dpf embryos were amputated and the fin tissues were pooled for RNA isolation and these samples were used as non-regenerating fin tissue (0 dpa). The amputated larvae were allowed to grow for 1, 2, or 3 days and the newly formed fin tissues were re-amputated as described above for the respective 1, 2, and 3 dpa time points. Three technical replicates, each comprised of regenerating fin tissue from 150 larvae were isolated at each time point. RNA was isolated from the fin tissue using the RNAqueous Micro kit (Ambion, Austin, TX). Adult zebrafish were amputated and the intact fin tissues were used as non regenerating fin tissue. The fin tissues were re-amputated at 1, 3, and 5 dpa for RNA isolation. Each replicate consisted of 10 fins. RNAlater was removed from the samples and total RNA was purified with TRI reagent (Molecular Research Laboratories, Cincinnati, OH) according to the manufacturer's instructions. The quality and quantity of RNA was determined by UV absorbance. Ribosomal RNA abundance and degree of degradation was determined in electropherogram patterns using the 2100 Bioanalyzer and RNA 6000 Nano chips (Agilent Technologies, Palo Alto, CA).

Affymetrix Microarray Processing

The microarray processing including probe synthesis, hybridization and scanning were conducted by the Center for Genome Research and Biocomputing at Oregon State University, Corvallis OR. For analysis of larval transcript abundance, 100 ng of total RNA from 0,1, 2 and 3 dpa larval fin tissue were used to generate biotinylated complementary RNA (cRNA) using the Two-Cycle Target Labeling kit (Affymetrix, Santa Clara, CA). Briefly, RNA samples were reverse transcribed using a T7-$(dT)_{24}$ primer and Superscript II reverse transcriptase (Invitrogen, Carlsbad, CA) and double stranded cDNA was synthesized. This was then used as a template for *in vitro* transcription for another round of double-stranded cDNA synthesis. For the adult fin regeneration study, 2.5 µg of total RNA was used to generate biotinylated cRNA for each treatment group using the One-Cycle Target Labeling kit (Affymetrix, Santa Clara, CA). From the double-stranded cDNA, biotinylated cRNA was synthesized using T7 RNA polymerase and a biotin-conjugated pseudouridine containing nucleotide mixture provided in the IVT Labeling Kit (Affymetrix, Santa Clara, CA). For both larval and adult fin regeneration experiments, 10 µg of purified and fragmented cRNA from each experimental sample was hybridized to zebrafish genome arrays (Zebrafish430_2) according to the Affymetrix GeneChip Expression Analysis Technical Manual (701021 Rev. 5). Arrays were scanned with an Affymetrix scanner 3000. For data analysis, the Affymetrix cel files were imported into GeneSpring 7.1 software (Agilent Technologies, Palo Alto, CA). The files were GC-RMA processed to discount for background signal and each transcript was normalized to the median signal to allow comparison between arrays on a relative scale for each gene. The differential effect of time on regeneration was performed by comparing the non-regenerating fin tissue (0 dpa) to other time points by one-way ANOVA assuming equal

variance employing Benjamini and Hochberg multiple testing corrections ($p < 0.05$). Only genes that were at least 1.7 fold differentially expressed from the 0 dpa gene levels were considered for analysis. The annotation of genes was performed by considering the sequence similarity to known mammalian proteins that was determined by conducting a BLAST search of each Affymetrix probe set against the Sanger database (http://www.sanger.ac.uk/Projects/D_rerio/). Additionally, other databases such as Genbank (http://www.ncbi.nlm.nih.gov/BLAST/) and the Zebrafish Affy Chip Annotation Project at Children's Hospital Boston (http://134.174.23.160/zfaca/hash/master020106public.aspx) were utilized. The fold difference values from microarray data of the published heart regeneration study were on a base 2-logarithm scale and those values were transformed to normal numbers for comparison with our studies. Experiments were MIAME certified, and the raw data are listed at the National Center for Biotechnology Information (NCBI) Gene Expression Omnibus (GEO) (http://www.ncbi.nlm.nih.gov/projects/geo/; series record GSE10188).

Morpholinos

The fluorescein tagged *raldh2* morpholino (Gene Tools, Philomath, OR) was used to transiently knockdown *raldh2* gene. The sequence of *raldh2* morpholino is 5'-GTTCAACTTCACTGGAGGTCATCGC-3'. Morpholinos were diluted to 3 mM in 1X Danieau's solution (58 mM NaCl, 0.7 mM KCl, 0.4 mM $MgSO_4$, 0.6 mM $Ca(NO_3)_2$, 5 mM HEPES, pH 7.6) as described [22]. A standard control morpholino (Gene Tools, Philomath, OR) (5'CTCTTACCTCAGTTACAATTTATA 3') was used as the control morpholino (Control-MO). Approximately 2 nl of 0.3mM MO solution was microinjected

into the embryos at the 1–2 cell stage. The fin tissue of control and *raldh2* morphants were amputated at 2dpf and exposed and allowed to grow for 3 days at 28°C.

Quantitative RT-PCR

Total RNA was isolated in triplicate from the regenerating fins at 0, 1, 2 and 3 dpa (n = 150/group). From the larval fin RNA, cDNA was prepared from 100 ng of total RNA per group using Superscript II (Life Technologies, Gaithersburg, MD) and oligo(dT) primers in a 20 μl volume. Quantitative RT-PCR (qRT-PCR) was conducted using gene specific primers (Table S8) with the Opticon 2 real-time PCR detection system (MJ Research, Waltham, MA). Briefly, 1 μl of cDNA was used for each PCR reaction in the presence of SYBR Green, using DyNAmo SYBR green qPCR kit according to the manufacturer's instructions (Finnzymes, Espoo Finland). All samples were normalized to their β-actin abundance. Quantitative differences between biological samples were determined by normalizing all samples to a common reference sample. Agarose gel electrophoresis and thermal denaturation (melt curve analysis) were conducted to ensure formation of specific products. Significant differences of mRNA abundance were assessed by one-way ANOVA on $\log_{10}$ transformed data using Tukey method ($p < 0.05$) (SigmaStat software, Chicago, IL).

Whole Mount *In situ* Hybridization

In situ hybridization was performed on the regenerating fin at respective time points as described previously [16]. The *mvp*, *msxe* and *dlx5a* probes were obtained from Atsushi Kawakami [16]. *Raldh2* probe was prepared by cloning the cDNA by RT-PCR from the RNA isolated from the whole adult zebrafish. The *wnt10a* probe was a gift

from Gilbert Weidinger (Biotechnological Center, Technical University of Dresden, Germany). The embryos were reared in phenylthiourea (Sigma) at a final concentration of 100μM from 24hpf to inhibit formation of pigmentation.

Cell Proliferation Assay

The cell proliferation assay was conducted as previously described [14] on the regenerating fin tissue after pulse labeling with Brdu (Roche, Indianapolis, IN) for 6hrs starting from 24 hpa or 48 hpa. Brdu assay was performed on vehicle- or DEAB exposed amputated larvae at the respective time points. After 6hrs of incubation with Brdu at 28°C, the larvae were fixed in 4% paraformaldehyde (PFA) overnight. The fixed larvae were dehydrated with methanol and then stored in methanol at -20°C. Briefly, immunochemistry was conducted on the stored larvae by rehydrating with a graded methanol/PBST (phosphate-buffered saline (PBS) and 0.1% Tween-20) series. The larvae were then treated with Proteinase K in PBST for 20 minutes at room temperature (RT) and then rinsed several times with PBST. The larvae were refixed in 4% PFA for 30 minutes and then washed several times in water, followed by quick rinses in 2N HCL and incubation in 2N HCL at RT for an hour. After several washes, the larvae were then blocked with 1% normal goat serum in PBST for an hour at RT and then incubated with anti-Brdu antibody (1:100; G3G4; Developmental Studies Hybridoma Bank, Iowa City, IA) overnight at 4°C. After four or more 30 min washes with PBST, the larvae were incubated with a secondary antibody (1:1000; Alexa-546 conjugated goat anti mouse; Molecular Probes, Eugene, OR) for 4 hrs at RT. The larvae were then washed 4x for 30 min in PBST and visualized by epifluorescence microscopy. The Brdu-labeled

fluorescent cells were quantified with the acquired images using ImagePro Plus software program (Media Cybernetics, Inc., Silver Spring, MD).

Results

Structural Morphogenesis of Larval to Adult Fin

Although both larvae and adult zebrafish regenerate their caudal fins following amputation, it is clear that there are structural differences in the regenerating tissues between the two life stages. Bright field imaging revealed that the lepidotrichia (fin rays) are not yet present in larvae at 5 days post fertilization (dpf). Instead, the larval fin primordia contained an abundance of actinotrichia (composed of collagenous fibrils) which populate the tissue. It is also noteworthy that the larval fin at this stage is not vascularized as revealed by *in vivo* imaging of the *Fli1-GFP* transgenic line. This led us to ask when the larval fin takes on adult fin morphology. To answer this question, fin developmental progression was systematically assessed to identify the structural morphogenesis until the fin developed an adult-like phenotype (Figure S1). Although vasculature in the trunk was functional with strong blood flow in 3- and 7- day-old zebrafish, vascularization of the caudal fin was not apparent until after 10dpf. At approximately 10dpf, the posterior end of the notochord begins to bend dorsally, and soon after, clusters of actinotrichia gather, like corn stalks tied with twine, to form ray-like structures ventral to the notochord (Figure S1). Concomitant with the formation of rays, the vasculature forms along these rigid tracks. By 19 dpf, 18 rays had developed, become vascularized and innervated (neuronal immunohistochemistry data not shown). By approximately 3 weeks, the caudal fin appears similar to the adult morphologically,

with fully formed vasculature including intersegmental vascular loops. These studies illustrate significant structural differences between the adult and 2 day old larval fin structures, yet at both life stages, the animals are equally able to regenerate their fin tissues following amputation.

Comparative Microarray Analysis Revealed Common Signaling Pathways during Zebrafish Regeneration.

Since regeneration is an orchestrated process of molecular events, we designed a broad-based microarray study to identify the gene expression changes that occur specifically in the isolated regenerates over time in larval fin tissues. The differential gene expression profiles for 1, 2 and 3 days post amputation (dpa) were created by filtering for genes that were at least 1.7 fold differentially abundant relevant to the non-regenerating fin (0 dpa). One-way ANOVA analysis was conducted for statistical significance and a total of 1851 transcripts were altered in at least one regeneration time point from 0 dpa (Figure 1A). From the 1851 genes, a shorter gene list was created and annotated by filtering for genes that were at least 2.5 fold differentially abundant at any regenerating time point when compared to 0 dpa (Table S1). These transcripts were grouped into functional categories such as wound healing and immune response, signal transduction, extracellular matrix and cell adhesion (Figure 1B). Our results were consistent with the previous studies conducted using RNA isolated from adult zebrafish caudal fins and the adult hearts [18, 19]. This prompted us to perform a comparative genomic analysis across three different regeneration platforms. We first compared the amputation-initiated gene expression changes between the larval and adult fin regenerates. As was done with the larval expression data, an adult fin regeneration expression list was created by filtering transcripts that were at least 1.7 fold differentially

expressed at 1, 3 or 5 dpa when compared to the non-regenerating 0 dpa fin. Statistical significance was analyzed by one-way ANOVA and a total of 3762 transcripts were changed at 1, 3, or 5 dpa from 0 dpa. The larval and the adult fin lists were cross-compared and 658 transcripts (approximately 36% of the larval list) were identified as common (Figure 1C). We further narrowed the common list by filtering for the transcripts that were at least 1.7 fold differentially abundant at 1 dpa in the larval gene list and this reduced the number of genes to 341. To acquire more meaningful data, we then analyzed the pattern of gene expression changes by assessing the similarity in the gene regulation between the larval and adult gene lists. Out of the 341 transcripts that were common in both lists, 109 and 107 genes were similarly induced and repressed, respectively, which comprised about 64% resemblance in the pattern of gene regulation between the two regenerating tissue platforms (Table S2). Similar to the previous adult regeneration studies, many genes involved in wound healing, signal transduction, transcriptional regulation and extracellular matrix components were regulated in both fin regeneration models (Table S3.)

The common gene expression profile identified during these two distinct fin regeneration models directed us to compare larval fin regeneration genomic response to the response in the regenerating adult heart. We utilized the published data from the study performed on zebrafish regenerating heart [18], in which a total of 662 genes were differentially expressed in the regenerating zebrafish heart in at least one of the three time points, 3, 7 or 14 dpa [18]. The larval fin regeneration expression list was compared to the adult heart regeneration list and we identified 189 common gene expression changes (Figure 1D). Of these genes, 116 were similarly induced and 18 were similarly repressed, which constitutes about 89% and 31% similarity in the gene regulation,

respectively, between larval fin and adult heart regeneration (Table S4). This suggests the existence of conserved biomolecules that are generally required for tissue regeneration (Table S5).

To further mine regeneration expression data, we performed a comparative analysis across three regeneration platforms, the two fin regeneration models and the zebrafish heart regeneration system. The goal was to identify the gene expression changes that are similarly modulated after amputation (Figure 1D). A total of 91 genes were common and 54% of these genes were similarly regulated across all three platforms (Table S6). A number of genes that were induced or repressed in either adult fin or heart regeneration were validated by qRT-PCR with the larval fin RNA (Figure S2). Wound healing transcripts such as *galectin 9, cathepsin S, C,* and *B* were similarly regulated indicating that the immediate response to amputation is conserved across the three regeneration platforms. Two members of the Maf protein family such as *krml2* and *krml2.2* which are involved in the control of cellular differentiation were also similarly regulated across three different platforms [23, 24]. The extracellular matrix components *timp2* and *mmp14* were highly induced indicating the importance for a proper foundation for the proliferating cells to migrate and adhere in a regulated fashion. We also identified many genes such as *fgf20a, msxe, msxc, wnt5b* that have been previously reported in different zebrafish fin regeneration studies in this larval fin regeneration microarray analysis (Table S7). Most importantly, *raldh2* (retinaldehyde dehydrogenase 2) was one of the genes that was highly induced across three regeneration models. The profound induction of this gene in the epicardium after amputation of zebrafish heart has been recently reported [18, 25]. This is significant as the caudal fin and heart are morphologically completely different, yet at the level of gene expression; common

genomic responses to amputation were observed, again suggesting that there are likely conserved “regenerative mechanisms”.

***Raldh2* is Highly Expressed During Caudal Fin Regeneration.**

From the comparative genomic analysis, r*aldh2*, a rate limiting enzyme for Retinoic acid (RA) synthesis was one of the highly induced genes during regeneration across the three regeneration platforms. The induction of *raldh2* was validated by qRT-PCR with the larval fin RNA (Figure S2). *In situ* localization of *raldh2* in regenerating larval fins revealed expression as early as 4 hours post amputation (hpa) continuing through 72 hpa (3 days post amputation) (Figure 2A). *Raldh2* was expressed during blastema formation (4, 12 and 24 hpa) suggesting a possible role in the development of the blastema. While not quantitative, *raldh2* signal intensity at 48 and 72 hpa was notably high, consistent with the microarray and qRT-PCR data (Table S1 and Figure S2), suggesting the importance of this rate limiting enzyme at the post-blastema phase of regeneration. In the adult regenerating fin tissue, *raldh2* was localized in the distal blastemal region just beneath the wound epithelium at 3 dpa (Figure 2B). This is consistent with the expression of *retinoic acid receptor gamma* in adult regenerating fin tissue beneath the wound epithelium [26], depicting the overlapping expression of RA signaling members in the regenerating fin tissue. In support of our data, previous mRNA localization studies have revealed that *raldh2* is very highly expressed in epicardium surrounding the ventricle, atrium and outflow tract as early as 1 dpa after partial ventricular amputation in zebrafish heart [25]. Together, the qRT-PCR data and the mRNA localization studies confirm the enhanced expression of *raldh2* during caudal fin regeneration in zebrafish.

Raldh2 is Required for Larval Fin Regeneration.

As *raldh2* is highly induced in three regeneration systems, we hypothesized that if Raldh2 is critical for regeneration, inhibition of RA synthesis by specific inhibitors should block regeneration. The larvae at 2dpf were amputated and exposed continuously to a specific Raldh2 inhibitor, 4-diethylaminobenzaldehyde (DEAB; 250 µM) and a RA synthesis inhibitor, 3,7-Dimethyl-2,6-Octadienal (Citral; 25 µM). The larvae exposed to DEAB and Citral were not able to accomplish regeneration, and the measurement studies clearly indicate the inhibitory effect on regeneration (Figure 3A, B, C, P). To further demonstrate the specific requirement of *raldh2* during regeneration, we utilized the available *raldh2/neckless* mutant, but the larvae were severely deformed making regeneration assessments impossible. As an alternative, we performed morpholino (MO) antisense repression of *raldh2* and analyzed the regeneration potential of the *raldh2* morphants. Our previous larval fin regeneration studies demonstrated that morpholinos can be effectively delivered at the one-cell stage and efficacy lasts for several days [14, 15]. Since complete knockdown of *raldh2* is detrimental to normal embryonic development and leads to early mortality [27], we titrated the amount of *raldh2* morpholino to only partially repress Raldh2 expression, and optimized the concentration of the *raldh2* morpholino to a level which did not affect normal fin development (data not shown). The control morphants completely regenerated their fin tissue after amputation at 3 dpa, whereas the *raldh2* morphants failed to regenerate (Figure 3D, E, Q). As the primary function of Raldh2 is the synthesis of RA, we next tested whether the inhibitory effect on regeneration by DEAB could be reversed using exogenous RA. All trans RA (0.01 µM) was co-exposed with DEAB immediately after caudal fin amputation for 24hrs. The use of exogenous RA rescued the inhibition of

regeneration by DEAB (n=32/46) (Figure 3R). Similarly, we successfully rescued the impaired regeneration of *raldh2* morphants by approximately 50%, using exogenous RA (data not shown). Of note, RA (at 0.01 µM) itself did not affect larval fin regeneration (data not shown). These results clearly suggest that *raldh2* expression is required for fin regeneration.

Inhibition of Raldh2 Impair Wound Epithelium, Blastema and Cell Proliferation during Larval Fin Regeneration.

To understand the phase(s) of regeneration affected by the inhibition of RA signaling, we performed *in situ* analysis with *dlx5a* and *msxe*, markers which define the wound epithelium and the blastema, respectively. The expression of *dlx5a* and *msxe* was lost in the DEAB and Citral exposed larvae at 1 dpa (Figure 2F, G, H, K, L M). To confirm the result that Raldh2 expression is essential for proper formation of wound epithelium and blastema, we further performed mRNA localization studies with the same markers in *raldh2* morphants. Very similar to the RA synthesis inhibitors, the expression of both *dlx5a* and *msxe* were significantly reduced in the regenerating fin tissue of the *raldh2* morphants when compared with the control morphants at 1 dpa (Figure 3I, J, N, O). Together, these results indicate that *raldh2* expression is essential for proper wound epithelium and the blastema formation during fin regeneration.

Since inhibition of Raldh2 affects wound epithelium and blastema formation, we next examined the role of raldh2 specifically on cell proliferation by performing *in vivo* Bromodeoxyuridine (Brdu) incorporation assays. Cell proliferation assays were conducted on larvae exposed to vehicle or DEAB at 24-30 hpa and 48-54 hpa. There was significant reduction in the number of Brdu-labeled cells in the regenerates of DEAB-exposed larvae at both 24-30 hpa and 48-54 hpa when compared to the vehicle-

exposed larvae (Figure 4A, B). We also performed Brdu incorporation assay on *raldh2* morphants to identify whether cellular proliferation is similarly affected using the antisense approach. Similar to the DEAB-exposed larvae, *raldh2* morphants had a significant reduction in the number of Brdu labeled cells at 24-30 hpa and 48-54 hpa when compared to the standard control morphants (Figure 4C, D). It is noteworthy that the inhibitory effects on cell proliferation are similar between DEAB-exposed larvae and *raldh2* morphants with a reduction of Brdu labeled cells at the posterior and ventral side of the notochord [14, 16]. Altogether, these results suggest that the expression of *raldh2* is required for cell proliferation at different regenerative stages.

Wnt Signaling Regulates *Raldh2* Expression during Fin Regeneration.

Since Raldh2 is functionally important for fin regeneration, it is important to begin to identify the factors that control *raldh2* expression. The functional importance of Wnt signaling during zebrafish adult fin regeneration was recently reported [7, 10]. First, to analyze whether Wnt signaling has any functional role during larval fin regeneration, we used a heat shock inducible dominant negative transgenic zebrafish line (Tg(hsp70:ΔTCF-GFP) that simultaneously expresses GFP and inhibits Wnt/β-catenin signaling. Two day old larvae were heat shocked for 2 hrs at 37^0C followed by amputation. The hsp70:ΔTCF-GFP transgenic larvae were unable to regenerate fin tissue at 3 dpa (Figure 5A, F). The expression of *dlx5a* and *msxe* was affected in hsp70:ΔTCF-GFP transgenic larvae (Figure 5B, C), suggesting similar requirement for Wnt signaling during both larval and adult fin regeneration. To directly test whether Wnt signaling regulates the expression of *raldh2*, *in situ* hybridization was performed on hsp70:ΔTCF-GFP transgenic larvae. *Raldh2* was completely absent in hsp70:ΔTCF-GFP transgenic larvae at 1 dpa, indicating the regulatory role for Wnt signaling (Figure 5D). In

order to confirm that Wnt signaling was inhibited after heat shock in the hsp70ΔTCF -GFP transgenic larvae, we quantitatively measured the expression of known Wnt target genes. qRT-PCR revealed that Axin2, DKK1 and cyclinD1 were significantly down-regulated in hsp70ΔTCF -GFP transgenic larvae (Figure 5E). Since Wnt signaling is considered to be upstream of all known molecular signaling pathways identified during fin regeneration, we proposed that *wnt10a* expression should not be affected by Raldh2 inhibition. *In situ* analysis revealed comparable *wnt10a* expression between vehicle, DEAB and Citral exposed larvae, indicating that *wnt10a* is unaffected by the inhibition of RA signaling (Figure 5 G).

FGF and ERK1/2 Signaling is Required for the Expression of *raldh2*.

One of the most well-studied pathways in zebrafish regeneration is FGF signaling [5, 8, 15, 16]. Similar expression of *fgf20a* was identified in the larval regenerating fin, underscoring the commonality at the molecular level between the adult and larval fin regeneration systems (Table S1, S3; Figure 6G). To identify whether FGF signaling controls *raldh2* expression, *in situ* hybridization was conducted on SU5402 (a chemical inhibitor of FGFR1) [5] exposed larvae at 1dpa. The *raldh2* expression was completely absent in the SU5402 exposed animals, suggesting that FGF signaling regulates its expression (Figure 6A). Furthermore, since FGF signaling is mediated through the phosphorylation of ERK1/2, we used an ERK1/2 inhibitor (U0126) to determine whether activation of ERK1/2 is required for the expression of *raldh2*. As the role of ERK1/2 signaling on fin regeneration has not been previously reported, 2 dpf larvae were amputated and exposed to vehicle or U0126 (100 µm) continuously for 3 days. The U0126 -exposed larvae failed to regenerate the amputated fin tissue and results in a complete loss of *dlx5a* and *msxe* expression in the regenerates at 1 dpa (Figure 6 B, H,

C, D). Similar to SU5402, inhibition of ERK1/2 activation completely abolished the expression of *raldh2* (Figure 6E). The inhibition of ERK1/2 signaling by U0126 was validated by analyzing the expression of *mvp*, an ERK target gene (Figure 6F) [28]. These results suggest that FGF signaling pathway, possibly through the phosphorylation of ERK1/2 is required for the expression of *raldh2* during larval fin regeneration in zebrafish.

RA Signaling is Sufficient to Rescue the Inhibitory Effect of FGFR1 and ERK1/2 Inhibitor on Larval Fin Regeneration.

Our *raldh2* expression analysis following Wnt and FGF signaling inhibition suggests that RA signaling is downstream to the Wnt and FGF pathways. It has been reported that Wnt is upstream to FGF signaling [7]. To directly determine whether RA signaling is downstream to FGF signaling, we asked whether the inhibitory effect of SU5402 could be overcome by exogenous RA. Amputated larvae at 2dpf were co-exposed with SU5402 and exogenous RA continuously for 3 days. Exogenous administration of RA rescued SU5402 mediated impairment of regeneration suggesting that RA signaling is downstream to FGF pathway (Figure 7A, C). Since ERK1/2 signaling is downstream to FGF singaling, we analyzed whether RA could rescue the inhibitory effect of ERK1/2 inhibitor. U0126 exposed larvae did not elicit inhibition of regeneration in the presence of exogenous RA, suggesting that RA signaling is downstream to ERK1/2 signaling (Figure 7B, D). This is a significant finding as it demonstrates a necessary role for RA signaling for larval fin regeneration.

Discussion

Since the early life stages of zebrafish are amenable to molecular and genetic techniques, the development of the larval fin regeneration model provides a unique platform to rapidly identify the gene products required for regeneration [11, 13-16]. Comparative gene expression analysis revealed significant common gene expression changes in larval fin, adult caudal fin and heart regenerating tissues, suggesting common molecular pathways choreographing the regeneration process.

The physiological progression of fin regeneration in larvae and adults is similar, as both initiate with the formation of a wound epithelium, blastema formation and the distal to proximal propagation of cell proliferation [16, 29]. Furthermore, there is also growing evidence to suggest that heart regeneration in zebrafish has a high degree of commonality with fin regeneration with respect to the order of events which occur after a surgical wound. Both tissues regenerate through the blastema formation followed by proliferation of cells to complete outgrowth [2, 18, 25, 30]. Gene expression of *msxB* and *msxC* encoding homeo-domain containing transcription factors are re-induced in regenerating zebrafish hearts as early as 3 dpa, and also in regenerating fin blastema [2, 18, 25, 30]. Additionally, the expression pattern of *notch1b* and *deltaC*, members of the Notch signaling pathway, are induced very early after heart amputation and in the regenerating fin blastema [30]. None of the four genes described above were detected in the non-amputated fin or heart tissue, indicating that the re-induction of these genes was specific to the regenerating tissue. Together, the current literature supports the existence of conserved molecular mechanisms across the three different regenerative platforms.

Recent studies illustrate that a proper balance of Wnt/β-catenin signaling is also critical for the formation and proliferation of blastemal cells [7, 10]. This is consistent with our result observed in the larval model: when canonical Wnt signaling is blocked, the

formation of wound epithelium and blastema are blocked (Figure 5A, B, and C). Moreover, Wif1, a feedback regulator of Wnt signaling pathway was one of the repressed transcripts in both adult and larval fin regeneration models suggesting that the Wnt signaling pathway is well-regulated during regeneration. Moreover, a significant number of Wnt target genes were identified in both the larval and adult fin regeneration gene expression list (Table S3).

FGF signaling is one of the well-studied signaling pathways during zebrafish regeneration. The necessity of FGF signaling during adult zebrafish fin and heart regeneration was demonstrated with the use of the FGFR1 inhibitor (SU5402) and the transgenic line (*hsp70:dn-fgfr1*) that expresses the dominant negative FGFR1 protein upon heat shock [5, 25, 31]. Predictably, the larval fin regeneration system also requires FGF signaling since SU5402 also blocked the early life stage regeneration [15, 16]. Moreover, *fgf20a* which was identified as an initiator of blastema formation in adult regenerating fin [8], is also highly induced in the larval fin tissue (Table S1). Even though *fgf20a* was detected by microarray analysis and qRT-PCR, the expression was too low to detect by *in situ* hybridization in the larval fin tissue. During zebrafish heart regeneration, among the several FGF ligands tested, only *fgf17b* was strongly expressed in the cardiomyocytes at the apical edge of the regenerating heart tissue [25]. The expression of different FGF ligands in these tissues is not unexpected considering the diversity of the regenerating tissues. But the data strongly indicates that epimorphic tissue regeneration requires functional FGF signaling in the early stages of the regenerative process.

Raldh2, a rate limiting enzyme for RA synthesis was one of the most highly induced genes in all three regeneration models. A profound induction of *raldh2* in the

epicardium after zebrafish heart amputation has been reported [18, 25]. This is significant as the caudal fin and heart are morphologically different, yet at the level of gene expression; common genomic responses to amputation were observed. RALDH2 enzyme activity is also highly induced in NG-2 cells after spinal cord injury in rats [32]. *Raldh2* is also expressed in the skin and perichondrium and in perivascular cells in cartilage during deer antler regeneration [33]. Whole body regeneration from a miniscule blood vessel fragment has been illustrated in the colonial urochordate *Botrylloides leachi,* and the homologue of the *RA receptor* and *raldh*-related gene were exclusively expressed in blood cells in the regeneration niches, suggesting the ancestral conservation of RA signaling during regeneration and body restoration events [34].

The functional role of RA signaling during amphibian and zebrafish regeneration has been studied for decades and RA is even referred to as a regeneration-inducing molecule [26, 35-40]. RA is mainly characterized as a signaling molecule that is required for the vertebrate pattern formation both in developing and regenerating tissues. Amphibian regeneration studies revealed that exposure of regenerating axolotl and urodele limbs to RA results in the modification of positional memory in the proximodistal axis and caused patterning defects such as duplication of the stump [41, 42]. Similarly, exposure of zebrafish with RA during fin regeneration resulted in remarkable morphological effects suggesting that exogenous RA can re-specify patterns in the regenerating fin tissue [26]. Most of the regeneration studies with RA signaling are related with the patterning of the structures during regeneration. Our chemical inhibition studies suggest that RA signaling is indeed required for the complete formation of wound epithelium and blastema. Moreover, we also illustrated the sufficient role of RA signaling

during larval fin regeneration. The complete understanding of the RA signaling requirement for wound epithelium and blastema formation requires further studies.

Since the expression of *raldh2* was continuously present from 4 hpa to 3 dpa, we presume that the requirement of RA signaling is continuous from the initiation of regeneration through pattern formation and regenerative outgrowth (Figure 2). However, the increased expression of *raldh2* at 2 dpa raises the possibility for a distinct flux of RA signaling (Figure 2, S2), and suggests a dual phase of RA signaling during regeneration. In support of our proposal, vertebrate limb developmental studies in mice have illustrated the existence of an early phase of RA signaling to initiate forelimb development, followed by a late phase of RA signaling required to develop the apical ectodermal ridge fully along the distal ectoderm to complete the limb outgrowth [43]. Moreover, studies with the *raldh2/neckless* zebrafish mutant revealed that RA signaling is required for the induction of the pectoral fin field and also to establish a prepattern of anteroposterior fates in the condensing fin mesenchyme [44]. Therefore, in addition to the well-established functional role of RA signaling during the regenerative outgrowth, it is also essential in the early stages of regeneration, suggesting the existence of two phases of RA signaling during regeneration.

Finally, we illustrated that the expression of *raldh2* is regulated by Wnt and FGF/ERK signaling and that RA signaling is downstream of FGF /ERK signaling during zebrafish fin regeneration (Figure 7). Even though multiple signaling pathways are active during regeneration, the functional interactions required to accomplish epimorphic regeneration are still not completely understood. Collectively, these studies reveal that the regenerative response choreographing epimorphic tissue regeneration is conserved which offers opportunities to use multiple models to unravel the regenerative program.

References

1. Bianco, P. and P.G. Robey, *Stem cells in tissue engineering.* Nature, 2001. **414**(6859): p. 118-21.
2. Akimenko, M.A., et al., *Old questions, new tools, and some answers to the mystery of fin regeneration.* Dev Dyn, 2003. **226**(2): p. 190-201.
3. Brockes, J.P., *New approaches to amphibian limb regeneration.* Trends Genet, 1994. **10**(5): p. 169-73.
4. Nechiporuk, A. and M.T. Keating, *A proliferation gradient between proximal and msxb-expressing distal blastema directs zebrafish fin regeneration.* Development, 2002. **129**(11): p. 2607-17.
5. Poss, K.D., et al., *Roles for Fgf signaling during zebrafish fin regeneration.* Dev Biol, 2000. **222**(2): p. 347-58.
6. Quint, E., et al., *Bone patterning is altered in the regenerating zebrafish caudal fin after ectopic expression of sonic hedgehog and bmp2b or exposure to cyclopamine.* Proc Natl Acad Sci U S A, 2002. **99**(13): p. 8713-8.
7. Stoick-Cooper, C.L., et al., *Distinct Wnt signaling pathways have opposing roles in appendage regeneration.* Development, 2007. **134**(3): p. 479-89.
8. Whitehead, G.G., et al., *fgf20 is essential for initiating zebrafish fin regeneration.* Science, 2005. **310**(5756): p. 1957-60.
9. Jazwinska, A., R. Badakov, and M.T. Keating, *Activin-betaA signaling is required for zebrafish fin regeneration.* Curr Biol, 2007. **17**(16): p. 1390-5.
10. Kawakami, Y., et al., *Wnt/-catenin signaling regulates vertebrate limb regeneration.* Genes and Dev, 2006. **Dec 2006; 20: 3232 - 3237 ; doi:10.1101/gad.1475106**.
11. Rojas-Munoz, A., et al., *ErbB2 and ErbB3 regulate amputation-induced proliferation and migration during vertebrate regeneration.* Dev Biol, 2009. **327**(1): p. 177-90.
12. Kizil, C., et al., *Simplet controls cell proliferation and gene transcription during zebrafish caudal fin regeneration.* Dev Biol, 2009. **325**(2): p. 329-40.
13. Mathew, L.K., et al., *Crosstalk between AHR and Wnt signaling through R-Spondin1 impairs tissue regeneration in zebrafish.* Faseb J, 2008. **22**(8): p. 3087-96.
14. Mathew, L.K., et al., *Unraveling tissue regeneration pathways using chemical genetics.* J Biol Chem, 2007. **282**(48): p. 35202-10.
15. Mathew, L.K., E.A. Andreasen, and R.L. Tanguay, *Aryl hydrocarbon receptor activation inhibits regenerative growth.* Mol Pharmacol, 2006. **69**(1): p. 257-65.

16. Kawakami, A., T. Fukazawa, and H. Takeda, *Early fin primordia of zebrafish larvae regenerate by a similar growth control mechanism with adult regeneration.* Dev Dyn, 2004. **231**(4): p. 693-9.
17. Zodrow, J.M. and R.L. Tanguay, *2,3,7,8-tetrachlorodibenzo-p-dioxin inhibits zebrafish caudal fin regeneration.* Toxicol Sci, 2003. **76**(1): p. 151-61.
18. Lien, C.L., et al., *Gene expression analysis of zebrafish heart regeneration.* PLoS Biol, 2006. **4**(8): p. e260.
19. Schebesta, M., et al., *Transcriptional profiling of caudal fin regeneration in zebrafish.* ScientificWorldJournal, 2006. **6 Suppl 1**: p. 38-54.
20. Andreasen, E.A., et al., *Aryl hydrocarbon receptor activation impairs extracellular matrix remodeling during zebra fish fin regeneration.* Toxicol Sci, 2007. **95**(1): p. 215-26.
21. Andreasen, E.A., L.K. Mathew, and R.L. Tanguay, *Regenerative growth is impacted by TCDD: gene expression analysis reveals extracellular matrix modulation.* Toxicol Sci, 2006. **92**(1): p. 254-69.
22. Nasevicius, A. and S.C. Ekker, *Effective targeted gene 'knockdown' in zebrafish.* Nat Genet, 2000. **26**(2): p. 216-20.
23. Kajihara, M., et al., *Isolation, characterization, and expression analysis of zebrafish large Mafs.* J Biochem, 2001. **129**(1): p. 139-46.
24. Schvarzstein, M., et al., *Expression of Zkrml2, a homologue of the Krml1/val segmentation gene, during embryonic patterning of the zebrafish (Danio rerio).* Mech Dev, 1999. **80**(2): p. 223-6.
25. Lepilina, A., et al., *A dynamic epicardial injury response supports progenitor cell activity during zebrafish heart regeneration.* Cell, 2006. **127**(3): p. 607-19.
26. White, J.A., et al., *A zebrafish retinoic acid receptor expressed in the regenerating caudal fin.* Development, 1994. **120**(7): p. 1861-72.
27. Begemann, G., et al., *The zebrafish neckless mutation reveals a requirement for raldh2 in mesodermal signals that pattern the hindbrain.* Development, 2001. **128**(16): p. 3081-94.
28. Krens, S.F., et al., *ERK1 and ERK2 MAPK are key regulators of distinct gene sets in zebrafish embryogenesis.* BMC Genomics, 2008. **9**: p. 196.
29. Poleo, G., et al., *Cell proliferation and movement during early fin regeneration in zebrafish.* Dev Dyn, 2001. **221**(4): p. 380-90.
30. Raya, A., et al., *Activation of Notch signaling pathway precedes heart regeneration in zebrafish.* Proc Natl Acad Sci U S A, 2003. **100 Suppl 1**: p. 11889-95.
31. Lee, Y., et al., *Fgf signaling instructs position-dependent growth rate during zebrafish fin regeneration.* Development, 2005. **132**(23): p. 5173-83.
32. Mey, J., et al., *Retinoic acid synthesis by a population of NG2-positive cells in the injured spinal cord.* Eur J Neurosci, 2005. **21**(6): p. 1555-68.

33. Allen, S.P., M. Maden, and J.S. Price, *A role for retinoic acid in regulating the regeneration of deer antlers.* Dev Biol, 2002. **251**(2): p. 409-23.
34. Rinkevich, Y., et al., *Systemic bud induction and retinoic acid signaling underlie whole body regeneration in the urochordate Botrylloides leachi.* PLoS Biol, 2007. **5**(4): p. e71.
35. Brockes, J.P., *Retinoic acid and limb regeneration.* J Cell Sci Suppl, 1990. **13**: p. 191-8.
36. Brockes, J.P., *Retinoid signalling and retinoid receptors in amphibian limb regeneration.* Biochem Soc Symp, 1996. **62**: p. 137-42.
37. Geraudie, J. and P. Ferretti, *Correlation between RA-induced apoptosis and patterning defects in regenerating fins and limbs.* Int J Dev Biol, 1997. **41**(3): p. 529-32.
38. Geraudie, J., et al., *Caudal fin regeneration in wild type and long-fin mutant zebrafish is affected by retinoic acid.* Int J Dev Biol, 1995. **39**(2): p. 373-81.
39. Geraudie, J., et al., *Is exogenous retinoic acid necessary to alter positional information during regeneration of the fin in zebrafish?* Prog Clin Biol Res, 1993. **383B**: p. 803-14.
40. Viviano, C.M. and J.P. Brockes, *Is retinoic acid an endogenous ligand during urodele limb regeneration?* Int J Dev Biol, 1996. **40**(4): p. 817-22.
41. Kim, W.S. and D.L. Stocum, *Retinoic acid modifies positional memory in the anteroposterior axis of regenerating axolotl limbs.* Dev Biol, 1986. **114**(1): p. 170-9.
42. Stocum, D.L. and K. Crawford, *Use of retinoids to analyze the cellular basis of positional memory in regenerating amphibian limbs.* Biochem Cell Biol, 1987. **65**(8): p. 750-61.
43. Mic, F.A., I.O. Sirbu, and G. Duester, *Retinoic acid synthesis controlled by Raldh2 is required early for limb bud initiation and then later as a proximodistal signal during apical ectodermal ridge formation.* J Biol Chem, 2004. **279**(25): p. 26698-706.
44. Gibert, Y., et al., *Induction and prepatterning of the zebrafish pectoral fin bud requires axial retinoic acid signaling.* Development, 2006. **133**(14): p. 2649-59.
45. Kian Tee, M., et al., *Estradiol and selective estrogen receptor modulators differentially regulate target genes with estrogen receptors alpha and beta.* Mol Biol Cell, 2004. **15**(3): p. 1262-72.
46. Jordan, V.C., *Selective estrogen receptor modulation: concept and consequences in cancer.* Cancer Cell, 2004. **5**(3): p. 207-13.
47. Wang, J.C., et al., *Novel arylpyrazole compounds selectively modulate glucocorticoid receptor regulatory activity.* Genes Dev, 2006. **20**(6): p. 689-99.

Acknowledgement

We would like to thank Anne-Marie Girard from the Center for Gene Research and Biotechnology at Oregon State University for her valuable assistance. The vascular specific fli directed EGFP transgenic fish were kindly provided by Dr. Brant Weinstein of the Unit on Vertebrate Organogenesis at NIH, Bathesda, MD. The *Tg(hsp70l:tcf3-GFP)* line was obtained from ZIRC (P40 RR12546). These studies were supported in part by NIEHS grants ES10820, ES00210, and ES03850, NSF #0641409, Oregon Medical Research Foundation grant and a pre-doctoral fellowship from the American Heart Association (LKM).

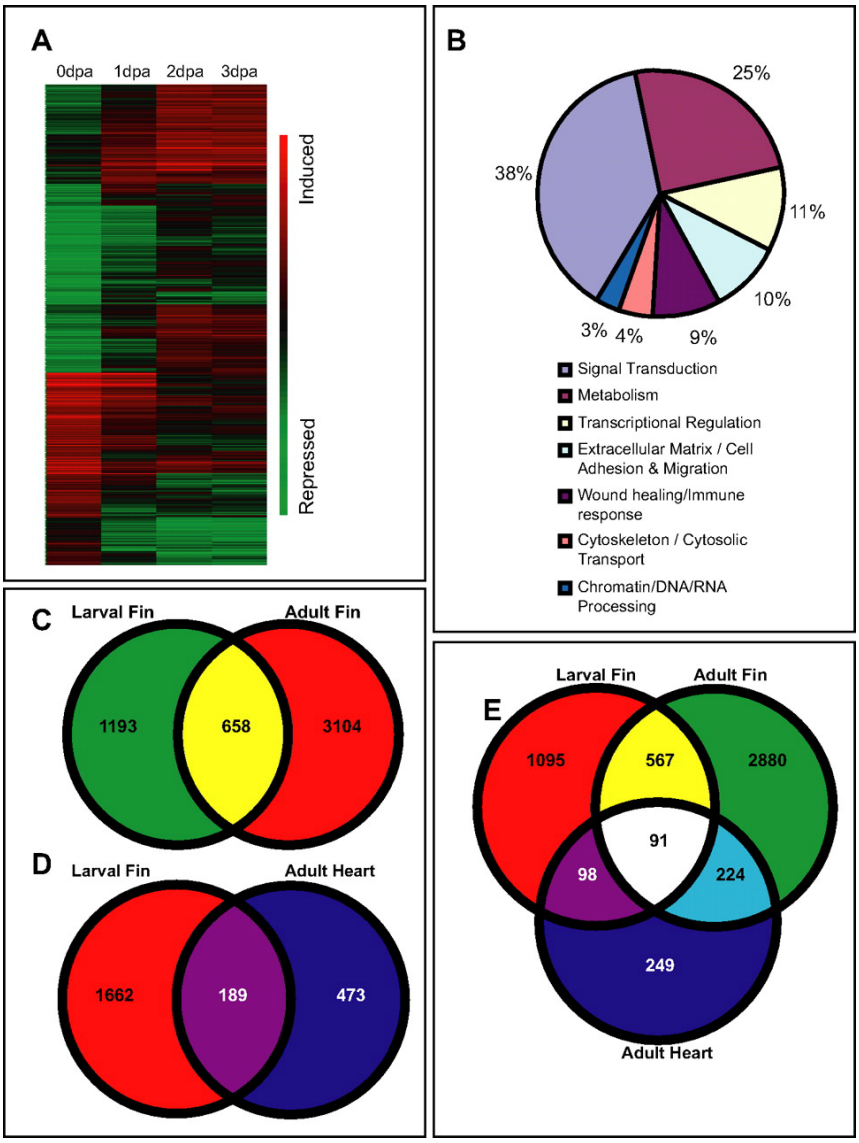

Figure 2- 1. Comparative genomic analysis during zebrafish generation

A) Heat map illustrating the changes in gene expression during the progression of larval fin regeneration. Non-amputated fin tissue at 2dpf (0 dpa) was used as the control to compare with the regenerating fin at 1, 2 and 3 dpa. **B)** The genes that were at least 2 fold differentially expressed were grouped based on the known function of the proteins. Comparative gene expression profiling was performed between larval fin, adult fin and adult heart regeneration systems in zebrafish. The Venn diagram comparing the genes that were modulated during regeneration between the **C)** larval and the adult fin regeneration, **D)** larval fin and the adult heart regeneration and **E)** larval fin, adult fin and adult heart regeneration models.

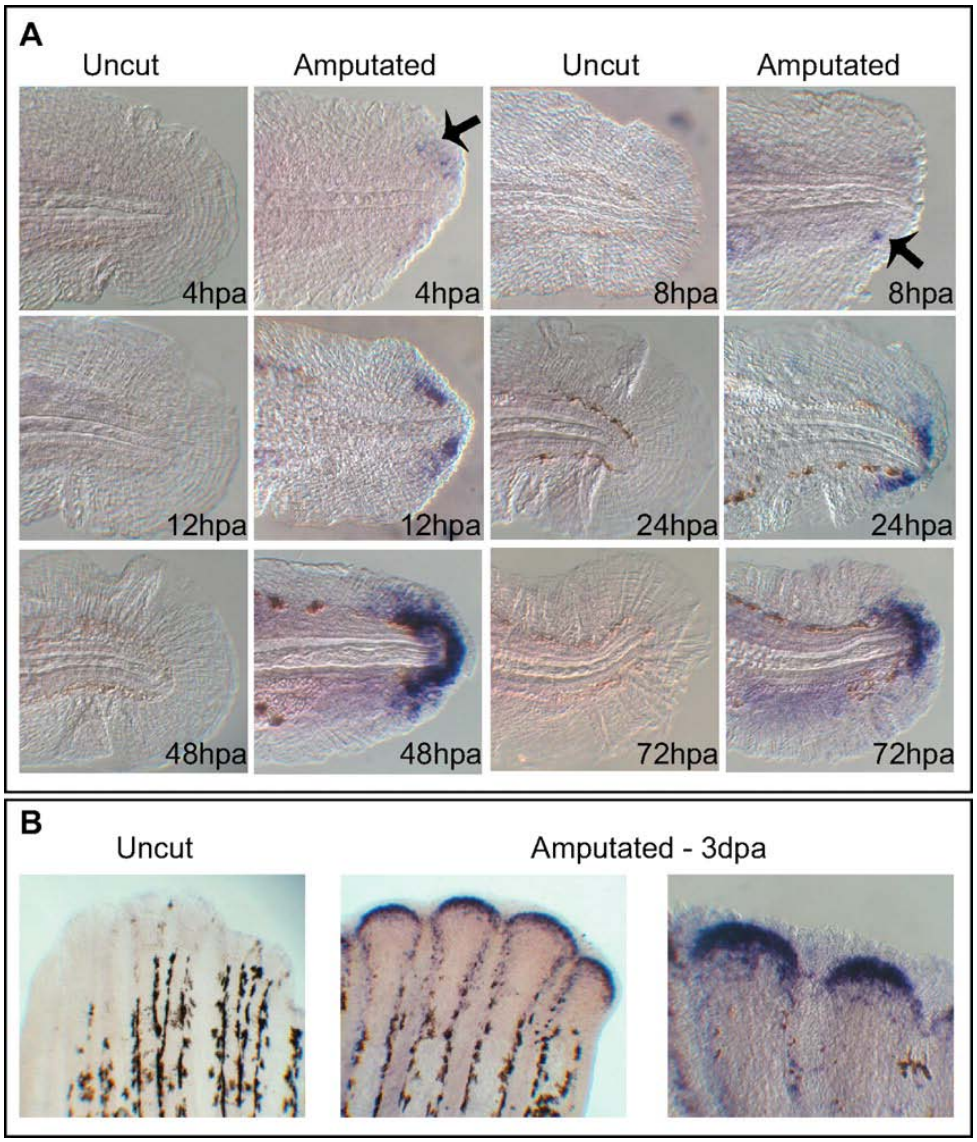

Figure 2- 2. In situ localization of raldh2 in the larval and adult regenerating fin tissue.

A) The mRNA localization of *raldh2* was performed in the regenerating fin tissue at various time points in the larval fin tissue. The expression was detected in the larval regenerate as early as 4 hpa and continuously till 3 dpa. The *raldh2* is clearly expressed beneath the wound epithelium at 4 & 8 hpa and in the blastema region at 12 hpa and 24 hpa. Similar to the microarray and qRT-PCR data, *raldh2* is highly expressed at 2 dpa when compared to the other time points. **B)** The expression of *raldh2* is present in the distal blastema region in the adult regenerating fin at 3 dpa and the transcript is completely absent in the uncut adult fin.

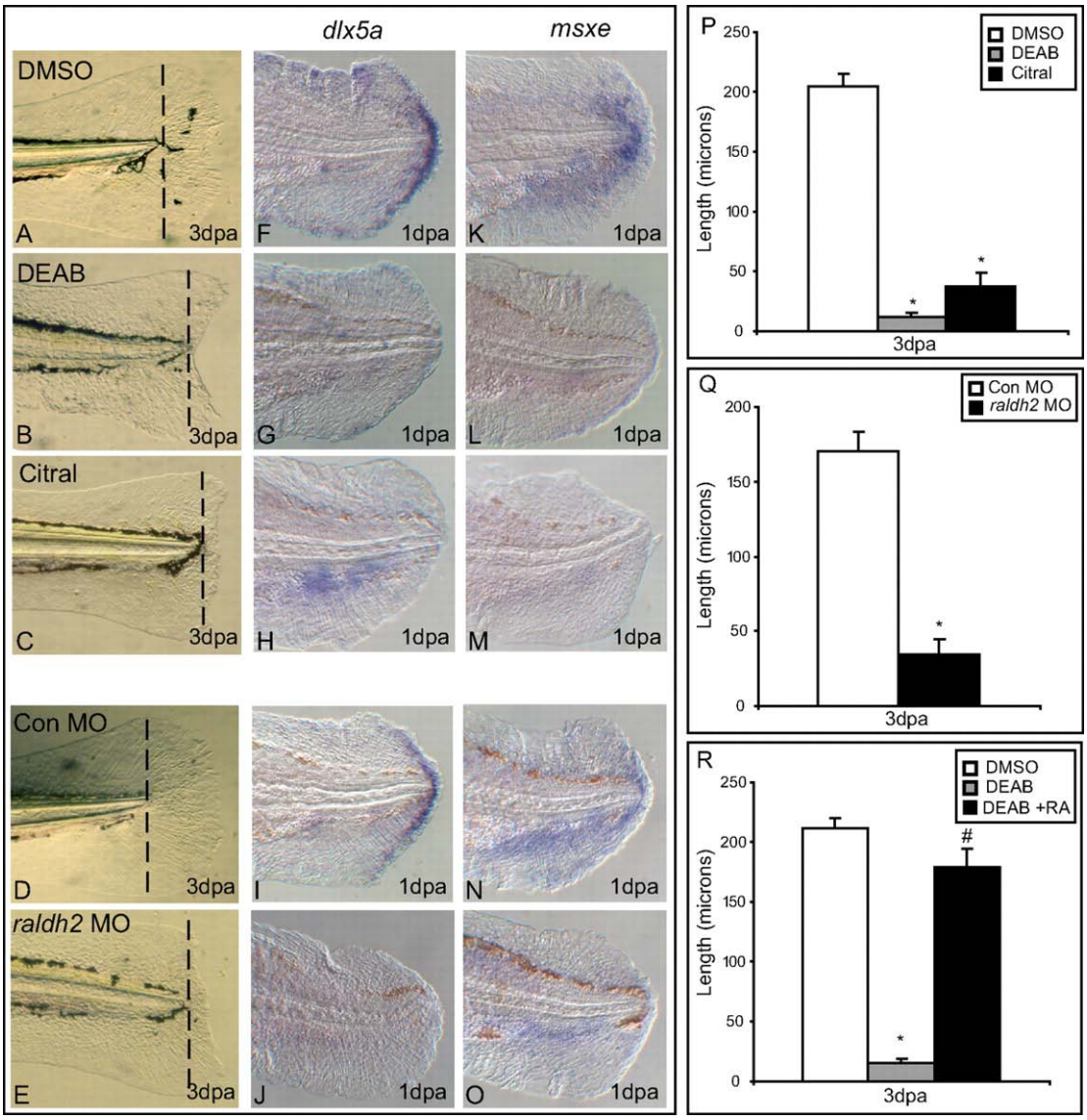

Figure 2- 3. Inhibition of RA signaling impairs wound epithelium and blastema formation and blocks fin regeneration.

A, B, C) The caudal fin of two day old larvae were amputated and exposed to vehicle, DEAB or Citral and the regeneration potential was assessed at 3 dpa. DEAB and Citral exposure completely blocked regenerative progression. **D, E)** Control and *raldh2* morphants were amputated and allowed to grow for 3 days at 28°C. *raldh2* repression impaired regeneration. The expression of wound epithelium marker *dlx5a* and blastema marker *msxe* were assessed in the regenerating fin at 1 dpa by *in situ* hybridization in the vehicle, DEAB and Citral exposed larvae. **(G, H, L, M)** DEAB and Citral exposed larvae failed to express *dlx5a* or *msxe* when compared with the vehicle exposed larvae

(F, K,). The expression of *dlx5a* and *msxe* in the regenerating fin at 1 dpa were highly reduced in the *raldh2* morphants **(N, O)** in comparison with the standard control morphants **(I, J). (P, Q)** Regenerative growth was quantified by measuring the distance from the plane of amputation to the tip of regenerating tissue (n=6 representative images). Both DEAB and Citral exposed larvae and the *raldh2* morphants had significantly less regenerative growth ($p < 0.001$). The respective values represent the mean $\pm$ S.E.M and the * sign refers to the significant difference statistically (One Way ANOVA). **(R)** Co-exposure of RA with DEAB rescued the inhibition of regeneration, and there was statistical difference in regeneration between DEAB alone and RA+DEAB (#; $p < 0.001$). All these experiments were conducted multiple times and the images are representative of more than 50 animals.

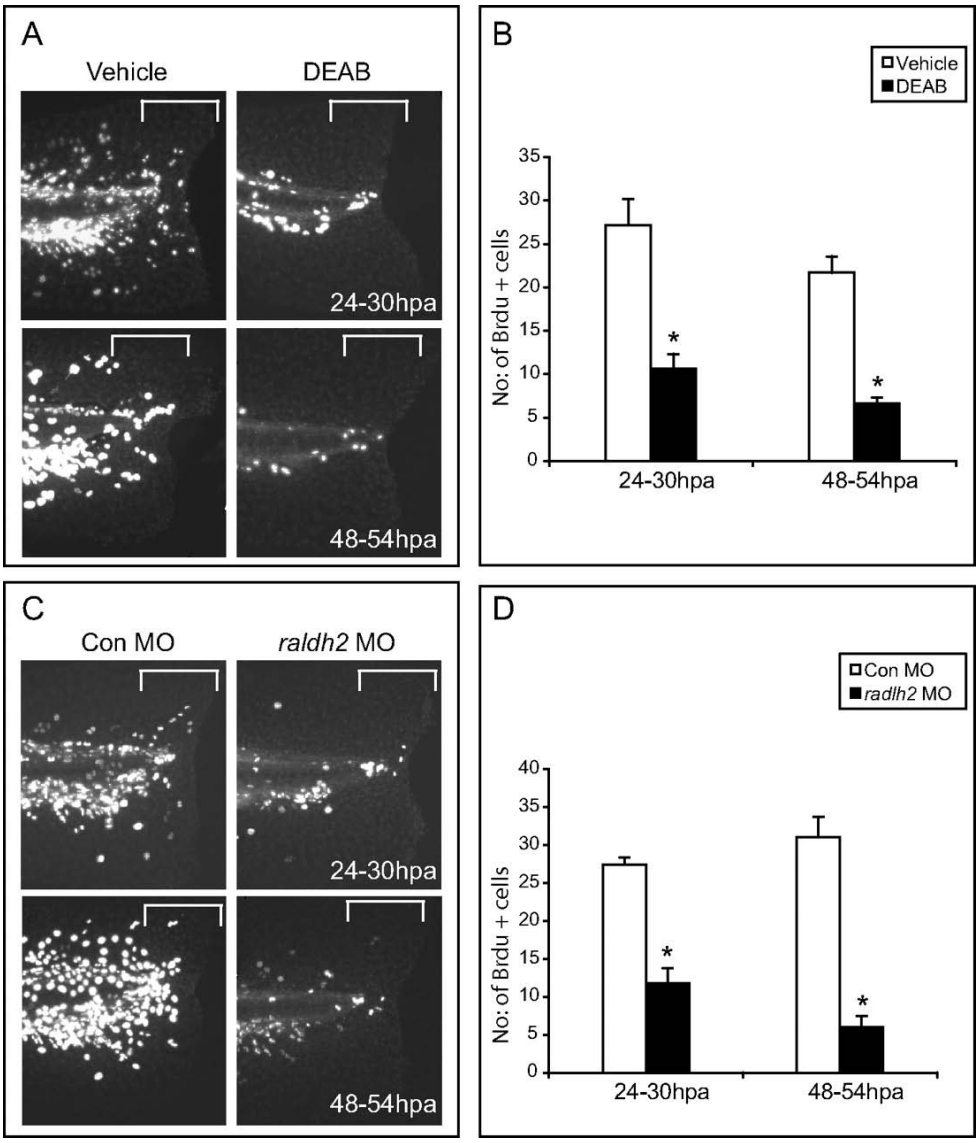

Figure 2- 4. Inhibition of RA signaling impacts cell proliferation during larval fin regeneration.

A) The amputated larvae exposed to vehicle or DEAB and Citral were incubated with Brdu at 24-30 and 48-54 hpa. The bracket represents the area analyzed for quantifying the proliferating cells. **B)** Cell proliferation was quantified between vehicle or DEAB (n=7) and Citral (n=9) exposed larvae. The respective values represent the mean $\pm$ S.E.M (One way ANOVA and Tukey method). The Brdu labeled cells were significantly reduced in DEAB and Citral exposed larvae at 24-30 and 48-54 hpa when compared with the vehicle ($p < 0.001$). **C)** The control and *raldh2* morphants were amputated and Brdu assay was performed as described above. **D)** Quantification of the cell proliferation between control and *raldh2* morphants. There was significant reduction in

the number of proliferating cells in the *raldh2* morphants at both 24-30 and 48-54 hpa when compared to the control morphants ($p < 0.001$). All the parameters were measured using the Image Pro-Plus software (Media Cybernetics, Silver Spring, MD).

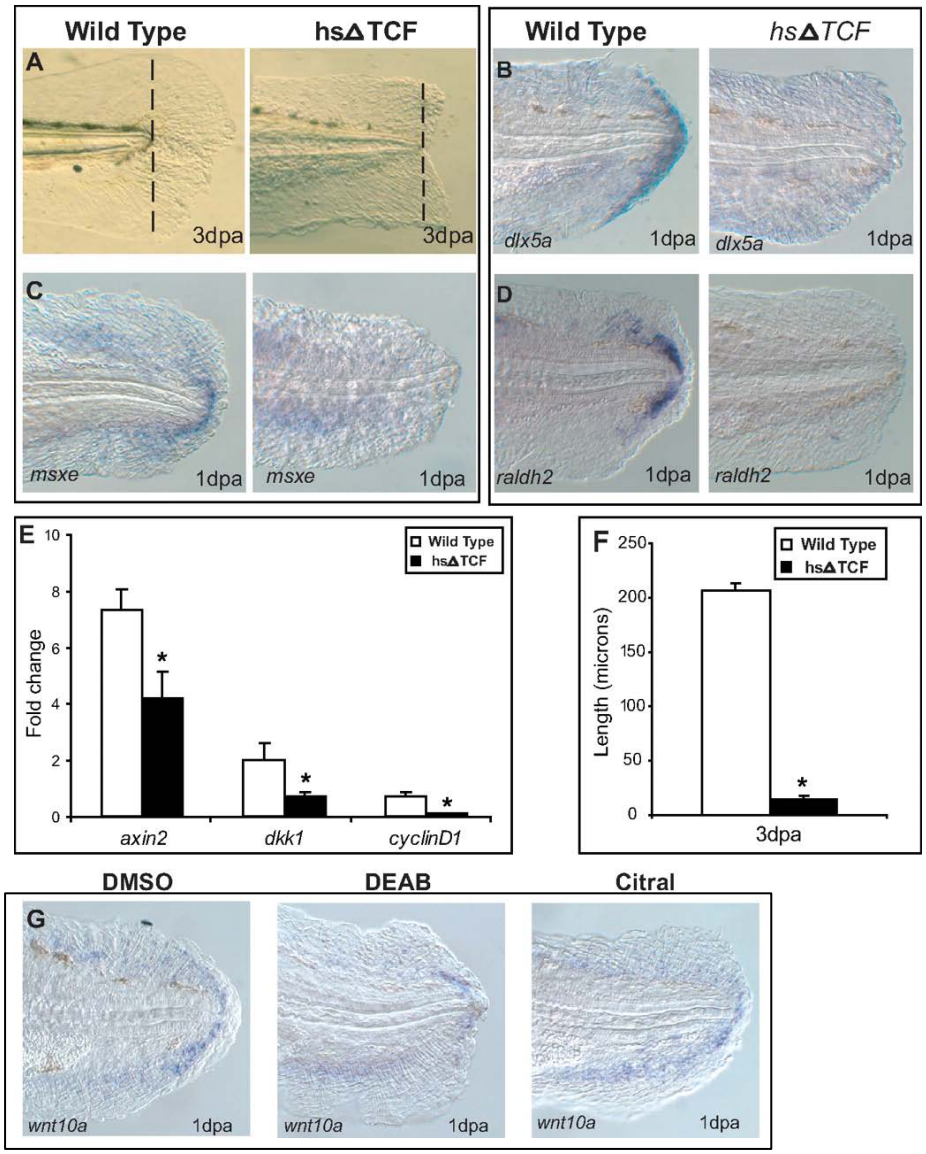

Figure 2- 5. Raldh2 expression during fin regeneration is controlled by Wnt Signaling.

Two day old wild type or homozygous *Tg(hsp70l:tcf3-GFP)* larvae were heat shocked at 37°C for 2 hours followed by amputation. **A)** The *Tg(hsp70l:tcf3-GFP)* larvae had impaired regeneration at 3 dpa. The dotted line indicates the plane of amputation. **B, C)** The expression of *dlx5a* in the wound epithelium and *msxe* in the blastema were not detectable in the *Tg(hsp70l:tcf3-GFP)* larvae. **D)** The expression of *raldh2* was completely lost in the *Tg(hsp70l:tcf3-GFP)* larvae at 1 dpa. **E)** Wnt target genes Axin2 ($p = 0.019$), DKK1 ($p<0.001$), and cyclinD1 ($p<0.001$) were down-regulated in *Tg(hsp70l:tcf3-GFP)* larvae. **F)** By measuring the length of new tissues in heat shocked larvae, regenerative growth is significantly inhibited in *Tg(hsp70l:tcf3-GFP)* larvae (p=

0.002). **G)** The expression of *wnt10a* was comparable between vehicle, DEAB or Citral exposed larvae at 1dpa.

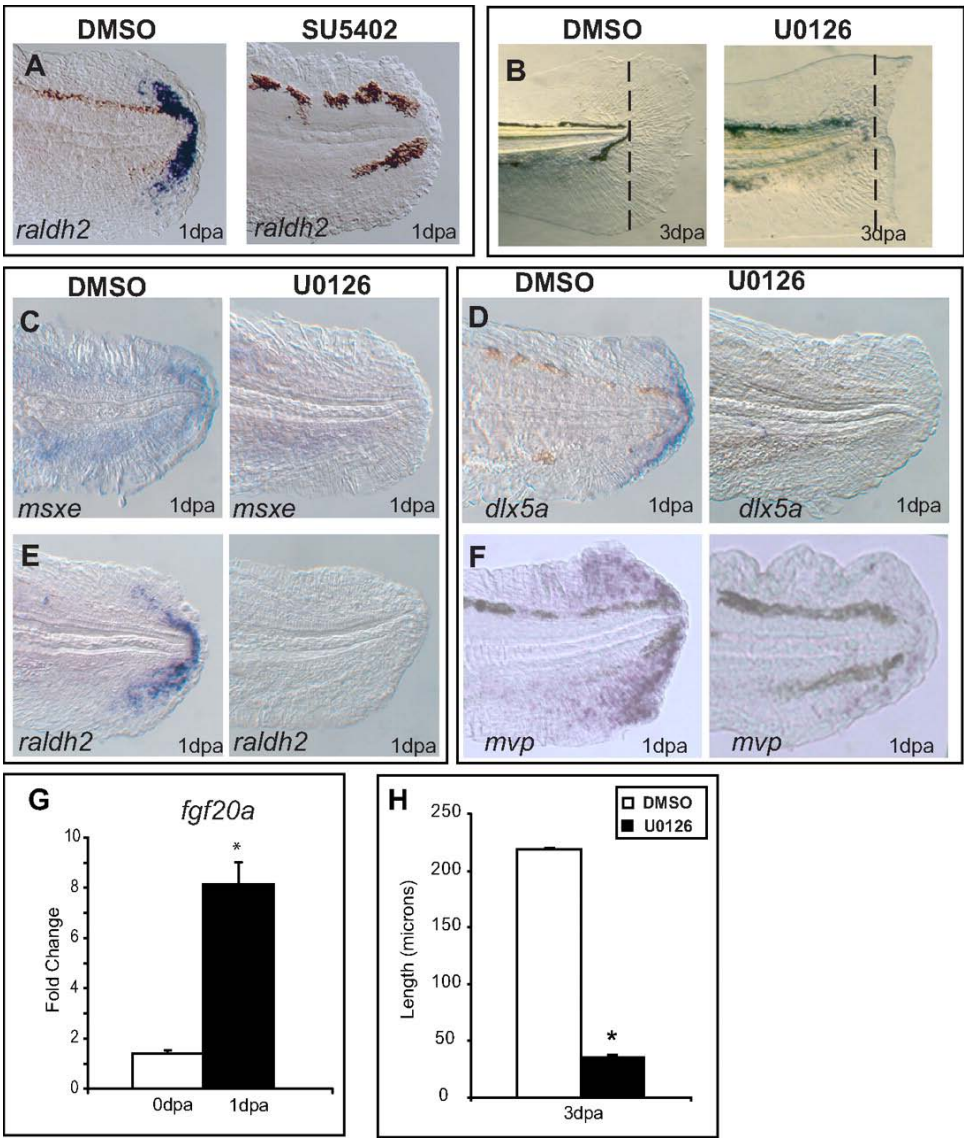

Figure 2- 6. Expression of raldh2 is dependent on FGF and ERK1/2 signaling during fin regeneration.
A) The expression of raldh2 was not present in the SU5402 exposed larval regenerating fin tissue at 1dpa. **B)** The vehicle exposed larvae completely regenerated by 3 dpa, whereas, U0126-exposed larvae failed to regenerate. **C, D)** The wound epithelium marker *dlx5a* and blastema marker *msxe* is not expressed in the U0126 exposed larvae. **E)** *Raldh2* is not expressed in the regenerating fin of U0126-exposed larvae. **F)** The expression of *mvp*, an ERK1/2 target gene was completely lost in U0126 larvae. **G)** Analysis of *fgf20a* in the regenerating fin tissue by qRT-PCR. **H)** By measuring the length of new fin tissue, it is clear that regeneration is significantly inhibited in U0126 exposed larvae ($p<0.001$)
.

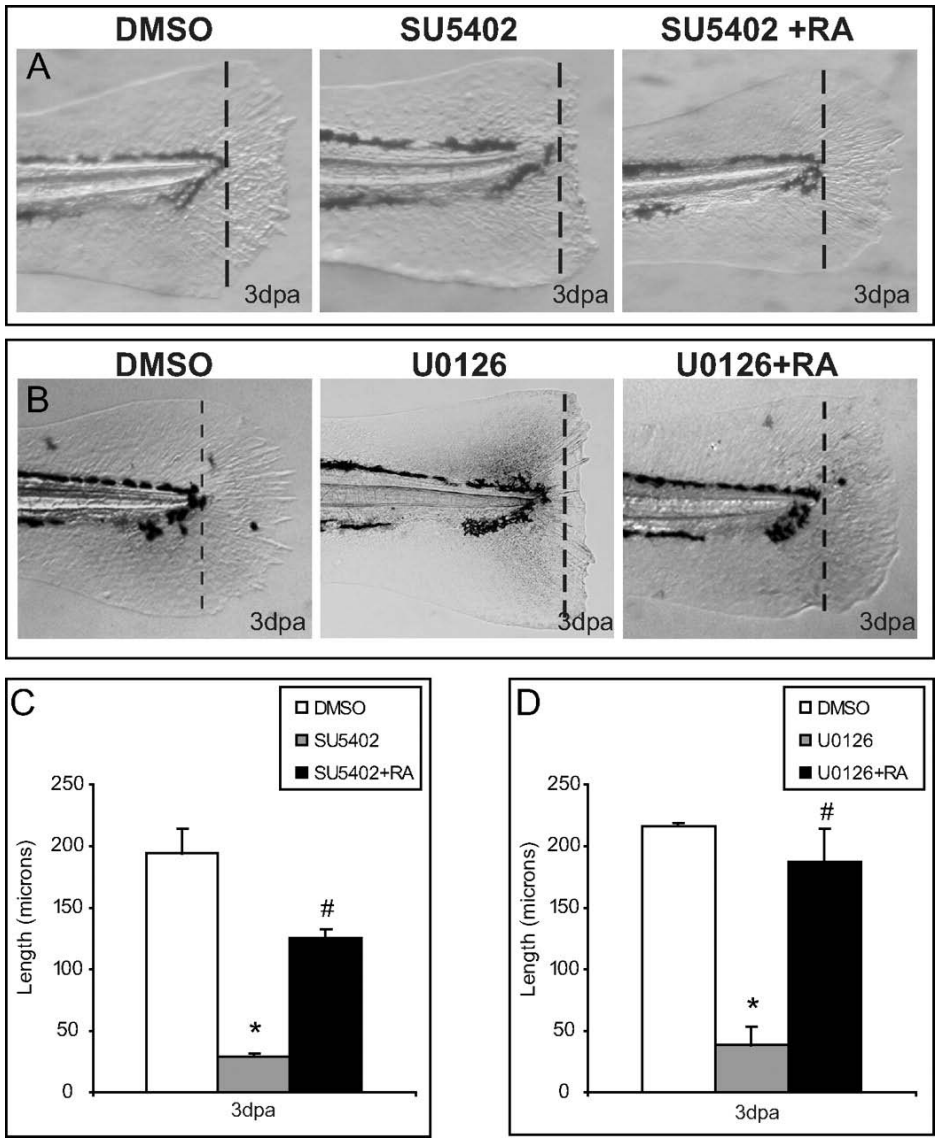

Figure 2- 7. RA is sufficient to rescue SU5402 and U0126 mediated inhibition of regeneration.

A) The 2dpf larvae were amputated and exposed to vehicle, SU5402, SU5402+RA. Co-exposure of SU5402 and RA rescued the impairment of regeneration (n = 31/48). **B)** Co-exposure of 2dpf amputated larvae with U0126 and RA rescued the U0126 mediated inhibition of regeneration (n = 36/46). **C, D)** Both SU5402 and U0126 mediated impairment of regeneration was rescued with RA (One Way ANOVA; #; $p<0.001$).

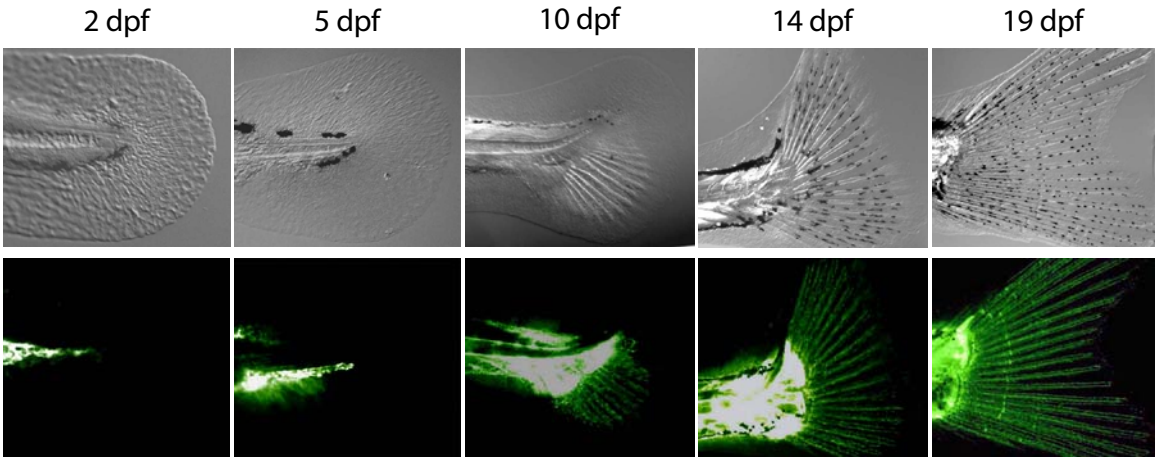

Figure 2-S 1. Fin Morphogenesis.
The development of the caudal fin was assessed and images were acquired periodically from 2-19dpf. The transgenic line (*Fli*) was used to analyze the development of blood vessels in the caudal fin.

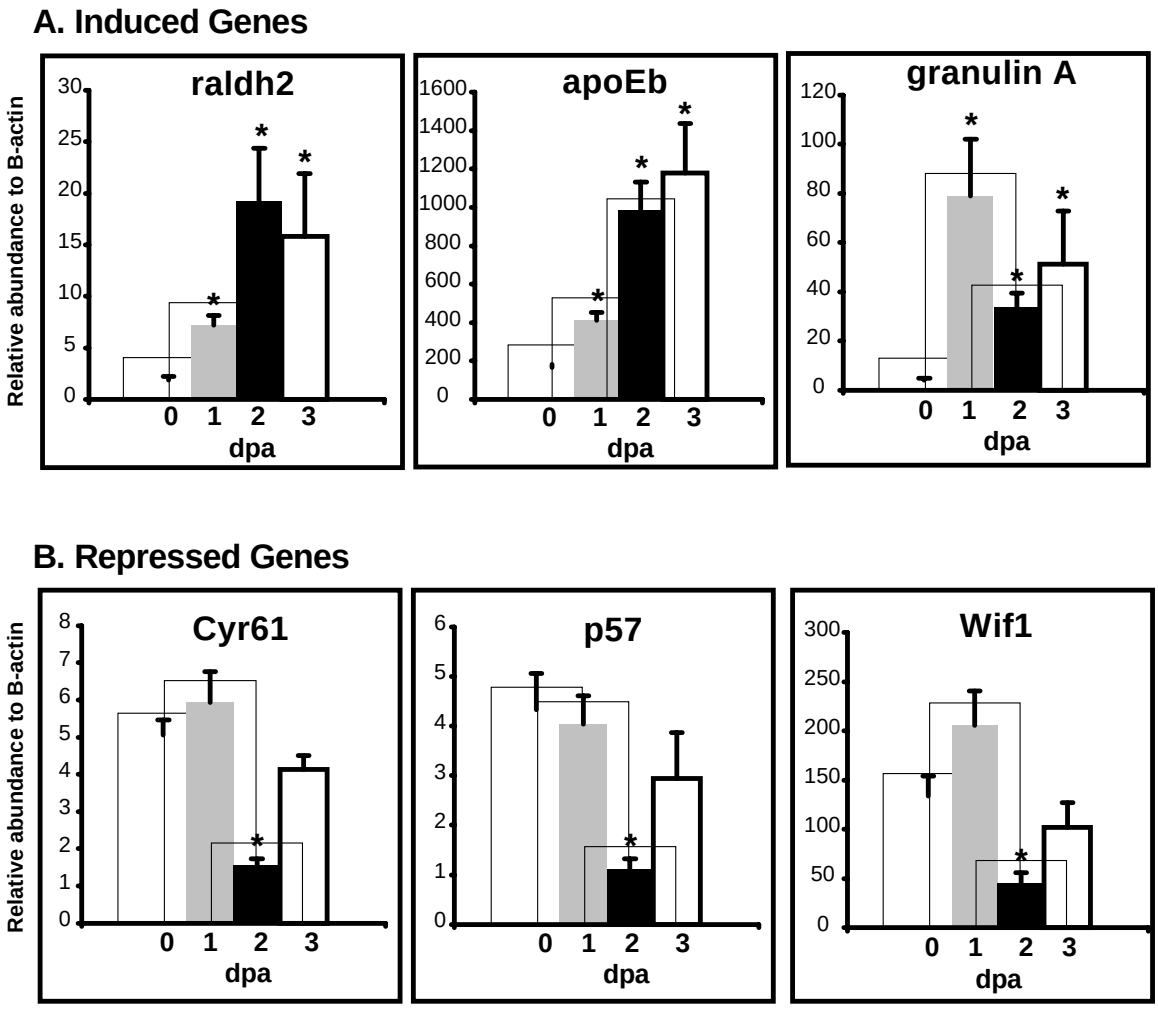

Figure 2-S2. Validation of genes by quantitative real time PCR (qRT-PCR).
A list genes that were commonly expressed during regeneration between the three different regeneration models were confirmed by qRT-PCR with the larval regenerating fin tissue. qRT-PCR was conducted using gene specific primers for *raldh2, apoEb, granulinA*, *cyr61, p57* and *wif1*. The abundance of the message levels were normalized to β-actin expression. The expression of *raldh2* ($p < 0.002$), *apoEb* ($p < 0.001$), *granulinA* ($p < 0.001$) were significantly induced in all the three regeneration time points and *cyr61* ($p < 0.001$), *p57* ($p < 0.010$) and *wif1* ($p < 0.005$) were statistically significant at 2 dpa only. The respective values represent the mean ± S.E.M. (One Way ANOVA, n=3).

Table 2-S1. List of selected genes that were at least 2.5 fold differentially abundant at any regenerating time point when compared to 0 dpa during larval fin regeneration.

Gene	Affymetrix ID	Fold Change 1 DPA	2 DPA	3DPA
Wound healing/Immune response				
cathepsin L2	Dr.15507.2.A1_at	202.16	87.16	106.55
granulin 2	Dr.4748.1.S1_at	11.71	33.73	19.66
cathepsin S	Dr.24219.5.S1_at	11.35	4.95	4.53
complement component 4B proprotein	Dr.12491.1.A1_at	11.30	17.33	26.12
lactotransferrin	Dr.1889.1.S1_at	9.88	2.39	2.72
granulin A	Dr.5809.1.A1_at	9.19	3.49	4.85
legumain	Dr.24341.1.S1_at	5.22	3.08	2.88
socs-3	Dr.6431.1.S1_at	5.10	14.54	8.92
complement component 6	Dr.16392.1.A1_at	3.60	4.65	5.54
cathepsin C	Dr.4782.1.S1_at	3.30	2.51	2.36
TCIRG1	Dr.3804.2.A1_a_at	2.99	2.47	2.17
galectin 9	Dr.4573.1.A1_at	2.76	4.02	3.24
cathepsin B	Dr.3374.2.S1_at	2.75	2.17	2.27
eosinophil peroxidase	Dr.9478.3.S1_a_at	2.68	2.17	1.62
Napsin 1 precursor	Dr.19238.1.S1_at	2.56	2.90	2.46
Galectin 8, isoform b	Dr.25862.1.A1_at	2.38	1.83	1.50
cathepsin K	Dr.4048.1.S1_at	2.25	4.41	3.63
cathepsin L	Dr.19902.1.S1_at	2.14	3.77	2.85
granulin 1	DrAffx.2.25.A1_at	2.08	4.02	2.52
TFPI	Dr.20029.1.A1_at	1.91	3.77	3.33
thromboxane A synthase 1	Dr.9661.1.A1_at	1.55	2.72	2.40
annexin A1	Dr.26404.1.S1_at	-2.08	-2.34	-2.75
interferon-related developmental regulator 1	Dr.5617.1.A1_at	-2.52	-1.64	-1.70
Thy-1 cell surface antigen	Dr.20019.1.S1_at	-2.54	-1.36	-1.48
Myelin and lymphocyte protein	Dr.1248.1.S1_at	-2.66	-3.11	-2.65
Signal Transduction				
raldh2	Dr.5206.1.S1_at	11.75	49.47	26.03
ms4a4a	Dr.22334.1.S1_at	8.39	21.60	15.68
CBFA2T1	Dr.10668.1.S2_at	7.21	2.40	2.87
protease, serine, 12	Dr.26268.1.A1_at	6.90	3.19	3.65
glia maturation factor, gamma	Dr.18605.1.A1_at	6.37	3.88	3.18
F-box only protein 25	Dr.25520.1.A1_at	4.44	13.67	11.31
fgf20a	Dr.17781.1.A1_at	4.29	10.41	4.57
IGFBP1	Dr.8587.1.A2_at	4.29	5.31	2.98
SAMSN1	Dr.919.1.A1_at	4.22	2.62	2.22
interferon regulatory factor 1	Dr.914.1.A1_a_at	4.04	3.27	25.85
PSME1	Dr.8135.1.S1_at	4.03	6.85	6.39
protein kinase C-like 2	Dr.16985.1.A1_at	3.15	1.89	1.95
PSME2	Dr.8134.1.S1_at	2.91	3.67	4.29
Apoptosis-inducing protein	Dr.13076.1.S1_at	2.88	7.48	5.60
ring finger protein 11	Dr.26465.1.S1_at	2.74	6.32	6.38
phospholipase C, gamma 2	Dr.11512.1.A1_at	2.60	3.57	4.44
glutamate receptor, ionotropic, kainate 2	Dr.3211.1.A1_at	2.60	2.11	1.91
rasl11b	Dr.2953.1.S1_at	2.59	3.11	1.64
SPRY domain-containing SOCS box protein 4	Dr.10211.1.A1_at	2.58	2.83	2.74
Serine/threonine protein kinase VRK2	Dr.15781.1.S1_at	2.55	2.76	3.78
arrestin domain containing 2	Dr.2047.1.A1_at	2.55	6.99	5.67
B-cell translocation gene 1	Dr.25187.3.S1_at	2.49	3.24	2.03
MPP1	Dr.1842.1.A1_at	2.48	3.88	3.46
mesoderm specific transcript	Dr.8060.1.S1_at	2.47	3.24	3.14
EIF4EBP3	Dr.4647.1.S1_at	2.38	4.31	3.40

pyruvate kinase, muscle	Dr.7952.1.S1_at	2.38	2.21	1.86
BCL2-like 10	Dr.15057.1.S2_at	2.35	8.03	4.88
G protein-coupled receptor 137ba	Dr.6999.1.A1_at	2.35	2.38	2.55
PSMA6	Dr.10120.1.S1_at	2.35	4.17	3.93
PSMB7	Dr.15777.1.A1_at	2.35	4.20	6.93
NR4A1	Dr.9243.1.A1_at	2.27	7.08	4.60
Ubiquitin-conjugating enzyme E2H	Dr.17520.1.S1_at	2.27	3.56	3.13
pleckstrin homology domain containing, family B (evectins) member 2	Dr.15849.1.S1_at	2.26	3.66	2.95
GADD45B	Dr.1378.1.S1_at	2.14	4.94	4.00
ankyrin repeat and SOCS box-containing 8	Dr.26472.1.S1_at	2.12	2.99	3.14
ADP-ribosylation factor-like 4	Dr.11322.1.S1_at	2.12	4.03	3.06
GBP1	Dr.14275.1.A1_at	2.08	3.13	5.89
syndecan binding protein	Dr.1778.1.S1_at	2.07	2.83	2.14
apolipoprotein Eb	Dr.1246.1.S1_at	2.05	3.47	3.17
serum/glucocorticoid regulated kinase	Dr.10320.1.S1_at	2.04	3.13	2.07
GTP cyclohydrolase I feedback regulatory	Dr.12454.1.S1_at	2.01	3.97	4.26
GABARAPL2	Dr.16079.1.S1_at	2.00	3.32	3.22
secernin 3	Dr.7392.1.S1_at	1.99	2.19	2.56
myeloid cell leukemia sequence 1a	Dr.4957.1.S1_at	1.89	2.79	2.73
C-type natriuretic peptide 4	Dr.18242.1.A1_at	1.85	5.60	3.14
Inositol hexakisphosphate kinase 2	Dr.15620.1.S1_at	1.74	3.67	3.81
maf	Dr.10168.1.S1_at	1.70	4.45	3.73
ADP-ribosylation factor-like protein 5B	Dr.15961.1.A1_at	1.68	3.52	2.66
Elongation factor 2 kinase	Dr.523.1.A1_at	1.64	2.56	2.27
dual specificity phosphatase 1	Dr.2413.1.S1_at	1.63	8.85	5.57
2-peptidylprolyl isomerase A	Dr.9654.1.A1_at	1.62	5.03	5.80
Caspase-9 precursor	Dr.16035.1.S1_at	1.58	3.07	2.34
early growth response 1	Dr.10183.1.S2_at	1.54	3.08	4.40
B-cell translocation gene 2	Dr.6511.1.S1_at	1.53	4.49	2.53
Ras-related protein Rab-1A	Dr.21919.1.A1_at	1.51	2.55	2.50
dachshund homolog	Dr.3413.1.S1_at	1.51	3.07	2.14
interferon regulatory factor 7	Dr.10428.1.S1_at	1.50	2.46	2.75
Secernin-2	Dr.12696.1.A1_at	1.47	3.72	2.91
Breast cancer associated protein BRAP1	Dr.7929.1.S1_at	1.44	2.70	2.45
inositol polyphosphate phosphatase-like 1	Dr.21368.1.A1_at	1.42	2.42	3.10
lipopolysaccharide-induced TNF factor	Dr.20110.1.S1_at	1.41	2.85	2.21
GADD45G	Dr.11828.1.A1_at	1.40	2.66	1.77
cyclin G2	Dr.20083.1.A1_at	1.38	3.23	2.35
Programmed cell death 4	Dr.14306.1.S1_a_at	1.35	2.67	3.04
bmp5	Dr.10625.1.A1_at	1.33	2.63	2.32
TGF-beta-inducible nuclear protein 1	Dr.10477.1.S1_at	1.30	2.76	2.62
E3 ubiquitin-protein ligase IBRDC2	Dr.17207.1.A1_at	1.29	4.83	3.33
FGF10	Dr.8853.1.S1_at	1.29	2.56	2.41
interleukin-1 receptor-associated kinase 4	Dr.13000.1.S1_at	1.28	3.07	2.44
SERPINE2 protein	Dr.10097.1.S1_at	1.21	1.86	2.60
WNT inhibitory factor 1	Dr.3690.1.S1_at	-1.17	-3.96	-4.29
caveolin 1	Dr.5678.1.S1_s_at	-1.24	-4.87	-3.72
Receptor expression-enhancing protein 2	Dr.16638.1.A1_at	-1.27	-2.61	-2.12
activated leukocyte cell adhesion molecule	Dr.20912.1.S2_at	-1.31	-3.41	-3.13
DLG7	Dr.20429.2.S1_a_at	-1.33	-3.30	-2.66
Transgelin-3	Dr.3966.1.A1_at	-1.34	-1.82	-2.68
fgfr4	Dr.409.1.S1_at	-1.37	-2.47	-3.20
cyclin D1	Dr.24753.1.S2_at	-1.37	-2.68	-1.93
calmodulin 3b	Dr.17933.1.S1_at	-1.38	-2.58	-2.35
cardiomyopathy associated 1	Dr.152.1.A1_at	-1.42	-4.40	-4.65
ODZ1	Dr.8281.1.S1_at	-1.42	-3.11	-3.37

GA17 protein	Dr.25580.1.S1_at	-1.47	-1.99	-2.63
neuropilin 1a	Dr.26440.1.S1_at	-1.58	-3.00	-2.86
p57	Dr.3502.1.S1_at	-1.61	-3.77	-4.65
elavl3	Dr.20167.3.S1_at	-1.64	-6.38	-5.03
protein kinase C, beta 1	Dr.15087.1.A1_at	-1.65	-2.98	-3.96
IMP-1	Dr.9189.1.A1_at	-1.78	-2.21	-3.00
pou23	Dr.21068.1.S1_s_at	-1.95	-3.18	-2.79
Ictacalcin	Dr.25140.5.S1_at	-1.97	-2.05	-3.90
Benzodiazapine receptor	Dr.20778.1.S1_at	-1.99	-2.60	-4.03
Oxidative stress induced growth inhibitor 2	Dr.6154.1.A1_at	-2.07	-7.57	-13.06
heat shock 70kDa protein 12A	Dr.15969.1.A1_at	-2.08	-2.98	-2.91
kdelr2	Dr.6631.1.A1_at	-2.11	-5.27	-5.12
pgrmc2	Dr.2911.1.S1_at	-2.14	-4.06	-4.21
stromal interaction molecule 1	Dr.25937.1.A1_at	-2.14	-2.42	-2.72
hey2	Dr.1899.3.A1_at	-2.20	-2.85	-2.89
lipoprotein lipase	Dr.20185.1.S1_at	-2.41	-3.32	-3.05
hsp90a	Dr.610.1.S1_at	-2.52	-11.72	-8.25
Purkinje cell protein 4 like 1	Dr.17014.1.S1_at	-2.52	-2.32	-2.35
calpain 2, (m/II) large subunit	Dr.10119.1.A1_at	-2.67	-3.52	-3.48
ITPK1	Dr.22569.1.S1_at	-2.75	-1.62	-1.33
cryptochrome 1	Dr.10329.1.S1_at	-2.88	-1.88	-2.15
calpain 9	Dr.4236.1.S1_at	-2.99	-4.51	-2.94
GTP cyclohydrolase 1	Dr.14668.1.S1_at	-3.05	-4.51	-8.58
insulin induced gene 1	Dr.19560.1.S1_at	-3.82	-2.15	-3.22
cryptochrome 2	Dr.10332.1.S1_at	-4.56	-5.24	-5.10
anterior gradient 2 homolog	Dr.25277.1.S1_at	-4.79	-8.07	-10.02
ppp1r3b	Dr.4453.1.S1_at	-8.78	-8.99	-10.89
ECM/Cell Adhesion & Migration				
versican	Dr.9682.1.A1_at	8.31	5.76	7.11
fibronectin 1b	Dr.24233.1.S1_at	4.94	3.12	2.63
col17a1	Dr.10041.1.A1_at	4.44	2.77	2.95
meprin A, beta	Dr.17470.1.S1_at	3.91	2.29	1.87
clusterin	Dr.20131.2.A1_at	3.41	6.06	5.06
Olfactomedin-like protein precursor	Dr.1154.1.S1_at	2.93	4.54	5.82
TIMP2	Dr.15281.1.A1_at	2.37	3.88	2.89
cartilage oligomeric matrix protein	Dr.1089.1.S1_at	2.28	2.60	4.06
FREM2	Dr.3300.2.A1_at	2.15	3.41	1.54
SPON2	Dr.563.1.S1_at	2.13	2.86	4.17
AAMP protein	Dr.11399.1.A1_at	2.07	2.31	2.81
Latexin	Dr.23294.1.S1_at	1.95	4.59	4.70
transmembrane 7 superfamily member 1	Dr.14044.1.A1_at	1.95	2.86	2.35
mmp14	Dr.23324.1.A1_at	1.86	3.46	3.65
lysyl oxidase	Dr.11427.1.S1_at	1.85	8.70	12.99
Membrane component, chromosome 11, surface marker 1.	Dr.941.1.S1_at	1.32	2.58	1.93
mmp14a	Dr.4229.1.S1_at	1.29	2.90	2.85
col1a2	Dr.5521.1.S1_at	-1.16	-3.58	-3.67
spondin 1b	Dr.565.1.S1_at	-1.33	-2.88	-3.82
fibronectin 1	Dr.19965.1.S1_at	-1.38	-3.44	-2.30
netrin 1	Dr.545.1.S1_at	-1.61	-4.17	-4.09
desmoplakin	Dr.4929.1.A1_at	-1.76	-2.35	-2.39
semaphorin 3aa	Dr.5060.1.A1_at	-1.89	-2.46	-2.71
EFEMP2	Dr.4543.1.S1_at	-2.73	-1.78	-3.86
Advillin	Dr.26109.1.A1_at	-2.98	-2.23	-3.23
claudin 9	Dr.12596.1.S1_at	-5.20	-8.21	-5.76
contactin 4	Dr.21041.1.S1_at	-9.99	-4.15	-4.15

Transcriptional Regulation				
krml2	Dr.23470.1.S1_s_at	8.82	4.67	4.88
krml2.2	Dr.8198.1.A1_at	7.67	4.98	4.80
spi1	Dr.7612.1.A1_at	5.31	2.45	2.30
junb	Dr.10326.1.S1_at	4.55	10.72	7.93
E74-like factor 3	Dr.1909.1.S1_at	3.62	5.10	4.66
Fos-related antigen 2	Dr.10410.1.A1_at	3.52	7.73	5.94
junbl	Dr.737.1.A1_at	2.98	4.65	3.58
stat1	Dr.257.1.A1_at	2.63	6.66	7.31
Kruppel-like factor 2a	Dr.3448.1.S1_at	2.55	6.29	7.80
sox4a	Dr.20124.1.A1_at	2.54	1.58	1.82
fos	Dr.12986.1.A1_a_at	2.37	6.88	5.71
histone deacetylase 9	Dr.14159.1.A1_at	2.23	3.02	3.59
suppressor of Ty 3 homolog	Dr.14718.1.A1_at	2.18	3.65	3.36
homeo box C12	Dr.10124.1.A1_at	2.00	3.83	2.52
transcription elongation factor A (SII), 3	Dr.15634.1.S1_at	1.49	3.21	1.48
sox9b	Dr.11850.1.S2_at	1.39	3.49	3.23
sox21b	Dr.14800.1.A1_at	-1.31	-3.53	-2.98
deltaD	Dr.20958.1.S1_at	-1.32	-5.99	-4.61
hoxb3a	Dr.5779.1.S1_at	-1.32	-5.90	-6.29
foxa	Dr.588.1.S1_at	-1.36	-3.44	-3.62
sox3	Dr.1691.12.S1_at	-1.38	-1.53	-2.61
hmgb2	Dr.9746.12.S1_at	-1.40	-2.12	-2.78
hoxa2b	Dr.5772.1.S1_at	-1.46	-3.28	-3.48
transcription factor 2, hepatic	Dr.14662.1.S2_at	-1.47	-2.61	-2.13
dmrt2	Dr.8088.1.S1_at	-1.59	-2.98	-3.02
sox19a	Dr.20910.1.S1_at	-1.71	-3.41	-6.28
deltaB	Dr.574.1.S1_at	-1.73	-6.38	-10.78
Kruppel-like factor 2b	Dr.9976.1.S1_at	-1.75	-2.50	-2.93
pou50	Dr.57.1.S1_at	-2.20	-4.27	-4.71
cdx4	Dr.11836.1.S1_at	-2.38	-4.21	-3.96
gastrulation brain homeo box 2	Dr.17548.1.S1_at	-3.38	-7.49	-7.65
endothelial PAS domain protein 1	Dr.25865.1.S1_at	-5.05	-5.27	-6.81
Chromatin/DNA/RNA Processing				
poly(A) binding protein cytoplasmic 1	Dr.12233.1.S1_at	1.59	2.98	2.32
chromodomain helicase DNA binding protein 2	Dr.859.1.S1_at	1.58	1.84	2.63
RNA binding motif protein 25	Dr.2606.1.A1_at	1.55	2.20	3.44
upstream binding transcription factor, RNA polymerase I	Dr.10946.1.A1_at	1.45	2.13	1.89
lamin B1	Dr.25051.1.S2_at	-1.26	-3.82	-3.46
Exportin-1	Dr.12499.1.A1_at	-1.31	-2.70	-2.56
SNRP70	Dr.25566.1.S1_at	-2.00	-2.72	-2.42
poly(A) binding protein cytoplasmic 1	Dr.12233.1.S1_at	1.59	2.98	2.32
chromodomain helicase DNA binding protein 2	Dr.859.1.S1_at	1.58	1.84	2.63
Cytoskeleton/Cytosolic Transport				
keratin 14	Dr.25556.1.S1_at	7.09	3.12	1.96
syntaxin 11	Dr.12309.1.A1_at	3.00	3.57	2.44
MYLIP	Dr.20935.1.S1_at	2.88	4.65	4.69
profilin family, member 4	Dr.16239.1.A1_at	2.17	3.78	3.83
nipsnap homolog 3A	Dr.17452.1.S1_at	1.87	2.18	2.67
Tubulin beta-2A chain	Dr.7928.1.A1_at	-1.26	-3.10	-3.01
secretory carrier membrane protein 5	Dr.19471.1.A1_at	-1.35	-4.12	-3.39
actin, alpha 1	Dr.24891.1.S1_at	-2.02	-4.60	-7.89
periplakin	Dr.9761.1.S1_at	-2.29	-2.69	-2.08
tubulin, alpha 1	Dr.7506.1.A1_at	-2.31	-2.68	-3.14

p76	Dr.349.1.A1_at	-2.59	-2.18	-2.43
envoplakin	Dr.5577.1.A1_at	-4.56	-6.73	-6.42
Metabolism				
ferritin, heavy polypeptide 1	Dr.12425.5.S1_at	14.25	35.56	14.56
Y+L amino acid transporter 1	Dr.18441.1.A1_at	6.43	7.15	6.16
acid phosphatase 5, tartrate resistant	Dr.1508.1.S1_at	5.35	2.34	2.72
Rhesus blood group, B glycoprotein	Dr.12749.1.A1_at	5.27	2.38	3.31
Palmitoyltransferase ZDHHC2	Dr.9870.1.A1_at	4.09	7.09	10.49
glucosamine-6-phosphate deaminase 1	Dr.18431.1.S1_at	4.07	6.57	5.75
argininosuccinate synthetase	Dr.4095.1.A1_at	3.67	2.86	2.32
cytoglobin	Dr.4925.1.S1_x_at	3.53	5.35	4.57
Cytochrome c oxidase subunit 4 isoform 2	Dr.12760.1.A1_at	3.47	2.47	5.61
SLC7A8	Dr.3789.1.A1_at	3.33	2.38	3.05
mpdu1a	Dr.1439.1.S1_at	-3.19	-4.08	-2.98
enolase 2	Dr.13441.1.A1_at	3.18	8.96	4.54
aldose reductase	Dr.6142.1.A1_at	3.18	9.79	7.99
carboxypeptidase N, polypeptide 1	Dr.1128.1.S1_at	2.98	1.77	2.28
UGT1A1	Dr.3029.1.A1_at	2.78	2.63	2.07
Multidrug resistance protein 1	Dr.8645.1.A1_at	2.51	1.70	4.08
SLC15A4	Dr.13966.1.S1_at	2.42	2.97	2.91
carboxypeptidase M	Dr.14571.1.A1_at	2.41	6.42	4.97
uncoupling protein 3	Dr.4905.1.S1_at	2.38	5.95	21.21
carboxypeptidase, vitellogenic-like	Dr.506.1.S1_at	2.33	2.63	2.54
argininosuccinate lyase	Dr.11501.1.S1_at	2.18	2.83	2.56
creatine kinase, muscle	Dr.22156.1.A1_at	2.15	2.69	3.69
CYP27A1	Dr.25700.1.A1_at	2.08	3.57	4.93
ATP6V1E1	Dr.4617.1.A1_at	2.06	2.63	2.20
glutathione peroxidase 2	Dr.8000.1.S1_at	2.01	2.35	3.27
cytochrome b-245, alpha polypeptide	Dr.17749.2.A1_a_at	2.00	2.84	2.57
glycogenin 1	Dr.13604.1.S1_at	2.00	2.85	2.77
Sialin	Dr.15485.1.A1_at	1.99	2.50	2.42
Phytanic acid oxidase	Dr.10186.1.A1_at	1.99	2.18	2.75
lysophospholipase 3	Dr.360.1.A1_at	1.96	3.20	3.02
bckdk	Dr.25159.1.S1_at	1.93	2.60	2.45
cyp3c1	Dr.938.1.S1_at	1.89	3.05	2.79
selenoprotein X, 1	Dr.147.1.A1_at	1.88	2.54	2.51
glutamate-ammonia ligase	Dr.4147.1.S1_at	1.86	5.48	4.78
peptidylprolyl isomerase A (cyclophilin A)	Dr.6264.1.A1_at	1.85	2.65	2.24
ywhabl	Dr.4607.1.A1_at	-1.67	-2.43	-2.76
Malonyl CoA-acyl carrier protein transacylase	Dr.13862.1.S1_at	1.61	5.21	4.14
methionine sulfoxide reductase A	Dr.14650.1.A1_at	1.51	4.79	4.26
slc40a1	Dr.8152.1.S1_at	1.43	2.73	2.26
Intestinal alkaline phosphatase 1	Dr.1104.1.A1_at	1.31	4.55	3.18
slc38a3	Dr.5364.1.A1_at	1.30	2.98	2.62
adenosine monophosphate deaminase 3	Dr.11670.1.S1_at	1.30	2.56	1.66
HSD3B7	Dr.10542.1.S1_at	1.17	2.86	2.87
atp1a1a.2	Dr.10343.1.S1_at	-1.25	-3.67	-3.49
cytochrome c oxidase subunit Vib polypeptide 1	Dr.956.1.S1_at	-1.28	-1.77	-2.58
Troponin I, fast skeletal muscle	Dr.17891.1.S1_at	-1.42	-13.19	-11.69
selenoprotein M	Dr.5565.1.S1_at	-1.43	-1.75	-2.62
alcohol dehydrogenase 8b	Dr.16130.1.S1_at	-1.45	-2.17	-2.54
lactate dehydrogenase B	Dr.4212.1.S1_at	-1.54	-3.10	-3.07
acetyl-CoA acetyltransferase 2	Dr.813.1.S1_at	-1.66	-3.33	-3.45
MTHFD2	Dr.5222.1.S1_at	-1.83	-2.43	-2.90

creatine kinase, mitochondrial 1	Dr.771.1.S1_at	-1.87	-2.73	-4.18
ABCF2	Dr.24208.1.S1_at	-1.87	-2.34	-2.91
atp1a1a.1	Dr.25976.1.A1_at	-2.15	-2.48	-3.13
SLC6A1	Dr.7076.1.A1_at	-2.15	-7.39	-5.74
phosphoserine aminotransferase 1	Dr.11425.1.S1_at	-2.28	-2.44	-3.59
7-dehydrocholesterol reductase	Dr.18226.1.A1_at	-2.51	-2.30	-1.90
cyp51	Dr.1603.1.A1_at	-2.55	-5.83	-6.27
ribonucleotide reductase M2 b	Dr.23801.1.A1_at	-2.59	-1.43	-1.86
phosphomannomutase 2	Dr.13747.1.S1_at	-2.60	-2.85	-3.30
adenylate kinase 3	Dr.1707.1.S1_at	-2.60	-2.37	-1.42
Cytidine deaminase	Dr.25811.1.S1_at	-2.65	-1.64	-2.13
phosphoglycerate dehydrogenase	Dr.24995.5.A1_at	-2.66	-2.41	-3.12
HMGCS1	Dr.2051.1.S1_at	-2.67	-3.26	-2.73
phosphoglucomutase 3	Dr.21347.1.S1_at	-2.68	-3.98	-4.45
galactose-4-epimerase, UDP-	Dr.987.1.S1_at	-2.82	-3.99	-3.94
cyp17a1	Dr.25390.1.A1_s_at	-2.86	-2.24	-3.96
N-acylsphingosine amidohydrolase	Dr.25118.1.S1_at	-2.92	-2.23	-2.24
SLC25A22	Dr.25199.1.A1_at	-4.43	-3.27	-3.77
folate hydrolase	Dr.16405.1.S1_at	-6.90	-10.71	-12.76

Table 2-S2. Summary of the pattern of gene regulation between adult and larval fin regeneration.
Out of the 341 genes that were common in both gene lists, 109 and 107 genes were similarly induced and repressed, respectively, which comprised about 64% resemblance in the pattern of gene regulation between the two regenerating tissue platforms.

	Induced	**Repressed**	**Total**
Common Genes	179	166	341
Similarly Regulated	109	107	216
Similarly Regulated (%)	60.9	64.5	63.3

Table 2-S3.Selected genes that were commonly expressed between larval and adult fin regeneration.

Gene	Affymetrix ID	Larval Fin Fold Change 1DPA	2DPA	3DPA	Adult Fin Fold Change 1DPA	3DPA	5DPA
Wound healing/Immune response							
cathepsin S	Dr.24219.5.S1_at	11.35	4.95	4.53	2.18	1.53	1.75
legumain	Dr.24341.1.S1_at	5.22	3.08	2.88	3.23	2.07	2.29
socs-3	Dr.9617.1.A1_at	4.54	7.59	4.12	4.09	4.20	2.19
cathepsin C	Dr.4782.1.S1_at	3.30	2.51	2.36	1.80	1.91	1.69
cathepsin L	Dr.19902.1.S1_at	2.14	3.77	2.85	4.22	3.56	3.60
granulin 1	DrAffx.2.25.A1_at	2.08	4.02	2.52	11.61	2.53	3.47
Signal Transduction							
raldh2	Dr.5206.1.S1_at	11.75	49.47	26.03	12.37	14.34	7.47
ms4a4a	Dr.22334.1.S1_at	8.39	21.60	15.68	1.85	2.26	1.87
fgf20a	Dr.17781.1.A1_at	4.29	10.41	4.57	11.50	9.62	3.17
Igfbp1	Dr.8587.1.A2_at	4.29	5.31	2.98	3.41	2.00	2.01
WNT inhibitory factor 1	Dr.3690.1.S1_at	-1.17	-3.96	-4.29	-3.04	-4.12	-3.36
deltaD	Dr.20958.1.S1_at	-1.32	-5.99	-4.61	-2.27	-1.79	-1.28
Notch 2	Dr.16720.1.A1_at	-1.39	-1.93	-1.79	-1.75	-1.43	-1.42
regulator of G-protein signalling 16	Dr.9926.1.S1_at	-1.71	-1.49	-1.53	-3.36	-3.37	-1.26
ECM/ Cell Adhesion & Migration							
fibronectin 1b	Dr.24233.1.S1_at	4.94	3.12	2.63	9.17	5.05	3.80
galectin 9	Dr.4573.1.A1_at	2.76	4.02	3.24	3.36	3.58	1.48
TIMP2	Dr.15281.1.A1_at	2.37	3.88	2.89	58.91	15.31	4.75
MMP14	Dr.23324.1.A1_at	1.86	3.46	3.65	2.81	5.13	5.39
metrn	Dr.3745.1.A1_at	-1.32	-2.15	-2.22	-4.83	-3.83	-3.03
semaphorin 3aa	Dr.5060.1.A1_at	-1.89	-2.46	-2.71	-2.32	-2.67	-1.61
envoplakin	Dr.5577.1.A1_at	-4.56	-6.73	-6.42	-2.02	-1.75	-1.52
Transcriptional Regulation							
krml2	Dr.23470.1.S1_s_at	8.82	4.67	4.88	2.12	1.75	1.64
krml2.2	Dr.8198.1.A1_at	7.67	4.98	4.80	2.36	2.20	1.86
spi1	Dr.7612.1.A1_at	5.31	2.45	2.30	3.78	2.56	2.78
Kruppel-like factor 2	Dr.3448.1.S1_at	2.55	6.29	7.80	3.16	3.89	4.73
sox4a	Dr.20124.1.A1_at	2.54	1.58	1.82	1.96	3.55	2.71
dachshund c	Dr.3413.1.S1_at	1.51	3.07	2.14	5.06	12.59	8.80
hes6	Dr.19467.1.A1_at	-1.19	-1.53	-1.93	-2.18	-1.71	-2.17
sox3	Dr.20010.8.A1_at	-1.78	-2.08	-2.80	-3.20	-2.02	-1.91
pou50	Dr.57.1.S1_at	-2.20	-4.27	-4.71	-1.85	-1.89	-1.85
Cytoskeleton/Cytosolic Transport							
nipsnap homolog 3A	Dr.17452.1.S1_at	1.87	2.18	2.67	2.86	3.65	2.81
vac14	Dr.18964.1.A1_at	1.60	1.59	2.13	2.91	2.01	1.34
keratin 18	Dr.890.1.S1_at	1.54	2.43	1.68	2.06	2.30	2.08
Clathrin-associated protein 19	Dr.1084.1.A1_at	-1.84	-1.89	-2.43	-2.49	-2.64	-1.95
tubulin, alpha 1	Dr.7506.1.A1_at	-2.31	-2.68	-3.14	-1.60	-2.05	-1.80
p76	Dr.349.1.A1_at	-2.59	-2.18	-2.43	-3.09	-2.28	-2.09
Chromatin/DNA/RNA Processing							
histone deacetylase 8	Dr.3849.1.A1_at	2.06	1.63	1.71	1.90	1.84	1.38
Orc6L	Dr.24945.1.S1_at	1.96	2.29	1.85	3.22	2.15	1.70
poly(A) binding protein cytoplasmic 1	Dr.12233.1.S1_at	1.59	2.98	2.32	25.99	12.39	23.62
HLA-B associated transcript 1	Dr.5423.1.A1_at	-1.39	-1.84	-1.71	-1.55	-1.93	-2.23
deoxyribonuclease I-like 3	Dr.20334.1.S1_at	-2.08	-1.31	-1.60	-3.35	-2.64	-1.90
ribonucleotide reductase M2 b	Dr.23801.1.A1_at	-2.59	-1.43	-1.86	-2.52	-2.34	-2.39

Table 2-S4.Summary of the pattern of gene regulation between larval fin and adult heart regeneration.

The larval fin regeneration gene list was compared to the adult heart regeneration gene list and identified 189 common gene expression changes. Of these genes, 116 were similarly induced and 18 were similarly repressed, which constitutes about 89% and 31% similarity in the gene regulation, respectively, between larval fin and adult heart regeneration.

	Induced	Repressed	Total
Common Genes	131	58	189
Similarly Regulated	116	18	132
Similarly Regulated (%)	88.5	31.0	69.8

Table 2-S5.Selected genes that were commonly expressed between larval and adult heart regeneration.

		Larval Fin Fold Change			Adult Heart Fold Change		
Gene	**Affymetrix ID**	**1DPA**	**2DPA**	**3DPA**	**3DPA**	**7DPA**	**14DPA**
Wound healing/Immune response							
granulin 2	Dr.4748.1.S1_at	11.71	33.73	19.66	9.95	4.91	3.76
cathepsin S	Dr.24219.5.S1_at	11.35	4.95	4.53	9.66	4.40	2.20
lactotransferrin	Dr.1889.1.S1_at	9.88	2.39	2.72	1.76	5.43	2.72
granulin a	Dr.5809.1.A1_at	9.19	3.49	4.85	8.23	4.50	2.07
legumain	Dr.24341.1.S1_at	5.22	3.08	2.88	5.58	3.21	1.80
galectin 9	Dr.4573.1.A1_at	2.76	4.02	3.24	3.89	1.96	1.92
Signal Transduction							
raldh2	Dr.5206.1.S1_at	11.75	49.47	26.03	3.17	2.55	1.25
krml2	Dr.23470.1.S1_s_at	8.82	4.67	4.88	3.95	1.72	1.01
krml2.2	Dr.8198.1.A1_at	7.67	4.98	4.80	3.90	1.87	1.09
jun B proto-oncogene	Dr.10326.1.S1_at	4.55	10.72	7.93	2.47	2.71	2.12
apolipoprotein Eb	Dr.1246.1.S1_at	2.05	3.47	3.17	15.37	4.39	1.17
CYR61	Dr.15501.1.S1_at	-1.34	-2.36	-1.83	1.70	3.03	1.77
p57 (kip2)	Dr.3502.1.S1_at	-1.61	-3.77	-4.65	-2.12	-2.09	-1.28
hsp90a	Dr.610.1.S1_at	-2.52	-11.72	-8.25	-3.10	-2.62	-2.50
ECM/ Cell Adhesion & Migration							
glia maturation factor, gamma	Dr.18605.1.A1_at	6.37	3.88	3.18	3.79	2.49	1.54
clusterin	Dr.20131.2.A1_at	3.41	6.06	5.06	1.37	7.44	3.41
TIMP2	Dr.15281.1.A1_at	2.37	3.88	2.89	10.90	6.44	2.72
MMP14	Dr.23324.1.A1_at	1.86	3.46	3.65	2.54	3.74	3.90
MMP2	Dr.2408.1.A1_at	1.40	2.24	2.55	1.13	3.08	2.65
decorin	Dr.16078.1.S1_at	-1.13	-2.16	-1.96	1.46	2.74	2.06
Transcriptional Regulation							
spi1	Dr.7612.1.A1_at	5.31	2.45	2.30	4.15	3.52	2.75
Negative elongation factor C/D	Dr.25468.1.A1_at	2.73	2.29	2.67	8.11	3.71	1.83
activating transcription factor 3	Dr.14282.1.S1_at	2.04	2.36	1.58	-1.38	2.36	1.39
Orc6L	Dr.24945.1.S1_at	1.96	2.29	1.85	3.60	2.73	1.42
Cytoskeleton/Cytosolic Transport							
syntaxin 11	Dr.12309.1.A1_at	3.00	3.57	2.44	2.84	1.85	1.52
keratin 18	Dr.890.1.S1_at	1.54	2.43	1.68	6.34	4.58	2.78
keratin 8	Dr.4387.1.S1_at	-1.22	-1.40	-1.89	3.88	2.81	1.29
unc45b	Dr.345.1.S1_at	-1.49	-2.59	-2.23	-2.18	-1.64	-1.44
p76	Dr.349.1.A1_at	-2.59	-2.18	-2.43	2.38	2.62	2.09
Metabolism							
ferritin, heavy polypeptide 1	Dr.12425.5.S1_at	14.25	35.56	14.56	47.84	19.27	5.64
Y+L amino acid transporter 1	Dr.18441.1.A1_at	6.43	7.15	6.16	16.03	6.85	2.46
glucosamine-6-phosphate deaminase 1	Dr.18431.1.S1_at	4.07	6.57	5.75	14.71	8.79	4.17
Thioredoxin	Dr.8723.1.S1_at	1.52	2.08	1.50	5.68	4.42	1.86
mical3	Dr.14768.1.A1_at	-1.88	-1.81	-1.60	-2.46	-1.57	-1.32
atp1a1a.1	Dr.25976.1.A1_at	-2.15	-2.48	-3.13	-2.10	-1.78	-1.21

Table 2-S6. List of selected genes commonly present between larval fin, adult fin and adult heart regeneration systems.

		Larval Fin Fold Change			Adult Fin Fold Change			Adult Heart Fold Change		
Gene	**Affymetrix ID**	**1DPA**	**2DPA**	**3DPA**	**1DPA**	**3DPA**	**5DPA**	**3DPA**	**7DPA**	**14DPA**
Wound healing/Immune response										
cathepsin S	Dr.24219.5.S1_at	11.35	4.95	4.53	2.18	1.53	1.75	9.66	4.40	2.20
legumain	Dr.24341.1.S1_at	5.22	3.08	2.88	3.23	2.07	2.29	5.58	3.21	1.80
cathepsin C	Dr.4782.1.S1_at	3.30	2.51	2.36	1.80	1.91	1.69	5.09	2.80	1.98
galectin 9	Dr.4573.1.A1_at	2.76	4.02	3.24	3.36	3.58	1.48	3.89	1.96	1.92
cathepsin B	Dr.3374.2.S1_at	2.75	2.17	2.27	2.16	1.64	1.63	4.29	1.99	-1.77
Napsin 1 precursor	Dr.19238.1.S1_at	2.56	2.90	2.46	2.18	1.77	1.95	4.18	2.33	1.35
Signal Transduction										
raldh2	Dr.5206.1.S1_at	11.75	49.47	26.03	12.37	14.34	7.47	3.17	2.55	1.25
krml2.2	Dr.23470.1.S1_s_at	8.82	4.67	4.88	2.12	1.75	1.64	3.95	1.72	1.01
krml2	Dr.8198.1.A1_at	7.67	4.98	4.80	2.36	2.20	1.86	3.90	1.87	1.09
Fos-related antigen 2	Dr.10130.1.S1_at	3.31	3.44	2.48	4.07	2.99	1.94	1.83	2.49	1.92
C-type natriuretic peptide 4	Dr.18242.1.A1_at	1.85	5.60	3.14	20.34	11.37	4.12	4.03	11.97	2.70
paired related homeobox 1	Dr.1410.1.S1_at	1.47	2.04	1.90	1.72	2.94	3.06	3.17	2.70	1.55
ECM/ Cell Adhesion & Migration										
fibronectin 1b	Dr.24233.1.S1_at	4.94	3.12	2.63	9.17	5.05	3.80	1.69	3.00	1.98
Olfactomedin-like protein precursor	Dr.1154.1.S1_at	2.93	4.54	5.82	2.80	6.60	5.72	3.78	4.26	2.31
timp2	Dr.15281.1.A1_at	2.37	3.88	2.89	58.91	15.31	4.75	10.90	6.44	2.72
mmp14	Dr.23324.1.A1_at	1.86	3.46	3.65	2.81	5.13	5.39	2.54	3.74	3.90

Table 2-S7.Expression of known zebrafish fin regeneration genes from the larval microarray analysis.

		Fold Change		
Gene	Affymetrix ID	1 DPA	2 DPA	3DPA
fgf20a	Dr.17781.1.A1_at	4.29	10.41	4.57
TIMP2	Dr.15281.1.A1_at	2.37	3.88	2.89
apoEb	Dr.1246.1.S1_at	2.05	3.47	3.17
msxc	Dr.16562.2.A1_at	1.81	2.55	2.51
keratin 18	Dr.1372.1.S1_at	1.14	1.01	0.74
beta catenin	Dr.10259.1.S2_at	1.12	0.99	0.99
dnajb11	Dr.1075.1.A1_a_at	0.85	1.19	1.59
msxe	Dr.41.1.A1_at	0.73	1.57	1.40
msxb	Dr.24779.1.S1_at	0.42	1.11	1.23
wnt5b	Dr.389.1.S1_at	0.38	1.24	0.86

Table 2-S8. List of gene specific primers used for qRT-PCR and cloning of raldh2 for probe synthesis.

Target Gene	Sequence 5′ to 3′
F raldh2	GGGGTAAAGTGGTAAAACGC
R raldh2	GCAGTGGTCAAAAGCATGGC
F apoEb	AGCTGCAGGAAGTCATGGAC
R apoEb	GTGCTAGTCCAATTGAGTCC
F granulin A	GAAGGACGTTCAGTGTGGTG
R granulin A	GGGCTCGTTTCTTTTTGGAG
F cyr 61	ATCCTCATTAGCTGCGTCCC
R cyr 61	TGATGTTGGTTTCCTCTAGC
F p57	TACATACATCAGTCCACCTG
R p57	CTGTTTAGAGCACTGTGGTC
F wif1	TAAGAGATTTCGCGGAGGAG
R wif1	TGAAATGGAGGTGCCTTGGC
F β-actin	AAGCAGGAGTACGATGAGTC
R β-actin	TGGAGTCCTCAGATGCATTG
F raldh2 for cloning cDNA	ACCGGCATCTTCAATAGACG
R raldh2 for cloning cDNA	ATCAGCTTGCCTACCTCAGT

CHAPTER 3 – Glucocorticoid-dependent *Cripto-1* Induction Inhibits Epimorphic Tissue Regeneration

Sumitra Sengupta, Lijoy K Mathew, Lisa Truong, Jane La Du and Robert L Tanguay.

Department of Environmental and Molecular Toxicology, Environmental Health Sciences Center, Oregon State University, Corvallis, OR, 97331.

Formatted for Publication in Journal of Biological Chemistry

Abstract

Previously we adopted a chemical genetic approach and utilized the larval regeneration model to identify modulators of tissue regeneration. This led to identification that exposure to glucocorticoids (GC) impacts tissue regeneration by inappropriate activation of the glucocorticoid receptor (GR). In order to elucidate the molecular mechanisms downstream of activated GR we performed global gene expression analysis specifically in regenerating tissues. *Cripto-1*, an inhibitor of Activin signaling, was one of the most highly expressed transcripts in the fin regenerates of beclomethasone dipropionate (BDP) exposed larvae. We hypothesized that mis-expression of *Cripto-1* is essential for the activated GR to block regeneration. Partial antisense repression and RA exposure repressed *Cripto-1* and reversed the inhibitory effect of BDP and restoring regenerative progression. This study demonstrates that inhibition of regeneration by GCs is mediated by *Cripto-1*. Since *Cripto-1* is a known inhibitor of Activin signaling, we perturbed Activin signaling using the chemical inhibitor SB431542, and demonstrated its importance in an early life stage model of tissue regeneration. In summary, the GR-dependent induction of *Cripto-1* expression offers a molecular explanation as to how glucocorticoid exposures impair epimorphic regeneration.

Introduction

Chemical genetics is a dynamic approach that utilizes small molecules to modulate molecular events in order to unravel the mechanisms underlying complex biological functions. The field of regenerative medicine holds promise for chemical genetics-based discovery of therapeutics for numerous disease conditions, injury and even aging. The stem cell paradigm, a major research focus of regenerative medicine, offers potentially powerful therapeutic advances, but an incomplete understanding of the underlying molecular signaling in need of correction. Deeper understanding of the signaling involved will create opportunities to potentiate a regenerative outcome in vertebrates that normally cannot regenerate. Vertebrates endowed with the capacity to regenerate such as zebrafish, salamanders and newts have been invaluable in revealing the underlying details of this process. To date, the literature suggests that numerous signaling molecules interact in a highly controlled spatio-temporal environment to permit tissue regeneration. Identification of these signaling molecules is essential to advance the field of regenerative medicine. By taking advantage of high throughput screening techniques, the field of stem cell biology has immensely progressed in the last century. However, most of this work has been completed *in vitro*. We have taken advantage of the rapid screening amenability of larval zebrafish and developed an early life stage larval regeneration model [1]. Our rapid chemical genetic approach facilitates investigating the underlying molecular signaling pathways involved in tissue regeneration [2] by identifying novel modulators. Our approach is centred on the tenet that if a chemical inhibits regeneration, then it has influenced a critical molecular target involved

in regeneration. Identification of such chemical targets will enable assembly of the molecular regeneration pathways. We initially screened a 2000 member FDA- approved library that identified glucocorticoids (GC) as modulators of tissue regeneration for the first time [2]. GCs are one of the oldest drugs in the market and are mainly used as anti-inflammatory agents. Endogenous GCs, such as cortisol, are steroid hormones synthesized from cholesterol in the adrenal cortex. In humans, cortisol is the principle GC and is involved in the regulation of metabolism, stress response and immune function [3]. Exogenous GCs are classified based on their anti-inflammatory and immune suppressing functions. Response to GCs is not uniform, differing not only among individuals but also within tissues of the same individual. GCs can both promote [4] and inhibit wound healing [5] in mammals. The physiological and pharmacological actions of GCs are predominantly mediated by the GC receptor (GR) which, upon ligand binding, translocates to the nucleus, and activates transcription of many genes. The pharmacology of GCs depends mostly on ligand concentration and receptor expression levels in target tissues; however, coactivators and corepressor recruitment are also important [6].

Previous chemical genetic approaches were used to probe zebrafish tissue regeneration and revealed that inappropriate aryl hydrocarbon receptor (AHR) activation blocks regeneration by misexpressing R-Spondin 1 [7]. Wound healing is the first stage of tissue regeneration and GCs impair this process by modulating TGFβ activity [8]. New investigations into the role of GCs as modulators of tissue regeneration have the potential to reveal the signaling pathways required for regeneration and expand understanding of GR biology. Previously we demonstrated that activation of GR, specifically during early stages of regeneration, negatively affects tissue regeneration.

Even though GCs are immunosuppressants, in the zebrafish larval regeneration model, neutrophil and macrophages are not required for tissue regeneration [2]. Since inflammatory cell migration doesnot not explain why glucocorticoids block regeneration, the downstream functional GR targets that are required for the impaired regeneration phenotype remain completely unknown.

To reveal the potential downstream effectors of inappropriately activated GR, we performed microarray analysis on regenerating fin tissue exposed to beclomethasone dipropionate (BDP). Our results revealed *Cripto-1* as a molecular target of activated GR. Cripto-1 is a member of the EGF-CFC family [9] and TDGF1 is the human *Cripto-1* ortholog. *Cripto-1* plays important roles in ventral neuroectoderm, endoderm [10] and cardiac development [11]. Functional studies with *Cripto-1* mutant (*oep)* in zebrafish have revealed that this gene is required for the formation of the prechordal plate [14]. Absence of *Cripto-1* prevents the formation of the prechordal plate, leading to fused eyes and a pin shaped head phenotype [12, 13]. *Cripto-1* inhibits TGFβ signaling pathway by acting as a cofactor to Nodal and by binding Activin, preventing its binding to the Alk receptor [10]. Prior to this study, the involvement of *Cripto-1* in regeneration and its relationship to GR activation was unknown. Our results conclusively demonstrate that inappropriate activation of GR results in *Cripto-1* over expression and that this misexpression leads to impaired regeneration.

Materials and Methods

Zebrafish Embryos

AB strain embryos were used for performing microarray experiments. The 5D strain was used to validate the BDP response and to perform the ensuing experiments. All embryos were raised following standard husbandry procedures [15]. Experimental groups consisted of sample size n=12. Caudal fins of 2 days post fertilization (dpf) larvae were amputated as previously described [2, 16-18].

Chemical Exposures

Embryos were exposed to Beclomethasone dipropionate (BDP) (Sigma), SB431542 (Sigma) and DEAB (Sigma) at a final concentration of 1µM, 100µM and 250µM respectively. All-*trans* – Retinoic acid (Sigma) was used at 0.1µM dose continuously for 8 hours followed by continuous co-exposure with 1µM BDP and 0.01µM RA for three days after amputation. All chemical stocks were prepared in dimethyl sulfoxide (DMSO).

Fin RNA Isolation

Caudal fins were amputated at 2 dpf and larvae were exposed to either a vehicle control (DMSO) or 1 µM BDP in individual, wells of a 96 well plate. At 24 hours post amputation (hpa) the regenerating fin tissues were amputated, collected followed by and RNA extraction using the RNAqueous Micro kit (Ambion). Amputated fin tissues from 150 embryos was pooled to produce a replicate, three replicates per treatment. UV absorbance analysis was used to determine the quality and quantity of isolated RNA. Degree of degradation and ribosomal RNA abundance were determined in electropherogram patterns using the 2100 Bioanalyzer and RNA 6000 Nano chips (Agilent Technologies).

Affymetrix Microarray Processing

Microarray processing was performed at the Center for Genome Research and Biocomputing at Oregon State University using the Affymetrix platform. 100ng RNA isolated from larval fin tissue (AB strain) (+/- 1 µM BDP in fish water) was reverse transcribed using T7-$(dT)_{24}$ primer and Superscript II reverse transcriptase (Invitrogen) to generate single stranded cDNA. Double stranded cDNA generated by a second round of cDNA synthesis was used as a template for synthesis of biotinylated cRNA using T7 polymerase and biotin conjugated pseudouridine containing nucleotide mixture provided in the IVT Labeling Kit (Affymetrix). Ten µg of biotinylated purified and fragmented cRNA from each experimental group was hybridized to zebrafish genome arrays (Zebrafish430_2) according to the Affymetrix GeneChip Expression Analysis Technical Manual (7010201 Rev. 5). Arrays were scanned using Affymetrix scanner 3000 and each array image was screened for nonspecific signals, scratches or debris. Experiments were certified under Minimum Information About a Microarray Experiment (MIAME) standards.

Generated Affymetrix CEL files were imported into GeneSpring software (Agilent Technologies). The files were gene chip-robust multiarray processed to eliminate background signal, and each transcript was normalized to the median signal to allow comparison between arrays on a relative scale for each gene. The differential expression of transcripts caused by exposure to BDP was evaluated by comparing the BDP exposed samples with the vehicle exposed samples by One way ANOVA assuming equal variance ($p<0.05$). Genes that were at least 2 fold differentially expressed were considered for further analysis and annotated by sequence similarity of each Affymetrix probe set sequence with known mammalian proteins using the Sanger database (http://www.sanger.ac.uk/Projects/D_rerio/). Other databases such as ENSEMBL

(http://uswest.ensembl.org/Danio_rerio/Info/Index) and Genbank were used to validate the annotated genes. Experiments were MIAME certified and the raw data were submitted to the National Centre for Biotechnology Information (NCBI) Gene Expression Omnibus (GEO) (http://www.ncbi.nlm.nih.gov/projects/geo/) [8, 19]. The gene list was exported into MultiExperiment Viewer (MEV) to generate bi-hierarchical clustering. A gene list was created from the heat map and the ZFIN and Ensembl databases were used to identify human orthologs of altered zebrafish transcripts.

Pathway Analysis

Ingenuity Pathway Analysis (IPA) software (Ingenuity Systems) was used to analyze altered transcripts based on their biological function. DAVID (Database for Annotation, Visualization, and Integrated Discovery) determined gene ontology and grouped the transcripts based on their function.

Quantitative Real Time Reverse Transcriptase Polymerase Chain Reaction (qRT-PCR)

Total RNA was isolated from regenerating larval fin tissue (+/- BDP). Each group had three replicates with n=60 per replicate and 1 µg of isolated RNA per group was used to synthesize cDNA using Superscript II (Life Technologies) with oligo(dT) primers. Gene specific primers listed in (Supplemental Table 2) were used to perform qRT-PCR in the Opticon 2 real time PCR detection system (MJ Research) using the SYBR green qPCR detection kit (Finnzymes). Each sample was normalized to endogenous β actin quantity. Agarose gel electrophoresis and melt curve analysis confirmed expected PCR product formation. Statistical significance of differences in mRNA abundance was determined by one way ANOVA on $\log_{10}$ transformed data with Tukeys post test ($p<0.05$) (Sigmastat Software).

Oligonucleotides

Primers were designed to amplify sequences located in the Affymetrix probe target sequence. Sequences for each primer can be found in (Supplemental Table 2). Forward and antisense reverse primers are prefixed with F and R accordingly.

In situ hybridization

In situ hybridization following published methodology [2, 8, 20] was performed for spatial localization of transcripts at 1dpa. *msxE, dlx5a , mvp , smarca4* and *ilf2* probes were generously gifted from Atsushi Kawakami (Tokyo Institute of Technology, Yokahama, Japan). *Cripto-1* probe (cb85) was purchased from ZFIN and full-length *Cripto-1* (coding sequence and 3'UTR) probe was synthesized in the lab.

Morpholinos

Fluorescein tagged zebrafish one eyed pinhead (*zf oep*) morpholino (5' GCCAATAAACTCCAAAACAACTCGA 3')(Gene Tools) [21] targeting the translation start site, and splice blocking zebrafish GC receptor(*zf GR*) morpholino (5' - CGGAACCCTAAAATACATGAAGCAG - 3') [2] targeting splicing of exons 7 and 8, were used to knockdown *Cripto-1* and GR expression. The morpholinos were diluted to a stock concentration of 3mM in 1x Danieau's solution (58 mM NaCl, 0.7 mM KCl, 0.4 mM $MgSO_4$, 0.6 mM $Ca(NO_3)_2$, 5 mM HEPES, pH 7.6) [22][22][22]. A standard control MO (Gene Tools) (5'CTCTTACCTCAGTTACAATTTATA 3') was used as control for injection. Approximately 2nl of 1.2mM *zfOep-MO* and 3mM *zfGR*-MO were injected in 1-4 cell stage embryos. Control morpholino was injected at matching concentrations. Embryos were screened for uniform fluorescence at 24hpf for uniform distribution of morpholino. Caudal fins of the morphants were amputated at 2dpf followed by exposure to vehicle or BDP and raised untill 3dpf according to the standard regeneration assay protocol [2][14][14].

Results

Microarray analysis identifies *Cripto-1* as a potential GR target

Previously we demonstrated that inappropriate GR activation leads to inhibition of tissue regeneration [2]. To determine the molecular target critical for this GR mediated inhibition, we performed global gene expression analysis of the regenerating fin tissue exposed to DMSO or BDP. The heat map illustrates two major clusters of mRNA that are differentially expressed either up or down relative to non amputated tissues. Only transcripts that were at least 2 fold differentially expressed in comparison to the controls were considered for analysis (Figure 1). Statistical significance determined by one way ANOVA revealed 169 transcripts with greater than a 2 fold change that were statistically significant ($p<0.05$) (Table 1). These transcripts were analyzed based on sequence homology and further grouped by function. Most of the transcripts are involved in wound healing, extracellularmatrix remodeling (ECM) remodeling and metabolism. Genes such as *fgf20a*, *sox9b* and *raldh2*, which play important roles in regeneration [1, 7] were differentially expressed in the BDP exposed samples. Other known GR target genes such as *gilz* [23], *fkbp506* [24] and *annexin a1b* [25] were also significantly affected(Figure 2). Notably, *Cripto-1* or One-eyed pinhead (Oep) were 8.5 fold induced in the regenerating fin tissue upon BDP exposure (Table1). QRT PCR analysis confirmed this elevated expression in the regenerating tissue as well as in the whole embryo (Figure 2). Although highly induced, it was not possible to localize *Cripto-1* expression in BDP exposed larvae by *in situ* hybridization analysis because of low basal expression.

Activin signaling is important for larval caudal fin regeneration

An established role of the murine form of *Cripto-1* is inhibition of Activin signaling [33-36]. As a first step to understand the downstream effectors of the inappropriately activated GR, we explored the role of Activin signaling in larval tissue regeneration. SB431542 is a specific inhibitor of endogenous Activin and TGFβ signaling [38-40]. Exposure of amputated 48hpf larvae to SB431542 at 100 µM impaired regeneration with the characteristic "V" shape as seen in BDP exposed larvae (Figure 3a). Comparative *in situ* analysis of regeneration markers *raldh2*, *mvp*, *dlx5a*, *junbl*, *smarca4*, *wnt10a* and *ilf2* between BDP and SB431542 exposed fin tissue revealed identical expression patterns suggesting inhibition of Activin signaling in BDP exposed larvae (Figure 3b). Since *Cripto-1* suppress Activin signaling in multiple cell types by binding Activin ligands [33-36, 41] we explored the role of *Cripto-1* in BDP impaired tissue regeneration.

Temporal sensitive misregulation of *Cripto-1* is required for GR mediated inhibition of regeneration

To determine the role of *Cripto-1* induction in GR mediated impairment of tissue regeneration, we determined if *Cripto-1* expression is GR dependent. Quantitative RT-PCR (qRT-PCR) of *Cripto-1* in 1 dpa GR morphants exposed to BDP showed significantly reduced *Cripto-1* expression compared to control morphants exposed to BDP (Figure 4a). This data clearly indicates that GR activation is required for increased *Cripto-1* expression. We previously determined that BDP exposure from 0-4 hours post amputation was sufficient to inhibit regeneration. Exposure to BDP beyond the 4 hour post-amputation window did not impact regeneration [2]. We reasoned that the expression of GR target genes critical for regeneration should not be affected by BDP exposure occurring after 4h post-amputation. Quantitative RT PCR analysis of *Cripto-1*

in whole embryos exposed to BDP after 4h post-amputation showed no change in *Cripto-1* expression relative to controls.

Cripto-1 **is required for the regenerative inhibition response to BDP**

To directly test the role of *Cripto-1* expression in mediating GR activated inhibition of regeneration, we utilized a translation blocking morpholino which completely knockdown Cripto-1 resulting in one eyed pinhead phenotype (Figure 5a) that was lethal by 5 dpf [21]. To avoid lethality, we injected 2-4 cell embryos with variable amounts of morpholino. The morphants were screened for fluorescence at 24 hpf and those with uniform fluorescence were selected for further study. Control and Cripto-1 morphants were exposed to vehicle or BDP following amputation at 2dpf. The transient antisense repression allowed us to bypass lethality and 80% of the Cripto-1 morphants rescued BDP impaired regeneration. These *Cripto-1* morphants regenerated normally suggesting suppression of *Cripto-1* does not interfere with normal regenerative progression in our larval model. The regenerative response was complteley abrogated in control morphants exposed to BDP. *Cripto-1* morphants exposed to BDP did not exhibit inhibitory effects on regenerative growth (Figure 5b). These studies clearly delineate that over expression of *Cripto-1* is necessary for GR mediated inhibition of regeneration.

Suppression of ***Cripto-1*** **by Retinoic acid rescues BDP inhibited regeneration**

Retinoic acid (RA) treatment suppresses *Cripto-1* expression in human and murine teratocarcinoma cells [42]. To further evaluate the role of *Cripto-1* in tissue regeneration, we utilized RA treatment to suppress *Cripto-1* expression. Analysis of *Cripto-1* expression in whole embryos exposed to 0.1 and 0.01 µM RA at 1dpa, revealed

reduced expression in a dose-dependent manner (Figure 6a). We previously showed that 0.01 µM RA rescued regeneration in the larval model after exposure to the regenerative inhibitor SU5402 [1]. Here, co-exposure of BDP with 0.01 µM RA did not rescue regeneration in the larval model suggesting the fold suppression of *Cripto-1* expression by RA was not sufficient to overcome the induction by BDP exposure. Exposure to RA greater than 0.01 µM is itself inhibitory to tissue regeneration. We, therefore, pre-exposed 2 dpf larvae to 0.1 µM RA for 8 hours prior to amputation in 2 treatment groups, then co-exposed one of these treatment groups to BDP and 0.01uM RA post-amputation. RA pre-exposure did not affect regeneration in larvae treated with vehicle (DMSO) following amputation. This is consistent with the result that *Cripto-1* morphants can regenerate normally and that suppression of *Cripto-1* expression does not abrogate regeneration. Pre exposure to 0.1 µM RA alone rescued regeneration in approximately 60% of amputated larvae after BDP exposure. This might be due to differential uptake of RA, since each embryo was pre- exposed separately in individual wells of a 96 well plate. Pre and co-exposure to RA suppressed *Cripto-1* expression compared to ectopic elevated expression in fin tissue of BDP-exposed larvae at 1dpa (Figure 6b). The presence of dlx5a and junbl in co-exposed fin tissue suggested normal regenerative progression (Figure 6c) while regeneration assay results confirmed rescue of BDP inhibition of tissue regeneration by RA (Figure 6d). These data further suggest that modulation of *Cripto-1* expression by RA was sufficient to rescue the inhibition of regeneration by BDP. Taken together, our studies illustrate that temporal mis-expression of *Cripto-1* is responsible for GR mediated impairment of regeneration and titrating the abundance of *Cripto-1* to normal level using morpholinos or RA exposure rescues the inhibitory phenotype.

Discussion

The zebrafish larval model is a powerful tool to study epimorphic tissue regeneration. Understanding the underlying signaling pathways of this complex and highly regulated process is essential to adopt a therapeutic approach for promoting tissue regeneration. Previously our lab has demonstrated the power of the larval regeneration assay that combines a chemical genetics approach with a larval fin regeneration model to reveal novel modulators of tissue regeneration such as TCDD [7]. Identification of the molecular targets of these modulators i.e Wnt in the case of TCDD can reveal critical molecules essential for normal regenerative outcome. We previously screened a 2000 member library of FDA approved drugs [2] to identify novel modulators of regeneration. This screen revealed that GCs inhibit tissue regeneration in a GR dependent manner. Even though GR is one of the most studied nuclear receptors, the tissue specific response of GCs has generated conflicting results. In addition, since most of the studies have been done in non regenerating tissue platforms we lack proper understanding of how molecular signaling events downstream of GR activation abrogate regenerative response. As GCs alter a diverse array of genes, identification of altered transcripts that dictate non-regenerative response will also provide better understanding of basic regeneration pathways as well as explore new avenues for the field of GR biology.

We performed global gene expression analysis in the fin regenerates exposed to BDP. The differentially expressed genes include known GR targets as well as genes involved in tissue regeneration. *Cripto-1* was highly induced in the regenerating fin by

BDP exposure, a novel role for this gene from any model Rescue of the regenerative response by suppressing *Cripto-1* using morpholino and RA exposure in the presence of BDP indicates that misexpression of this gene is absolutely required for inhibition of tissue regeneration by GR activation. *Cripto-1* or TDGF1, the human orthologue, is a marker for undifferentiated ES cells. It is involved in maintaining the pluripotential and self-renewal capacity of mouse and human ES cells [26-28] and is responsible for promoting cardiomyocyte differentiation in embryonic stem cells [29]. Besides its role in differentiation [30, 31], *Cripto-1* knock out embryos also demonstrate reduced wound healing capacity [32]. An established role of the murine form of *Cripto-1* is inhibition of Activin signaling [33-36]. It is one of the key molecular pathway involved in tissue regeneration in the adult caudal fin model of zebrafish [37] *Cripto-1* expression declines with development and is generally not detectable in adult tissue. However, its absence during early embryonic development is detrimental. *Cripto-1* is over expressed in 75-80% of human breast, colon, and lung cancers, as well as 50-60% of testicular, stomach, pancreatic, and ovarian cancers [43]. Because of its characteristic localized expression during breast cancer progression, it has been suggested that plasma Cripto-1 might represent a novel biomarker for the early detection of breast and colon carcinomas [44]. An important role of *Cripto-1* is that it antagonizes Activin signaling and facilitates Nodal signaling by forming complexes with both ligands [34]. Inhibition of Activin signaling by *Cripto-1* impacts Activin signaling in epithelial progenitor cells that undergo rapid expansion during pancreatic islet cell regeneration and development [45].

Activins belong to the transforming growth factor beta (TGFß) protein superfamily. They initially bind to a type II activin receptor (ActRII or ActRIIB) and recruit type I activin receptor (ActRIB). Receptor hetero-dimerization activates the type II and

type I receptor phosphorylating the recruited regulatory r-Smad, Smad2, and Smad3 which subsequently modulate the expression of a large variety of genes. Activin plays an important role in wound repair [46, 47] and is important for caudal fin regeneration [37]. Increased Activin levels appear to enhance the healing rate, but lead to increased scarring. On the other hand, inhibition of Activin function delays the repair process, but the outcome of the healed wound appears to be improved. This suggests that levels of Activin can be therapeutically targeted to modify wound healing [47]. GCs are known to impact wound healing by suppressing Activin signaling [8, 48][49][50]. Our data suggests that *Cripto-1* might be another player in mediating the impact of GCs on Activin signaling.

This is the first report of modulation of *Cripto-1* by GCs. The functional consequence of induced *Cripto-1* expression extends beyond the field of regenerative biology. Keeping in mind the association of *Cripto-1* misexpression in cancer and during development exploring the mechanism of how GCs impact *Cripto-1* expression may result in expanding the understanding of GR biology and contribute towards the development of novel therapeutics. This study also identifies a new approach to inhibit Activin signaling by GCs. Since Activin A knockout mice [51] do not survive, administration of GCs during pregnancy might reveal unexplored effects of GCs on embryonic development. Data from animal research have revealed that fetal GC exposure may have a role in programming the individual to become susceptible to developing adult degenerative diseases [52]. In summary, this paper describes a particularly exciting outcome of a chemical genetic screen resulting in the discovery of a previously unknown role of GR.

References

1. Mathew, L.K., et al., *Comparative expression profiling reveals an essential role for raldh2 in epimorphic regeneration.* J Biol Chem, 2009. 284(48): p. 33642-53.

2. Mathew, L.K., et al., *Unraveling tissue regeneration pathways using chemical genetics.* J Biol Chem, 2007. 282(48): p. 35202-10.

3. *Glucocorticoids and mood: clinical manifestations, risk factors and molecular mechanisms. Proceedings of a meeting. June 20-21, 2008. La Jolla, California, USA.* Ann N Y Acad Sci, 2009. 1179: p. vii-viii, 1-233.

4. De Panfilis, G., et al., *Dexamethasone-induced healing of chronic leg ulcers in a patient with defective organization of the extracellular matrix of fibronectin.* Br J Dermatol, 2000. 142(1): p. 166-70.

5. Beranek, J.T., *Transformation of capillaries into interstitial tissue: further evidence in favour of the angiogenic hypothesis of repair and fibrosis.* Br J Plast Surg, 1989. 42(6): p. 725.

6. van der Laan, S. and O.C. Meijer, *Pharmacology of glucocorticoids: beyond receptors.* Eur J Pharmacol, 2008. 585(2-3): p. 483-91.

7. Frank, S., M. Madlener, and S. Werner, *Transforming growth factors beta1, beta2, and beta3 and their receptors are differentially regulated during normal and impaired wound healing.* J Biol Chem, 1996. 271(17): p. 10188-93.

8. Mathew, L.K., et al., *Crosstalk between AHR and Wnt signaling through R-Spondin1 impairs tissue regeneration in zebrafish.* FASEB J, 2008. 22(8): p. 3087-96.

9. Bianco, C., et al., *Role of the cripto (EGF-CFC) family in embryogenesis and cancer.* Growth Factors, 2004. 22(3): p. 133-9.

10. Gritsman, K., et al., *The EGF-CFC protein one-eyed pinhead is essential for nodal signaling.* Cell, 1999. 97(1): p. 121-32.

11. Liu, H., et al., *Cardiac myocyte differentiation: the Nkx2.5 and Cripto target genes in P19 clone 6 cells.* Funct Integr Genomics, 2005. 5(4): p. 218-39.

12. Solnica-Krezel, L., et al., *Mutations affecting cell fates and cellular rearrangements during gastrulation in zebrafish.* Development, 1996. 123: p. 67-80.

13. Schier, A.F., et al., *Mutations affecting the development of the embryonic zebrafish brain.* Development, 1996. 123: p. 165-78.

14. Schier, A.F., et al., *The one-eyed pinhead gene functions in mesoderm and endoderm formation in zebrafish and interacts with no tail.* Development, 1997. 124(2): p. 327-42.

15. Westerfield, M., *The zebrafish book : a guide for the laboratory use of zebrafish (Danio rerio)*. Ed. 4. ed. 2000, [Eugene, Or.]: M. Westerfield. 1 v. (unpaged).

16. Poss, K.D., et al., *Mps1 defines a proximal blastemal proliferative compartment essential for zebrafish fin regeneration.* Development, 2002. 129(22): p. 5141-9.

17. Mathew, L.K., E.A. Andreasen, and R.L. Tanguay, *Aryl hydrocarbon receptor activation inhibits regenerative growth.* Mol Pharmacol, 2006. 69(1): p. 257-65.

18. Andreasen, E.A., et al., *Aryl hydrocarbon receptor activation impairs extracellular matrix remodeling during zebra fish fin regeneration.* Toxicol Sci, 2007. 95(1): p. 215-26.

19. Andreasen, E.A., L.K. Mathew, and R.L. Tanguay, *Regenerative growth is impacted by TCDD: gene expression analysis reveals extracellular matrix modulation.* Toxicol Sci, 2006. 92(1): p. 254-69.

20. Poss, K.D., J. Shen, and M.T. Keating, *Induction of lef1 during zebrafish fin regeneration.* Dev Dyn, 2000. 219(2): p. 282-6.

21. Feldman, B. and D.L. Stemple, *Morpholino phenocopies of sqt, oep, and ntl mutations.* Genesis, 2001. 30(3): p. 175-7.

22. Nasevicius, A. and S.C. Ekker, *Effective targeted gene 'knockdown' in zebrafish.* Nat Genet, 2000. 26(2): p. 216-20.

23. Wang, J.C., et al., *Chromatin immunoprecipitation (ChIP) scanning identifies primary glucocorticoid receptor target genes.* Proc Natl Acad Sci U S A, 2004. 101(44): p. 15603-8.

24. Phuc Le, P., et al., *Glucocorticoid receptor-dependent gene regulatory networks.* PLoS Genet, 2005. 1(2): p. e16.

25. Roviezzo, F., et al., *The annexin-1 knockout mouse: what it tells us about the inflammatory response.* J Physiol Pharmacol, 2002. 53(4 Pt 1): p. 541-53.

26. Assou, S., et al., *A meta-analysis of human embryonic stem cells transcriptome integrated into a web-based expression atlas.* Stem Cells, 2007. 25(4): p. 961-73.

27. Minchiotti, G., *Nodal-dependant Cripto signaling in ES cells: from stem cells to tumor biology.* Oncogene, 2005. 24(37): p. 5668-75.

28. Minchiotti, G., S. Parisi, and M.G. Persico, *Cripto signaling in differentiating embryonic stem cells.* Methods Mol Biol, 2006. 329: p. 151-69.

29. Kirby, M.L., *Why don't they beat?: Cripto, apelin/APJ, and myocardial differentiation.* Circ Res, 2009. 105(3): p. 211-3.

30. Parisi, S., et al., *Nodal-dependent Cripto signaling promotes cardiomyogenesis and redirects the neural fate of embryonic stem cells.* J Cell Biol, 2003. 163(2): p. 303-14.

31. Xu, C., et al., *Specific arrest of cardiogenesis in cultured embryonic stem cells lacking Cripto-1.* Dev Biol, 1998. 196(2): p. 237-47.

32. Xu, C., et al., *Abrogation of the Cripto gene in mouse leads to failure of postgastrulation morphogenesis and lack of differentiation of cardiomyocytes.* Development, 1999. 126(3): p. 483-94.

33. Gray, P.C., et al., *Cripto binds transforming growth factor beta (TGF-beta) and inhibits TGF-beta signaling.* Mol Cell Biol, 2006. 26(24): p. 9268-78.

34. Kelber, J.A., et al., *Cripto is a noncompetitive activin antagonist that forms analogous signaling complexes with activin and nodal.* J Biol Chem, 2008. 283(8): p. 4490-500.

35. Shani, G., et al., *GRP78 and Cripto form a complex at the cell surface and collaborate to inhibit transforming growth factor beta signaling and enhance cell growth.* Mol Cell Biol, 2008. 28(2): p. 666-77.

36. Yeo, C. and M. Whitman, *Nodal signals to Smads through Cripto-dependent and Cripto-independent mechanisms.* Mol Cell, 2001. 7(5): p. 949-57.

37. Jazwinska, A., R. Badakov, and M.T. Keating, *Activin-betaA signaling is required for zebrafish fin regeneration.* Curr Biol, 2007. 17(16): p. 1390-5.

38. Callahan, J.F., et al., *Identification of novel inhibitors of the transforming growth factor beta1 (TGF-beta1) type 1 receptor (ALK5).* J Med Chem, 2002. 45(5): p. 999-1001.

39. Inman, G.J., et al., *SB-431542 is a potent and specific inhibitor of transforming growth factor-beta superfamily type I activin receptor-like kinase (ALK) receptors ALK4, ALK5, and ALK7.* Mol Pharmacol, 2002. 62(1): p. 65-74.

40. Laping, N.J., et al., *Inhibition of transforming growth factor (TGF)-beta1-induced extracellular matrix with a novel inhibitor of the TGF-beta type I receptor kinase activity: SB-431542.* Mol Pharmacol, 2002. 62(1): p. 58-64.

41. Gray, P.C., C.A. Harrison, and W. Vale, *Cripto forms a complex with activin and type II activin receptors and can block activin signaling.* Proc Natl Acad Sci U S A, 2003. 100(9): p. 5193-8.

42. Ciccodicola, A., et al., *Molecular characterization of a gene of the 'EGF family' expressed in undifferentiated human NTERA2 teratocarcinoma cells.* EMBO J, 1989. 8(7): p. 1987-91.

43. Zhong, X.Y., et al., *Positive association of up-regulated Cripto-1 and down-regulated E-cadherin with tumour progression and poor prognosis in gastric cancer.* Histopathology, 2008. 52(5): p. 560-8.

44. Bianco, C., et al., *Identification of Cripto-1 as a novel serologic marker for breast and colon cancer.* Clin Cancer Res, 2006. 12(17): p. 5158-64.

45. Zhang, Y.Q., et al., *Inhibition of activin signaling induces pancreatic epithelial cell expansion and diminishes terminal differentiation of pancreatic beta-cells.* Diabetes, 2004. 53(8): p. 2024-33.

46. Sulyok, S., et al., *Activin: an important regulator of wound repair, fibrosis, and neuroprotection.* Mol Cell Endocrinol, 2004. 225(1-2): p. 127-32.

47. Munz, B., et al., *Overexpression of activin A in the skin of transgenic mice reveals new activities of activin in epidermal morphogenesis, dermal fibrosis and wound repair.* EMBO J, 1999. 18(19): p. 5205-15.

48. Shao, L.E., et al., *Contrasting effects of inflammatory cytokines and glucocorticoids on the production of activin A in human marrow stromal cells and their implications.* Cytokine, 1998. 10(3): p. 227-35.

49. Parrelli, J.M., N. Meisler, and K.R. Cutroneo, *Identification of a glucocorticoid response element in the human transforming growth factor beta 1 gene promoter.* Int J Biochem Cell Biol, 1998. 30(5): p. 623-7.

50. Oursler, M.J., B.L. Riggs, and T.C. Spelsberg, *Glucocorticoid-induced activation of latent transforming growth factor-beta by normal human osteoblast-like cells.* Endocrinology, 1993. 133(5): p. 2187-96.

51. Wankell, M., et al., *Impaired wound healing in transgenic mice overexpressing the activin antagonist follistatin in the epidermis.* EMBO J, 2001. 20(19): p. 5361-72.

52. Rajadurai, V.S. and K.H. Tan, *The use and abuse of steroids in perinatal medicine.* Ann Acad Med Singapore, 2003. 32(3): p.e 324-34.

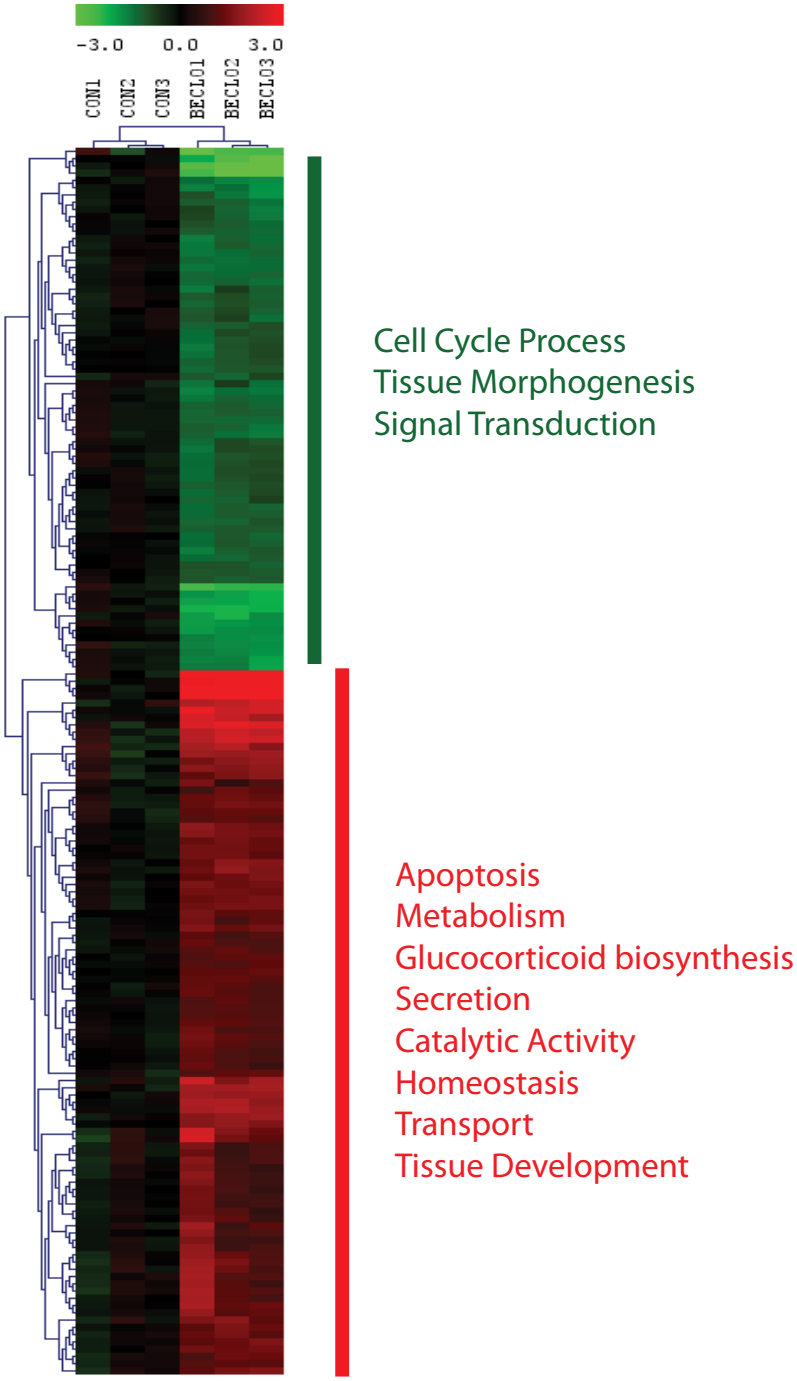

Figure 3- 1.Gene expression changes in larval regenerating fin tissue after exposure to BDP.
Heat map demonstrate bihierarchical clustering of 169 statistically significant ($p<0.05$) transcripts greater than two fold differentially expressed**.**

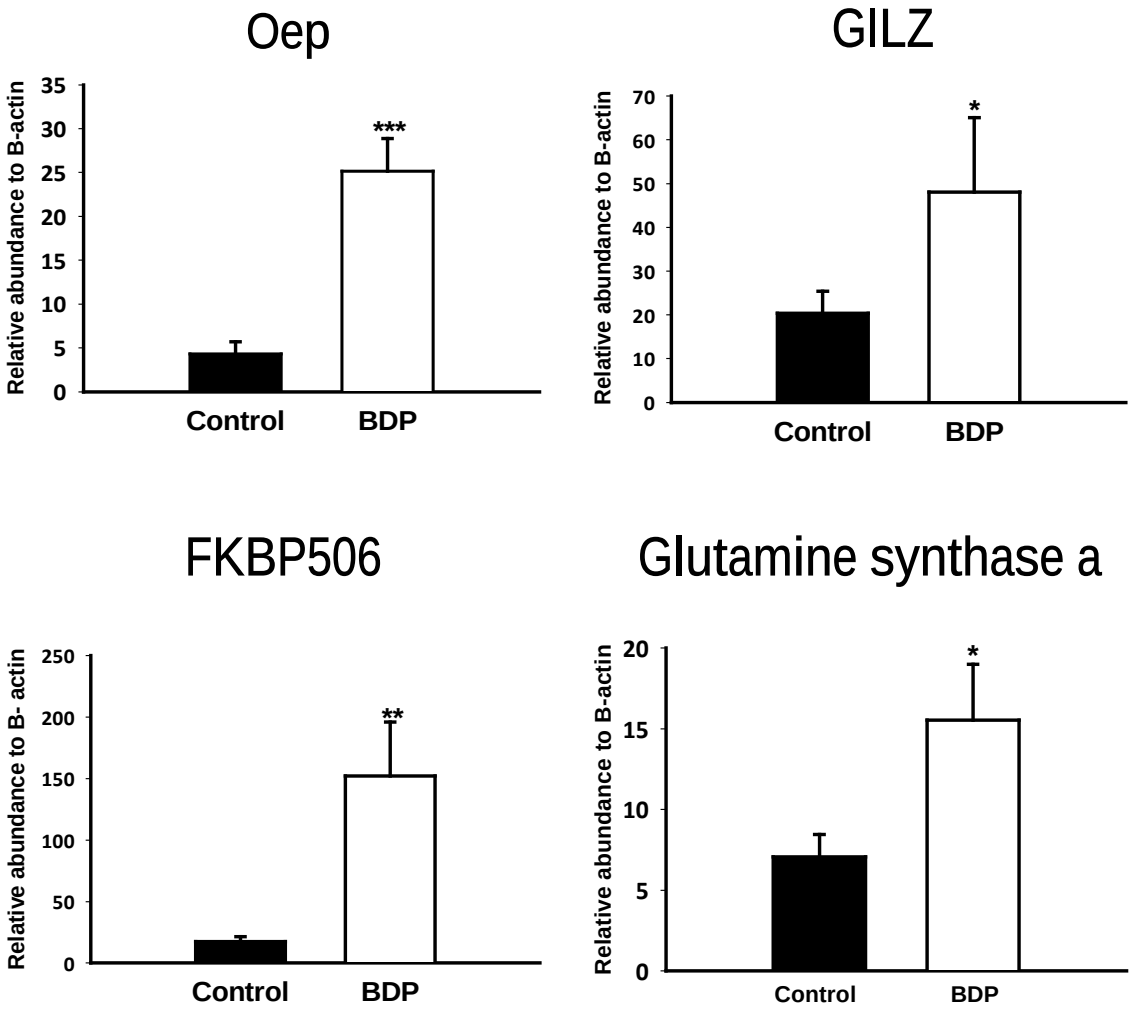

Figure 3- 2. qRT-PCR analysis of BDP enhanced transcripts in DMSO or BDP treated larval fin tissue at 1dpa.

The expression of *Cripto-1, GILZ, FKBP506* and *Glutamine synthase a* are illustrated as relative abundance to β actin mRNA levels. Gene specific primers were used to quantify mRNAs using real time qRT-PCR. Data presented as mean ±SEM (n=3). One way ANOVA was conducted to determine differences in expression. Asterisk indicate significant difference between vehicle and treatment ($p<0.05$).

a.

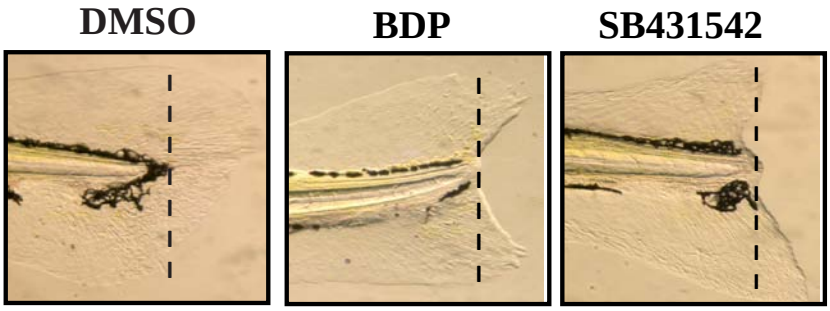
DMSO
BDP
SB431542

b.

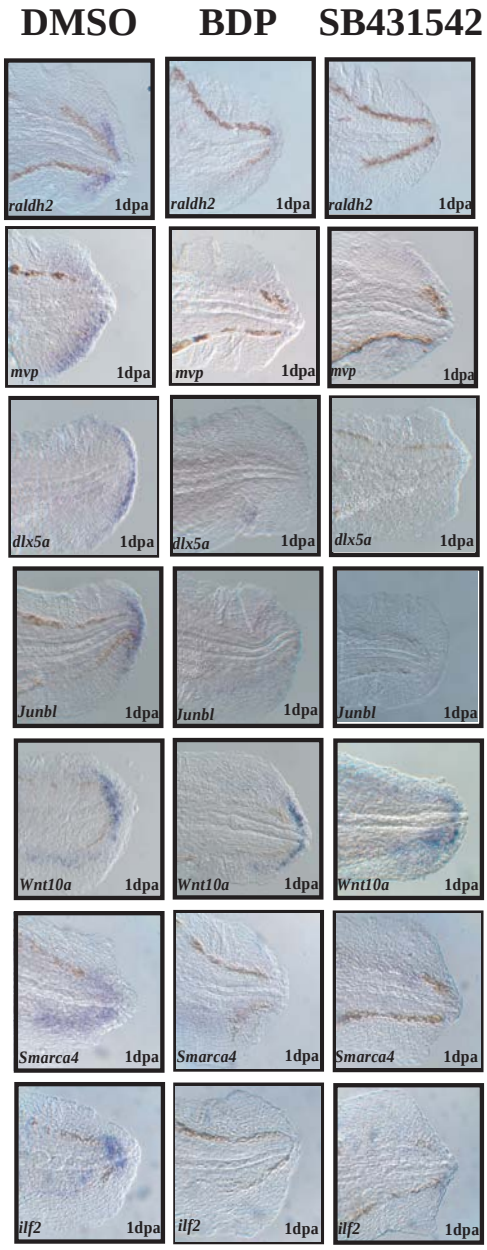
DMSO
BDP
SB431542
raldh2 1dpa
raldh2 1dpa
raldh2 1dpa
mvp 1dpa
mvp 1dpa
mvp 1dpa
dlx5a 1dpa
dlx5a 1dpa
dlx5a 1dpa
Junbl 1dpa
Junbl 1dpa
Junbl 1dpa
Wnt10a 1dpa
Wnt10a 1dpa
Wnt10a 1dpa
Smarca4 1dpa
Smarca4 1dpa
Smarca4 1dpa
ilf2 1dpa
ilf2 1dpa
ilf2 1dpa

Figure 3- 3. BDP and SB431542 impact larval regeneration.
a) Caudal fins of 2dpf larvae were amputated and exposed to 100 µM SB431542. Regenerative progression was evaluated and pictures taken at 3dpa **b)** *In situ* localization of *dlx5a, junbl, Wnt10a, ilf2, smarca4, raldh2 and mvp* in larvae exposed to BDP and SB431542 demonstrated a similar expression pattern.

a.

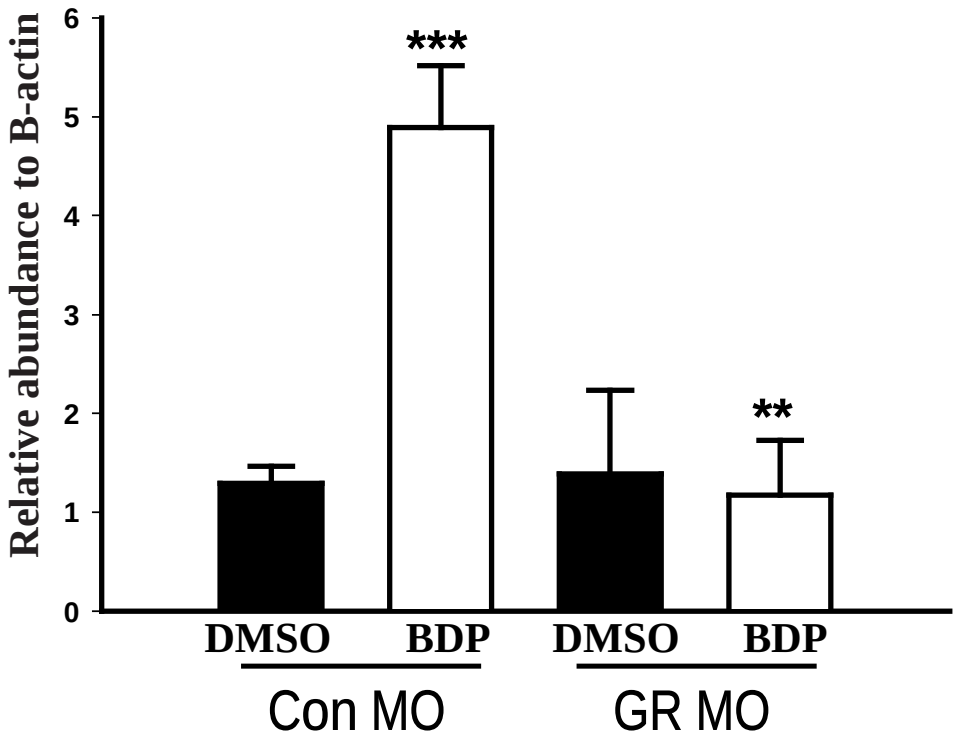
Relative abundance to B-actin
0
1
2
3
4
5
6
***
**
DMSO
BDP
DMSO
BDP
Con MO
GR MO

b.

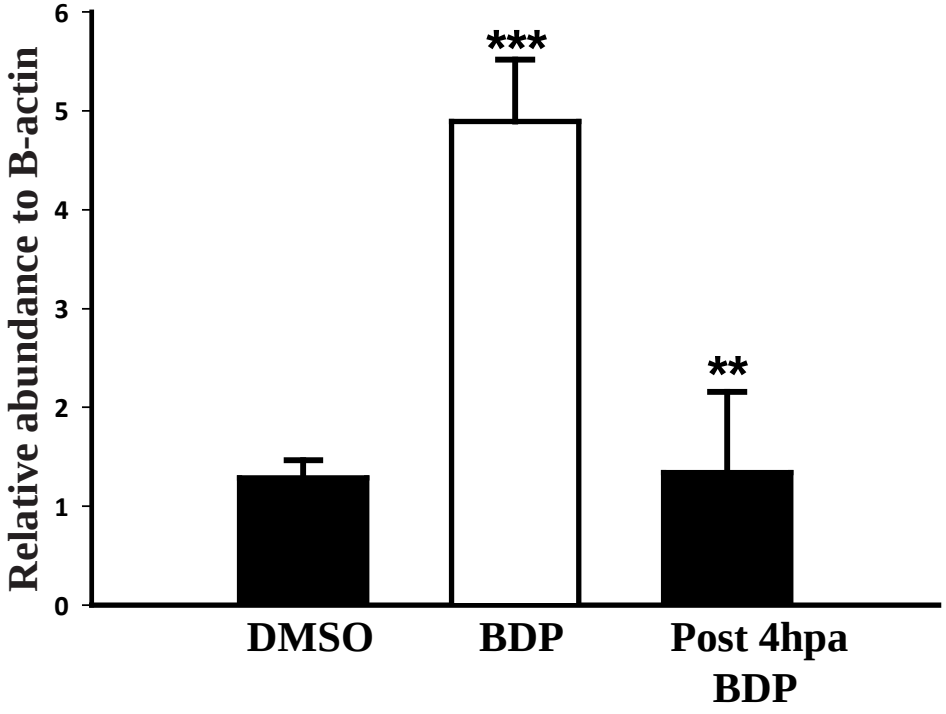
Relative abundance to B-actin
0
1
2
3
4
5
6
***
**
DMSO
BDP
Post 4hpa BDP

Figure 3- 4. BDP and SB431542 impact larval regeneration.
a) Caudal fins of 2dpf larvae were amputated and exposed to 100 µM SB431542. Regenerative progression was evaluated and pictures taken at 3dpa **b)** *In situ* localization of *dlx5a, junbl, Wnt10a,ilf2, smarca4, raldh2 and mvp* in larvae exposed to BDP and SB431542 demonstrated a similar expression pattern.

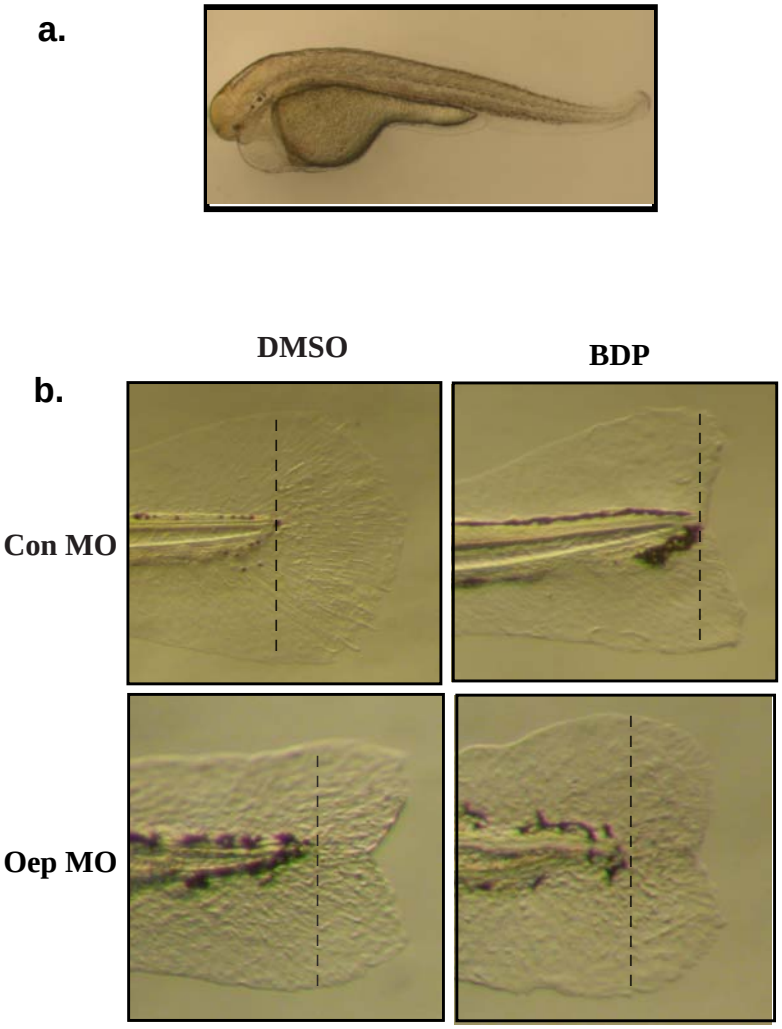

Figure 3- 5. Partial antisense repression of *Cripto-1* rescues inhibition of regeneration by BDP.
a) *Cripto-1* morphants Translation blocking *Cripto-1* MO transiently knocked down *Cripto-1.* The morphants developed characteristic one eyed pinhead phenotype by 2dpf. **b)** *Cripto-1* MO transiently knocked down *Cripto-1* compared to standard control morpholino injected embryo. The control and *Cripto-1* morphants were exposed to DMSO or BDP at 2dpf following amputation. The dotted lines mark the plane of amputation. Regenerative progression was evaluated and pictures taken at 3dpa.The experiments were repeated multiple times and ~80% of the *Cripto-1* morphants were resistant to inhibition of regeneration by BDP exposure.

a.

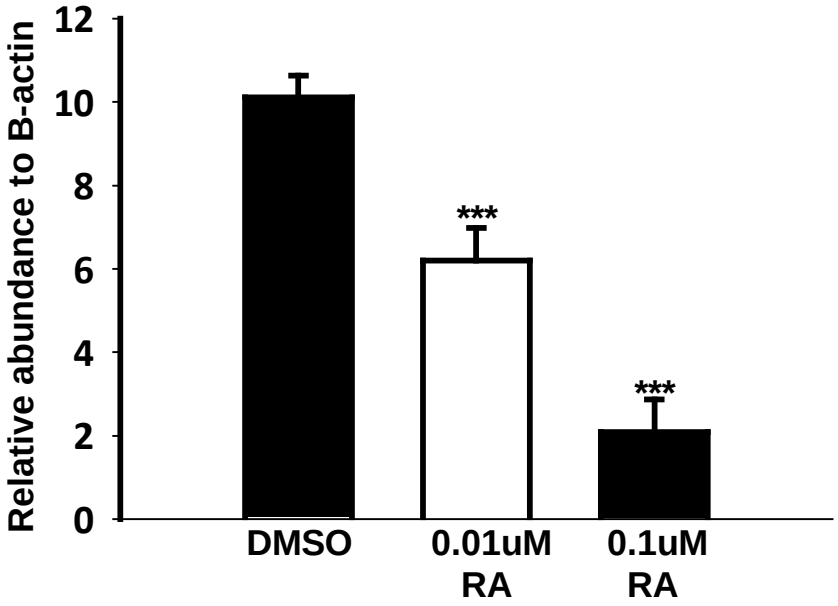
Relative abundance to B-actin
12
10
8
6
4
2
0
***
***
DMSO
0.01uM RA
0.1uM RA

b.

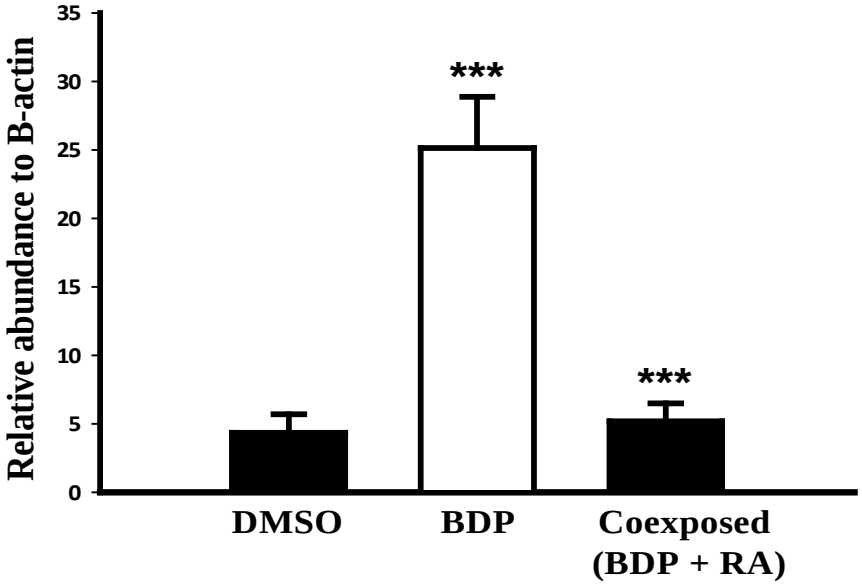
Relative abundance to B-actin
35
30
25
20
15
10
5
0
***
***
DMSO
BDP
Coexposed (BDP + RA)

c.

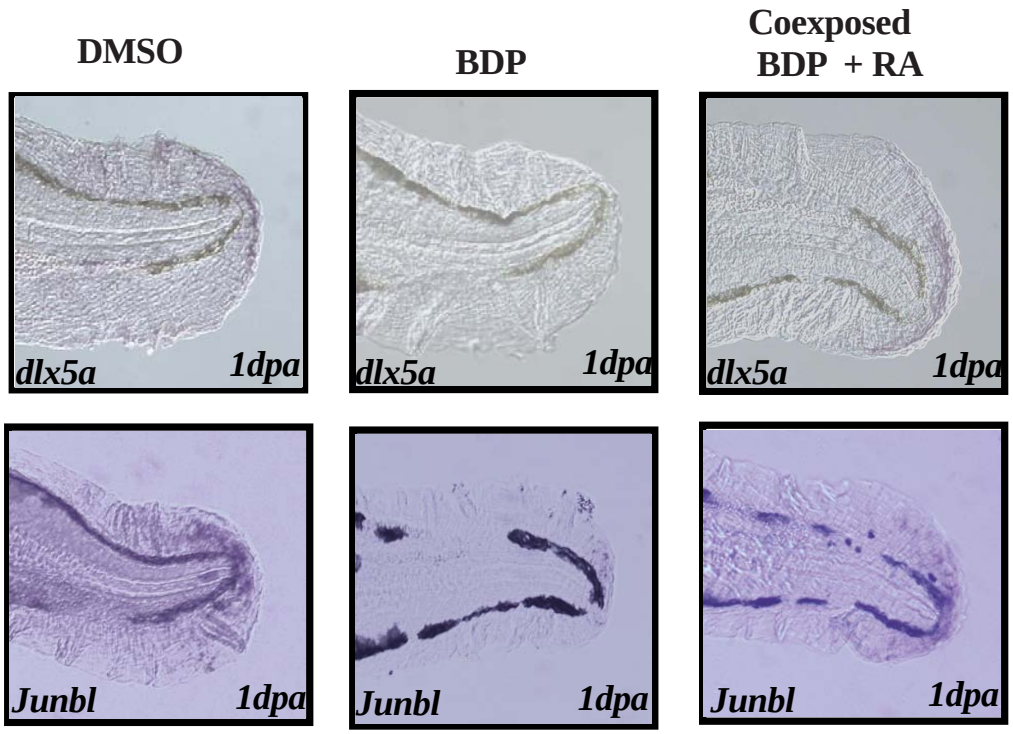
DMSO
BDP
Coexposed
BDP + RA
dlx5a
1dpa
dlx5a
1dpa
dlx5a
1dpa
Junbl
1dpa
Junbl
1dpa
Junbl
1dpa

d.

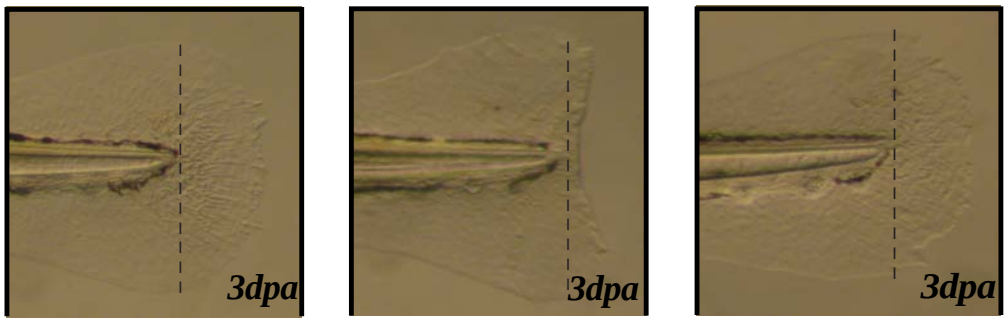
3dpa
3dpa
3dpa

Figure 3- 6.RA exposure suppress *Cripto-1* expression in the fin tissue and rescues BDP impaired regeneration.

a) Caudal fin of 2dpf embryos were amputated and exposed to DMSO or 0.01uM and 0.1uM RA. The abundance of *Cripto-1* was estimated in the regenerating fin tissues. The expression of *Cripto-1* was significantly reduced in a dose dependent manner compared to the control. The respective values represent the mean ±SEM and the asterisk indicate statistical significance (One way ANOVA, n=3).**b)** 2 dpf larvae were exposed to 0.1 µM RA for 8 hours followed by amputation and co exposure with 0.01uM RA with BDP. The abundance of *Cripto-1* was evaluated at 1dpa in the regenerating fin tissue by qRT-PCR. Co exposure with RA significantly suppresses *Cripto-1* expression compared to BDP exposure. The respective values represent the mean ±SEM and the asterisk indicate statistical significance (One way ANOVA, n=3). **c)** *In situ* localization of *dlx5a* and *junbl* in the regenerating fin tissue at 1dpa demonstrated restoration of regeneration markers in the caudal fin of larvae co exposed with BDP and RA. **d)** Amputated 2dpf larvae pre exposed with 1 µM RA were exposed to DMSO, BDP and co exposed with BDP and 0.01 µM RA. Regenerative progression was monitored and pictures were taken at 3dpa. The experiment was repeated multiple times and regeneration was restored in ~90% embryos co exposed to BDP and RA compared to BDP alone.

a.

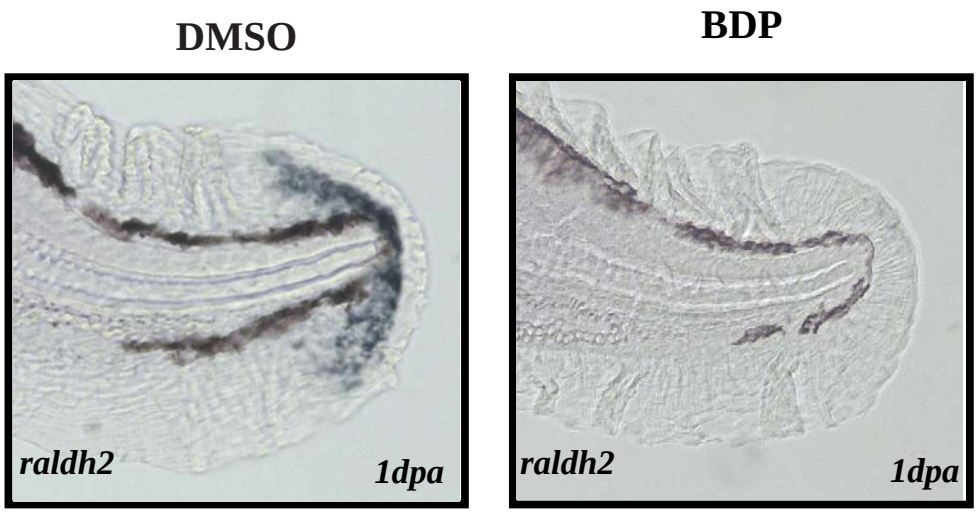

b.

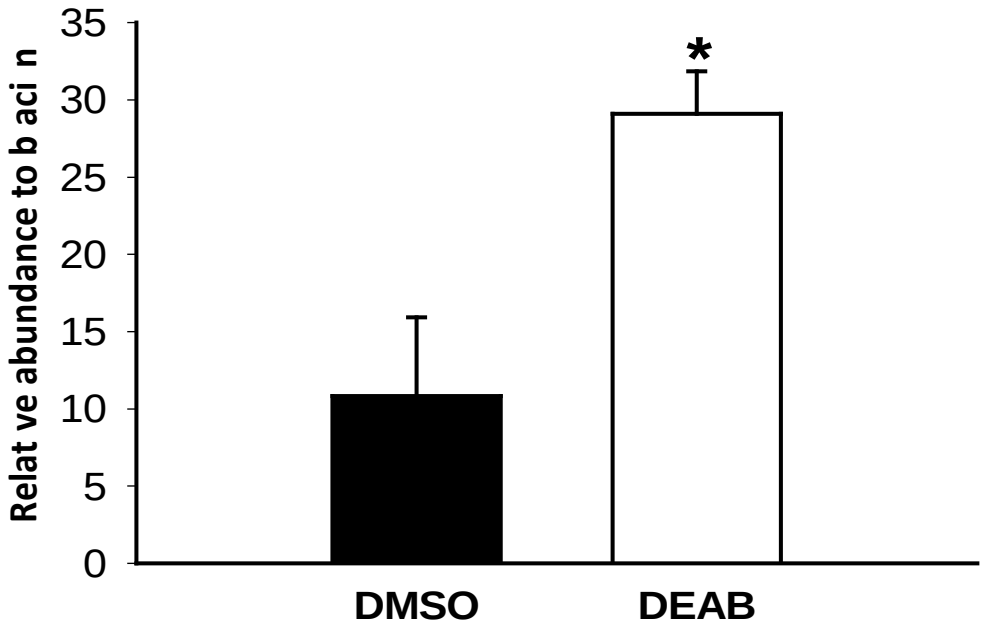

Figure 3- 7. BDP exposure suppress RA signaling.
a) BDP suppressed *raldh2* expression. 2dpf larvae were amputated and exposed to DMSO and BDP. *In situ* hybridization analysis revealed loss of *raldh2* expression in the fin tissue of the BDP exposed larvae. **b)** DEAB exposure induce *Cripto-1* expression at 1dpa. 2dpf larvae were amputated and exposed to DMSO and DEAB. qRT-PCR analysis of *Cripto-1* in DEAB exposed embryos demonstrate induced expression at 1dpa.

Table 3- 1.Classification of transcripts altered by BDP exposure according to function.

Human orthologues of transcripts altered greater than 2 fold by BDP exposure were analyzed by Ingenuity software and grouped according to their biological function.

Genes	Fold change	
Cell Death		
SOCS3	2.03	UP
ANGPT2	2.46	UP
CDC20	2.12	DOWN
DLX4b	2.06	DOWN
BCL2L13	2.26	UP
ATP1A1	2.50	UP
DKK3	4.33	DOWN
ANXA1	6.44	DOWN
HSD11B2	14.36	UP
GFAP	2.04	UP
FKBP5	6.33	UP
SNCB	2.18	UP
TYMS	2.05	DOWN
DLL1	2.00	UP
UCP2	2.57	UP
RRM2	2.09	DOWN
TDGF1	8.53	UP
ANXA4	3.13	UP
PLK1	2.08	DOWN
GSN	2.25	DOWN
XIAP	2.41	UP
PFKM	2.43	UP
DUSP1	3.87	UP
DCT	2.05	UP
ADCYAP1	2.03	UP
HMGB2	2.18	DOWN
Connective Tissue Development and Function		
SOCS3	2.03	UP
ANGPT2	2.46	UP
SLC4A2	2.04	DOWN
ANXA1	6.44	DOWN
HMX3	2.04	UP
HSD11B2	14.36	UP
ADCYAP1	2.03	UP
GSN	2.25	DOWN
Cellular Growth and Proliferation		
KIF23	2.29	DOWN
TYMS	2.05	DOWN
SOCS3	2.03	UP
DLL1		
SLC4A2	2.04	DOWN
TDGF1	8.53	UP
PLK1	2.08	DOWN
XIAP	2.41	UP
DUSP1	3.87	UP
DKK3	4.33	DOWN
ANXA1	6.44	DOWN
HSD11B2	14.36	UP
FKBP5	6.33	UP
ADCYAP1	2.03	UP

Cell Signaling		
SOCS3	2.03	UP
SYT4	2.52	UP
ANGPT2	2.46	UP
UCP2	2.57	UP
DUSP1	3.87	UP
CPLX2	3.44	UP
ANXA1	6.44	DOWN
GSN	2.25	DOWN
ADCYAP1	2.03	UP
XIAP	2.41	UP

Connective Tissue Disorders		
SOCS3	2.03	UP
SLC4A2	2.04	DOWN

Gene Expression		
SOCS3	2.03	UP
PTGES3 (includes EG:10728)	2.04	UP
SMC2	2.49	DOWN
DLX4	2.06	DOWN
ADCYAP1	2.03	UP
HMGB2	2.18	DOWN

Cell-To-Cell Signaling and Interaction		
TYMS	2.05	DOWN
ANGPT2	2.46	UP
SLC4A2	2.04	DOWN
UCP2	2.57	UP
DKK3	4.33	DOWN
ANXA1	6.44	DOWN
GFAP	2.04	UP
GPM6A	2.13	UP
DCT	2.05	UP
ADCYAP1	2.03	UP

Inflammatory Response		
SOCS3	2.03	UP
ANGPT2	2.46	UP
UCP2	2.57	UP
DUSP1	3.87	UP
ANXA1	6.44	DOWN
ADCYAP1	2.03	UP
GSN	2.25	DOWN

Cell Cycle		
TYMS	2.05	DOWN
KIF23	2.29	DOWN
NUSAP1	2.01	DOWN
CDC20	2.01	UP
ORC6L	2.33	DOWN
PLK1	2.08	DOWN
PTGES3 (includes EG:10728)	2.04	UP
SMC2	2.49	DOWN
DUSP1	3.87	UP
ASPM	2.09	DOWN
ANXA1	6.44	DOWN
ADCYAP1	2.03	UP
KIF11	2.25	DOWN

Cellular Movement		
KIF23	2.29	DOWN
SOCS3	2.03	UP
SYT4	2.52	UP
NUSAP1	2.01	DOWN
ANGPT2	2.46	UP
UCP2	2.57	UP
CDC20	2.12	DOWN
TDGF1	8.53	UP
PLK1	2.08	DOWN
GSN	2.25	DOWN
DKK3	4.33	DOWN
DUSP1	3.87	UP
CPLX2	3.44	UP
ANXA1	6.44	DOWN
Tissue Morphology		
TYMS	2.05	DOWN
SOCS3	2.03	UP
CA2	2.57	DOWN
ANGPT2	2.46	UP
SLC4A2	2.04	DOWN
TDGF1	8.53	UP
GSN	2.25	DOWN
XIAP	2.41	UP
DKK3	4.33	DOWN
ANXA1	6.44	DOWN
HSD11B2	14.36	UP
GFAP	2.04	UP
ADCYAP1	2.03	UP
Tissue Development		
SOCS3	2.03	UP
CA2	2.57	DOWN
ANGPT2	2.46	UP
DLL1		
DKK3	4.33	DOWN
TDGF1	8.53	UP
HMX3	2.04	UP
PLK1	2.08	DOWN
GSN	2.25	DOWN
ADCYAP1	2.03	UP

Table 3- 2. Identification of GREs upstream of TSS of *Cripto-1*.

GREs	Strand	Start position from TSS
GR alpha /PR /PR /GR beta	R	-68
AR / GR /PR / PR /PR	N	-68
GR/PR	N	-68
GR	R	-68
GR	R	-69
GR	N	-86
GR	R	-98
GR	N	-257
GR	R	-268
GR	N	-627
GR	R	-702
GR	R	-755
GR	R	-808
GR	N	-1033
GR	R	-1076
GR	N	-1153
GR	N	-1317
GR/PR	R	-1339
GR	N	-1470
GR	N	-1509

Table 3S- 1.List of selected genes that were at least 2.5 fold differentially abundant in BDP exposed fin regenerates compared to vehicle control.

Gene	Affymetrix probe ID	Fold change	
Endocrine System Development and Function			
CYP17A1	Dr.25390.1.A1_s_at	2.2035047	DOWN
atp1a1a.2	Dr.10343.1.S1_at	2.5449067	UP
ANGPT2	Dr.12620.1.S1_at	2.4642771	UP
anxa1b	Dr.1190.1.S1_at	6.4396889	DOWN
anxa1c	Dr.4833.1.S1_at	2.3146753	DOWN
hsd11b2	Dr.12359.1.A1_at	14.363574	UP
fkbp5	Dr.2675.1.A1_at	6.3346811	UP
adcyap1b	Dr.10739.2.S1_a_at	2.0281092	UP
Lipid Metabolism			
CYP17A1	Dr.25390.1.A1_s_at	2.2035047	DOWN
socs3a	Dr.6431.1.S1_at	2.0352392	UP
atp1a1a.2	Dr.10343.1.S1_at	2.5449067	UP
ANGPT2	Dr.12620.1.S1_at	2.4642771	UP
ptges3	Dr.5031.1.S1_at	2.0355733	UP
ucp2	Dr.21244.1.S1_at	2.5751274	UP
anxa1b	Dr.1190.1.S1_at	6.4396889	DOWN
anxa1c	Dr.4833.1.S1_at	2.3146753	DOWN
hsd11b2	Dr.12359.1.A1_at	14.363574	UP
gsnb	Dr.4727.1.A1_at	2.2533439	DOWN
fkbp5	Dr.2675.1.A1_at	6.3346811	UP
adcyap1b	Dr.10739.2.S1_a_at	2.0281092	UP
Small Molecule Biochemistry			
tyms	Dr.1047.1.S1_at	2.0492052	DOWN
ca2	Dr.10405.1.S1_at	2.5744109	DOWN
syt4	Dr.13868.1.S1_at	2.5230733	UP
socs3a	Dr.6431.1.S1_at	2.0352392	UP
ANGPT2	Dr.12620.1.S1_at	2.4642771	UP
ucp2	Dr.21244.1.S1_at	2.5751274	UP
rrm2	Dr.1691.1.S1_at	2.0947138	DOWN
TDGF1(oep)	Dr.581.1.S1_at	8.5301637	UP
gsnb	Dr.4727.1.A1_at	2.2533439	DOWN
xiap	Dr.12645.1.S1_at	2.4127052	UP
RRM1 (includes EG:6240)(LOC561592)	Dr.1691.1.S1_at	2.0947138	DOWN
dusp1	Dr.2413.1.S1_at	3.8725208	UP
anxa1b	Dr.1190.1.S1_at	6.4396889	DOWN
anxa1c	Dr.4833.1.S1_at	2.3146753	DOWN
hsd11b2	Dr.12359.1.A1_at	14.363574	UP
glula	Dr.4147.1.S1_at	2.8466879	UP
fkbp5	Dr.2675.1.A1_at	6.3346811	UP

fkbp5	Dr.2675.1.A1_at	6.3346811	UP
sncb	Dr.7855.1.A1_at	2.1825081	UP
gldc	Dr.24995.4.S1_at	4.9345554	UP
adcyap1b	Dr.10739.2.S1_a_at	2.0281092	UP
gatm	Dr.1064.1.S1_at	2.7011572	UP
Vitamin and Mineral Metabolism			
CYP17A1	Dr.25390.1.A1_s_at	2.2035047	DOWN
ATP1A1	Dr.10343.1.S1_at	2.5449067	UP
ANGPT2	Dr.12620.1.S1_at	2.4642771	UP
anxa1b	Dr.1190.1.S1_at	6.4396889	DOWN
anxa1c	Dr.4833.1.S1_at	2.3146753	DOWN
HSD11B2	Dr.12359.1.A1_at	14.363574	UP
GSN	Dr.4727.1.A1_at	2.2533439	DOWN
ADCYAP1	Dr.10739.2.S1_a_at	2.0281092	UP
Cell Death			
SOCS3	Dr.6431.1.S1_at	2.0352392	UP
CA2	Dr.10405.1.S1_at	2.5744109	DOWN
ANGPT2	Dr.12620.1.S1_at	2.4642771	UP
CDC20	Dr.26337.1.A1_at	2.1234569	DOWN
DLX4	Dr.153.1.S1_at	2.0558797	DOWN
BCL2L13	Dr.9893.1.A1_at	2.2586546	UP
ATP1A1	Dr.10343.1.S1_at	2.5449067	UP
DKK3	Dr.19049.1.A1_at	4.325465	DOWN
anxa1b	Dr.1190.1.S1_at	6.4396889	DOWN
anxa1c	Dr.4833.1.S1_at	2.3146753	DOWN
HSD11B2	Dr.12359.1.A1_at	14.363574	UP
GFAP	Dr.14127.1.S1_at	2.0415683	UP
FKBP5	Dr.2675.1.A1_at	6.3346811	UP
SNCB	Dr.7855.1.A1_at	2.1825081	UP
TYMS	Dr.1047.1.S1_at	2.0492052	DOWN
UCP2	Dr.21244.1.S1_at	2.5751274	UP
RRM2	Dr.1691.1.S1_at	2.0947138	DOWN
TDGF1	Dr.581.1.S1_at	8.5301637	UP
ANXA4	Dr.7269.1.A1_at	3.126881	UP
PLK1	Dr.20131.4.S1_at	2.0847763	DOWN
GSN	Dr.4727.1.A1_at	2.2533439	DOWN
XIAP	Dr.12645.1.S1_at	2.4127052	UP
PFKM	Dr.13621.1.A1_at	2.4286138	UP
DUSP1	Dr.2413.1.S1_at	3.8725208	UP
DCT	Dr.10336.1.S1_at	2.0475848	UP
ADCYAP1	Dr.10739.2.S1_a_at	2.0281092	UP
HMGB2	Dr.9746.12.S1_at	2.1815386	DOWN
Antigen Presentation			
ANGPT2	Dr.12620.1.S1_at	2.4642771	UP
UCP2	Dr.21244.1.S1_at	2.5751274	UP

anxa1b	Dr.1190.1.S1_at	6.4396889	DOWN
anxa1c	Dr.4833.1.S1_at	2.3146753	DOWN
ADCYAP1	Dr.10739.2.S1_a_at	2.0281092	UP
Cell-To-Cell Signaling and Interaction			
TYMS	Dr.1047.1.S1_at	2.0492052	DOWN
ANGPT2	Dr.12620.1.S1_at	2.4642771	UP
SLC4A2	Dr.1658.1.A1_at	2.0370382	DOWN
UCP2	Dr.21244.1.S1_at	2.5751274	UP
DKK3	Dr.19049.1.A1_at	4.325465	DOWN
anxa1b	Dr.1190.1.S1_at	6.4396889	DOWN
anxa1c	Dr.4833.1.S1_at	2.3146753	DOWN
GFAP	Dr.14127.1.S1_at	2.0415683	UP
GPM6A	Dr.5434.3.S1_at	2.1269987	UP
DCT	Dr.10336.1.S1_at	2.0475848	UP
ADCYAP1	Dr.10739.2.S1_a_at	2.0281092	UP
Hematological System Development and Function			
SOCS3	Dr.6431.1.S1_at	2.0352392	UP
ANGPT2	Dr.12620.1.S1_at	2.4642771	UP
UCP2	Dr.21244.1.S1_at	2.5751274	UP
DKK3	Dr.19049.1.A1_at	4.325465	DOWN
DUSP1	Dr.2413.1.S1_at	3.8725208	UP
anxa1b	Dr.1190.1.S1_at	6.4396889	DOWN
anxa1c	Dr.4833.1.S1_at	2.3146753	DOWN
GFAP	Dr.14127.1.S1_at	2.0415683	UP
GSN	Dr.4727.1.A1_at	2.2533439	DOWN
ADCYAP1	Dr.10739.2.S1_a_at	2.0281092	UP
Immune Cell Trafficking			
SOCS3	Dr.6431.1.S1_at	2.0352392	UP
ANGPT2	Dr.12620.1.S1_at	2.4642771	UP
UCP2	Dr.21244.1.S1_at	2.5751274	UP
DUSP1	Dr.2413.1.S1_at	3.8725208	UP
anxa1b	Dr.1190.1.S1_at	6.4396889	DOWN
anxa1c	Dr.4833.1.S1_at	2.3146753	DOWN
GFAP	Dr.14127.1.S1_at	2.0415683	UP
ADCYAP1	Dr.10739.2.S1_a_at	2.0281092	UP
GSN	Dr.4727.1.A1_at	2.2533439	DOWN
Inflammatory Response			
SOCS3	Dr.6431.1.S1_at	2.0352392	UP
ANGPT2	Dr.12620.1.S1_at	2.4642771	UP
UCP2	Dr.21244.1.S1_at	2.5751274	UP
DUSP1	Dr.2413.1.S1_at	3.8725208	UP
anxa1b	Dr.1190.1.S1_at	6.4396889	DOWN
anxa1c	Dr.4833.1.S1_at	2.3146753	DOWN
ADCYAP1	Dr.10739.2.S1_a_at	2.0281092	UP
GSN	Dr.4727.1.A1_at	2.2533439	DOWN

Amino Acid Metabolism			
DUSP1	Dr.2413.1.S1_at	3.8725208	UP
TDGF1	Dr.581.1.S1_at	8.5301637	UP
GLUL	Dr.4147.1.S1_at	2.8466879	UP
GLDC	Dr.24995.4.S1_at	4.9345554	UP
GATM	Dr.1064.1.S1_at	2.7011572	UP
Nucleic Acid Metabolism			
TYMS	Dr.1047.1.S1_at	2.0492052	DOWN
UCP2	Dr.21244.1.S1_at	2.5751274	UP
RRM2	Dr.1691.1.S1_at	2.0947138	DOWN
ADCYAP1	Dr.10739.2.S1_a_at	2.0281092	UP
GATM	Dr.1064.1.S1_at	2.7011572	UP
RRM1 (includes EG:6240)	Dr.1691.1.S1_at	2.0947138	DOWN
Post-Translational Modification			
DUSP1	Dr.2413.1.S1_at	3.8725208	UP
TDGF1	Dr.581.1.S1_at	8.5301637	UP
GLUL	Dr.4147.1.S1_at	2.8466879	UP
GSN	Dr.4727.1.A1_at	2.2533439	DOWN
GLDC	Dr.24995.4.S1_at	4.9345554	UP
GATM	Dr.1064.1.S1_at	2.7011572	UP
Infectious Disease			
CYP17A1	Dr.25390.1.A1_s_at	2.2035047	DOWN
TYMS	Dr.1047.1.S1_at	2.0492052	DOWN
PTGES3 (includes EG:10728)	Dr.5031.1.S1_at	2.0355733	UP
RRM2	Dr.1691.1.S1_at	2.0947138	DOWN
PLK1	Dr.20131.4.S1_at	2.0847763	DOWN
MUS81	Dr.977.2.A1_at	2.0307253	DOWN
XIAP	Dr.12645.1.S1_at	2.4127052	UP
RRM1 (includes EG:6240)	Dr.1691.1.S1_at	2.0947138	DOWN
PFKM	Dr.13621.1.A1_at	2.4286138	UP
Inflammatory Disease			
CYP17A1	Dr.25390.1.A1_s_at	2.2035047	DOWN
TYMS	Dr.1047.1.S1_at	2.0492052	DOWN
SOCS3	Dr.6431.1.S1_at	2.0352392	UP
ATP1A1	Dr.10343.1.S1_at	2.5449067	UP
DUSP1	Dr.2413.1.S1_at	3.8725208	UP
RRM2	Dr.1691.1.S1_at	2.0947138	DOWN
RRM1 (includes EG:6240)	Dr.1691.1.S1_at	2.0947138	DOWN
Neurological Disease			
CA2	Dr.10405.1.S1_at	2.5744109	DOWN
ANGPT2	Dr.12620.1.S1_at	2.4642771	UP
SQRDL (includes EG:58472)			
ATP1A1	Dr.10343.1.S1_at	2.5449067	UP
PTGES3 (includes EG:10728)	Dr.5031.1.S1_at	2.0355733	UP
DKK3	Dr.19049.1.A1_at	4.325465	DOWN

CPLX2	Dr.3989.1.A1_at	3.4392884	UP
ASPM	Dr.19463.1.S1_at	2.0901034	DOWN
GFAP	Dr.14127.1.S1_at	2.0415683	UP
SNCB	Dr.7855.1.A1_at	2.1825081	UP
FKBP5	Dr.2675.1.A1_at	6.3346811	UP
GATM	Dr.1064.1.S1_at	2.7011572	UP
TYMS	Dr.1047.1.S1_at	2.0492052	DOWN
SYT4	Dr.13868.1.S1_at	2.5230733	UP
UCP2	Dr.21244.1.S1_at	2.5751274	UP
RRM2	Dr.1691.1.S1_at	2.0947138	DOWN
PLK1	Dr.20131.4.S1_at	2.0847763	DOWN
GNG3	Dr.10136.1.S1_at	2.4031136	UP
GSN	Dr.4727.1.A1_at	2.2533439	DOWN
XIAP	Dr.12645.1.S1_at	2.4127052	UP
RRM1 (includes EG:6240)	Dr.1691.1.S1_at	2.0947138	DOWN
PFKM	Dr.13621.1.A1_at	2.4286138	UP
PDLIM7	Dr.16051.1.S1_at	2.2162526	UP
HCN2	Dr.22826.1.A1_at	2.6670146	UP
ADCYAP1	Dr.10739.2.S1_a_at	2.0281092	UP
GLDC	Dr.24995.4.S1_at	4.9345554	UP
KIF11	Dr.1557.1.S1_at	2.2506299	DOWN
HMGB2	Dr.9746.12.S1_at	2.1815386	DOWN

Cancer

KIF23	Dr.8295.1.S1_at	2.2917949	DOWN
SOCS3	Dr.6431.1.S1_at	2.0352392	UP
CA2	Dr.10405.1.S1_at	2.5744109	DOWN
ANGPT2	Dr.12620.1.S1_at	2.4642771	UP
CDC20	Dr.26337.1.A1_at	2.1234569	DOWN
CYP17A1	Dr.25390.1.A1_s_at	2.2035047	DOWN
ATP1A1	Dr.10343.1.S1_at	2.5449067	UP
anxa1b	Dr.1190.1.S1_at	6.4396889	DOWN
anxa1c	Dr.4833.1.S1_at	2.3146753	DOWN
HSD11B2	Dr.12359.1.A1_at	14.363574	UP
GFAP	Dr.14127.1.S1_at	2.0415683	UP
TYMS	Dr.1047.1.S1_at	2.0492052	DOWN
UCP2	Dr.21244.1.S1_at	2.5751274	UP
RRM2	Dr.1691.1.S1_at	2.0947138	DOWN
TDGF1	Dr.581.1.S1_at	8.5301637	UP
PPL	Dr.9761.1.S1_at	2.1069557	DOWN
ANXA4	Dr.7269.1.A1_at	3.126881	UP
PLK1	Dr.20131.4.S1_at	2.0847763	DOWN
GSN	Dr.4727.1.A1_at	2.2533439	DOWN
XIAP	Dr.12645.1.S1_at	2.4127052	UP
RRM1 (includes EG:6240)	Dr.1691.1.S1_at	2.0947138	DOWN
DUSP1	Dr.2413.1.S1_at	3.8725208	UP
GLUL	Dr.4147.1.S1_at	2.8466879	UP
GPM6A	Dr.5434.3.S1_at	2.1269987	UP

DCT	Dr.10336.1.S1_at	2.0475848	UP
KIF11	Dr.1557.1.S1_at	2.2506299	DOWN
HMGB2	Dr.9746.12.S1_at	2.1815386	DOWN
Genetic Disorder			
SOCS3	Dr.6431.1.S1_at	2.0352392	UP
CA2	Dr.10405.1.S1_at	2.5744109	DOWN
SLC4A2	Dr.1658.1.A1_at	2.0370382	DOWN
CDC20	Dr.26337.1.A1_at	2.1234569	DOWN
CYP17A1	Dr.25390.1.A1_s_at	2.2035047	DOWN
ATP1A1	Dr.10343.1.S1_at	2.5449067	UP
CPLX2	Dr.3989.1.A1_at	3.4392884	UP
DKK3	Dr.19049.1.A1_at	4.325465	DOWN
HSD11B2	Dr.12359.1.A1_at	14.363574	UP
GFAP	Dr.14127.1.S1_at	2.0415683	UP
SNCB	Dr.7855.1.A1_at	2.1825081	UP
ESCO2	Dr.3337.1.S1_at	2.0632125	DOWN
TYMS	Dr.1047.1.S1_at	2.0492052	DOWN
SYT4	Dr.13868.1.S1_at	2.5230733	UP
UCP2	Dr.21244.1.S1_at	2.5751274	UP
RRM2	Dr.1691.1.S1_at	2.0947138	DOWN
ANXA4	Dr.7269.1.A1_at	3.126881	UP
PLK1	Dr.20131.4.S1_at	2.0847763	DOWN
GNG3	Dr.10136.1.S1_at	2.4031136	UP
GSN	Dr.4727.1.A1_at	2.2533439	DOWN
XIAP	Dr.12645.1.S1_at	2.4127052	UP
RRM1 (includes EG:6240)	Dr.1691.1.S1_at	2.0947138	DOWN
PFKM	Dr.13621.1.A1_at	2.4286138	UP
PDLIM7	Dr.16051.1.S1_at	2.2162526	UP
DUSP1	Dr.2413.1.S1_at	3.8725208	UP
GLUL	Dr.4147.1.S1_at	2.8466879	UP
GLDC	Dr.24995.4.S1_at	4.9345554	UP
KIF11	Dr.1557.1.S1_at	2.2506299	DOWN
HMGB2	Dr.9746.12.S1_at	2.1815386	DOWN
Respiratory Disease			
CYP17A1	Dr.25390.1.A1_s_at	2.2035047	DOWN
TYMS	Dr.1047.1.S1_at	2.0492052	DOWN
SOCS3	Dr.6431.1.S1_at	2.0352392	UP
CDC20	Dr.26337.1.A1_at	2.1234569	DOWN
DUSP1	Dr.2413.1.S1_at	3.8725208	UP
RRM2	Dr.1691.1.S1_at	2.0947138	DOWN
PLK1	Dr.20131.4.S1_at	2.0847763	DOWN
GSN	Dr.4727.1.A1_at	2.2533439	DOWN
XIAP	Dr.12645.1.S1_at	2.4127052	UP
KIF11	Dr.1557.1.S1_at	2.2506299	DOWN
RRM1 (includes EG:6240)	Dr.1691.1.S1_at	2.0947138	DOWN

Reproductive System Disease			
TYMS	Dr.1047.1.S1_at	2.0492052	DOWN
SOCS3	Dr.6431.1.S1_at	2.0352392	UP
CDC20	Dr.26337.1.A1_at	2.1234569	DOWN
RRM2	Dr.1691.1.S1_at	2.0947138	DOWN
TDGF1	Dr.581.1.S1_at	8.5301637	UP
PLK1	Dr.20131.4.S1_at	2.0847763	DOWN
GSN	Dr.4727.1.A1_at	2.2533439	DOWN
RRM1 (includes EG:6240)	Dr.1691.1.S1_at	2.0947138	DOWN
CYP17A1	Dr.25390.1.A1_s_at	2.2035047	DOWN
DUSP1	Dr.2413.1.S1_at	3.8725208	UP
anxa1b	Dr.1190.1.S1_at	6.4396889	DOWN
anxa1c	Dr.4833.1.S1_at	2.3146753	DOWN
GPM6A	Dr.5434.3.S1_at	2.1269987	UP
KIF11	Dr.1557.1.S1_at	2.2506299	DOWN
Nervous System Development and Function			
SYT4	Dr.13868.1.S1_at	2.5230733	UP
ANGPT2	Dr.12620.1.S1_at	2.4642771	UP
ASPM	Dr.19463.1.S1_at	2.0901034	DOWN
CPLX2	Dr.3989.1.A1_at	3.4392884	UP
anxa1b	Dr.1190.1.S1_at	6.4396889	DOWN
anxa1c	Dr.4833.1.S1_at	2.3146753	DOWN
HSD11B2	Dr.12359.1.A1_at	14.363574	UP
GPM6A	Dr.5434.3.S1_at	2.1269987	UP
GFAP	Dr.14127.1.S1_at	2.0415683	UP
SNCB	Dr.7855.1.A1_at	2.1825081	UP
ADCYAP1	Dr.10739.2.S1_a_at	2.0281092	UP
Skeletal and Muscular System Development and Function			
SOCS3	Dr.6431.1.S1_at	2.0352392	UP
SYT4	Dr.13868.1.S1_at	2.5230733	UP
ANGPT2	Dr.12620.1.S1_at	2.4642771	UP
SLC4A2	Dr.1658.1.A1_at	2.0370382	DOWN
DUSP1	Dr.2413.1.S1_at	3.8725208	UP
HCN2	Dr.22826.1.A1_at	2.6670146	UP
HMX3	Dr.10448.1.S1_at	2.0356157	UP
HSD11B2	Dr.12359.1.A1_at	14.363574	UP
SNCB	Dr.7855.1.A1_at	2.1825081	UP
ADCYAP1	Dr.10739.2.S1_a_at	2.0281092	UP
GSN	Dr.4727.1.A1_at	2.2533439	DOWN
Cell Cycle			
TYMS	Dr.1047.1.S1_at	2.0492052	DOWN
KIF23	Dr.8295.1.S1_at	2.2917949	DOWN
NUSAP1	Dr.7155.2.S1_a_at	2.0110543	DOWN
CDC20	Dr.26337.1.A1_at	2.1234569	DOWN

ORC6L	Dr.24945.1.S1_at	2.3332334	DOWN
PLK1	Dr.20131.4.S1_at	2.0847763	DOWN
PTGES3 (includes EG:10728)	Dr.5031.1.S1_at	2.0355733	UP
SMC2	Dr.20402.1.A1_at	2.4920971	DOWN
DUSP1	Dr.2413.1.S1_at	3.8725208	UP
ASPM	Dr.19463.1.S1_at	2.0901034	DOWN
anxa1b	Dr.1190.1.S1_at	6.4396889	DOWN
anxa1c	Dr.4833.1.S1_at	2.3146753	DOWN
ADCYAP1	Dr.10739.2.S1_a_at	2.0281092	UP
KIF11	Dr.1557.1.S1_at	2.2506299	DOWN
Cellular Assembly and Organization			
KIF23	Dr.8295.1.S1_at	2.2917949	DOWN
SYT4	Dr.13868.1.S1_at	2.5230733	UP
ANGPT2	Dr.12620.1.S1_at	2.4642771	UP
SLC4A2	Dr.1658.1.A1_at	2.0370382	DOWN
PLK1	Dr.20131.4.S1_at	2.0847763	DOWN
GSN	Dr.4727.1.A1_at	2.2533439	DOWN
SLC26A5	Dr.4948.1.A1_at	2.1235644	UP
SMC2	Dr.20402.1.A1_at	2.4920971	DOWN
CPLX2	Dr.3989.1.A1_at	3.4392884	UP
HCN2	Dr.22826.1.A1_at	2.6670146	UP
anxa1b	Dr.1190.1.S1_at	6.4396889	DOWN
anxa1c	Dr.4833.1.S1_at	2.3146753	DOWN
GPM6A	Dr.5434.3.S1_at	2.1269987	UP
GFAP	Dr.14127.1.S1_at	2.0415683	UP
SNCB	Dr.7855.1.A1_at	2.1825081	UP
KIF11	Dr.1557.1.S1_at	2.2506299	DOWN
Renal and Urological Disease			
TYMS	Dr.1047.1.S1_at	2.0492052	DOWN
CA2	Dr.10405.1.S1_at	2.5744109	DOWN
PTGES3 (includes EG:10728)	Dr.5031.1.S1_at	2.0355733	UP
PPL	Dr.9761.1.S1_at	2.1069557	DOWN
RRM2	Dr.1691.1.S1_at	2.0947138	DOWN
HSD11B2	Dr.12359.1.A1_at	14.363574	UP
PLK1	Dr.20131.4.S1_at	2.0847763	DOWN
MUS81	Dr.977.2.A1_at	2.0307253	DOWN
XIAP	Dr.12645.1.S1_at	2.4127052	UP
PFKM	Dr.13621.1.A1_at	2.4286138	UP
RRM1 (includes EG:6240)	Dr.1691.1.S1_at	2.0947138	DOWN
Cellular Movement			
KIF23	Dr.8295.1.S1_at	2.2917949	DOWN
SOCS3	Dr.6431.1.S1_at	2.0352392	UP
SYT4	Dr.13868.1.S1_at	2.5230733	UP
NUSAP1	Dr.7155.2.S1_a_at	2.0110543	DOWN
ANGPT2	Dr.12620.1.S1_at	2.4642771	UP

UCP2	Dr.21244.1.S1_at	2.5751274	UP
CDC20	Dr.26337.1.A1_at	2.1234569	DOWN
TDGF1	Dr.581.1.S1_at	8.5301637	UP
PLK1	Dr.20131.4.S1_at	2.0847763	DOWN
GSN	Dr.4727.1.A1_at	2.2533439	DOWN
DKK3	Dr.19049.1.A1_at	4.325465	DOWN
DUSP1	Dr.2413.1.S1_at	3.8725208	UP
CPLX2	Dr.3989.1.A1_at	3.4392884	UP
anxa1b	Dr.1190.1.S1_at	6.4396889	DOWN
anxa1c	Dr.4833.1.S1_at	2.3146753	DOWN
GFAP	Dr.14127.1.S1_at	2.0415683	UP
HMGB2	Dr.9746.12.S1_at	2.1815386	DOWN
DNA Replication, Recombination, and Repair			
KIF23	Dr.8295.1.S1_at	2.2917949	DOWN
TYMS	Dr.1047.1.S1_at	2.0492052	DOWN
SOCS3	Dr.6431.1.S1_at	2.0352392	UP
ANGPT2	Dr.12620.1.S1_at	2.4642771	UP
NUSAP1	Dr.7155.2.S1_a_at	2.0110543	DOWN
CDC20	Dr.26337.1.A1_at	2.1234569	DOWN
TDGF1	Dr.581.1.S1_at	8.5301637	UP
ORC6L	Dr.24945.1.S1_at	2.3332334	DOWN
PLK1	Dr.20131.4.S1_at	2.0847763	DOWN
RRM1 (includes EG:6240)	Dr.1691.1.S1_at	2.0947138	DOWN
SMC2	Dr.20402.1.A1_at	2.4920971	DOWN
DUSP1	Dr.2413.1.S1_at	3.8725208	UP
ADCYAP1	Dr.10739.2.S1_a_at	2.0281092	UP
MUS81	Dr.977.2.A1_at	2.0307253	DOWN
KIF11	Dr.1557.1.S1_at	2.2506299	DOWN
HMGB2	Dr.9746.12.S1_at	2.1815386	DOWN
Cardiovascular Disease			
ANGPT2	Dr.12620.1.S1_at	2.4642771	UP
anxa1b	Dr.1190.1.S1_at	6.4396889	DOWN
anxa1c	Dr.4833.1.S1_at	2.3146753	DOWN
HSD11B2	Dr.12359.1.A1_at	14.363574	UP
EGLN3	Dr.9457.1.A1_at	4.8330303	UP
GSN	Dr.4727.1.A1_at	2.2533439	DOWN
ADCYAP1	Dr.10739.2.S1_a_at	2.0281092	UP
XIAP	Dr.12645.1.S1_at	2.4127052	UP
ESCO2	Dr.3337.1.S1_at	2.0632125	DOWN
Gastrointestinal Disease			
TYMS	Dr.1047.1.S1_at	2.0492052	DOWN
CA2	Dr.10405.1.S1_at	2.5744109	DOWN
SOCS3	Dr.6431.1.S1_at	2.0352392	UP
ANGPT2	Dr.12620.1.S1_at	2.4642771	UP
SLC4A2	Dr.1658.1.A1_at	2.0370382	DOWN

CDC20	Dr.26337.1.A1_at	2.1234569	DOWN
RRM2	Dr.1691.1.S1_at	2.0947138	DOWN
ANXA4	Dr.7269.1.A1_at	3.126881	UP
PLK1	Dr.20131.4.S1_at	2.0847763	DOWN
GSN	Dr.4727.1.A1_at	2.2533439	DOWN
RRM1 (includes EG:6240)	Dr.1691.1.S1_at	2.0947138	DOWN
ATP1A1	Dr.10343.1.S1_at	2.5449067	UP
DUSP1	Dr.2413.1.S1_at	3.8725208	UP
anxa1b	Dr.1190.1.S1_at	6.4396889	DOWN
anxa1c	Dr.4833.1.S1_at	2.3146753	DOWN
GLUL	Dr.4147.1.S1_at	2.8466879	UP
HSD11B2	Dr.12359.1.A1_at	14.363574	UP
HMGB2	Dr.9746.12.S1_at	2.1815386	DOWN
Drug Metabolism			
CYP17A1	Dr.25390.1.A1_s_at	2.2035047	DOWN
SYT4	Dr.13868.1.S1_at	2.5230733	UP
HSD11B2	Dr.12359.1.A1_at	14.363574	UP
ADCYAP1	Dr.10739.2.S1_a_at	2.0281092	UP
SNCB	Dr.7855.1.A1_at	2.1825081	UP
FKBP5	Dr.2675.1.A1_at	6.3346811	UP
XIAP	Dr.12645.1.S1_at	2.4127052	UP
Molecular Transport			
SYT4	Dr.13868.1.S1_at	2.5230733	UP
CA2	Dr.10405.1.S1_at	2.5744109	DOWN
ANGPT2	Dr.12620.1.S1_at	2.4642771	UP
UCP2	Dr.21244.1.S1_at	2.5751274	UP
RRM2	Dr.1691.1.S1_at	2.0947138	DOWN
GSN	Dr.4727.1.A1_at	2.2533439	DOWN
XIAP	Dr.12645.1.S1_at	2.4127052	UP
RRM1 (includes EG:6240)	Dr.1691.1.S1_at	2.0947138	DOWN
ATP1A1	Dr.10343.1.S1_at	2.5449067	UP
CPLX2	Dr.3989.1.A1_at	3.4392884	UP
anxa1b	Dr.1190.1.S1_at	6.4396889	DOWN
anxa1c	Dr.4833.1.S1_at	2.3146753	DOWN
ADCYAP1	Dr.10739.2.S1_a_at	2.0281092	UP
SNCB	Dr.7855.1.A1_at	2.1825081	UP
Skeletal and Muscular Disorders			
TYMS	Dr.1047.1.S1_at	2.0492052	DOWN
SOCS3	Dr.6431.1.S1_at	2.0352392	UP
CA2	Dr.10405.1.S1_at	2.5744109	DOWN
SLC4A2	Dr.1658.1.A1_at	2.0370382	DOWN
RRM2	Dr.1691.1.S1_at	2.0947138	DOWN
GNG3	Dr.10136.1.S1_at	2.4031136	UP
XIAP	Dr.12645.1.S1_at	2.4127052	UP
PFKM	Dr.13621.1.A1_at	2.4286138	UP
RRM1 (includes EG:6240)	Dr.1691.1.S1_at	2.0947138	DOWN
PDLIM7	Dr.16051.1.S1_at	2.2162526	UP

DKK3	Dr.19049.1.A1_at	4.325465	DOWN
CPLX2	Dr.3989.1.A1_at	3.4392884	UP
GFAP	Dr.14127.1.S1_at	2.0415683	UP
KIF11	Dr.1557.1.S1_at	2.2506299	DOWN
ESCO2	Dr.3337.1.S1_at	2.0632125	DOWN
HMGB2	Dr.9746.12.S1_at	2.1815386	DOWN
Connective Tissue Development and Function			
SOCS3	Dr.6431.1.S1_at	2.0352392	UP
ANGPT2	Dr.12620.1.S1_at	2.4642771	UP
SLC4A2	Dr.1658.1.A1_at	2.0370382	DOWN
anxa1b	Dr.1190.1.S1_at	6.4396889	DOWN
anxa1c	Dr.4833.1.S1_at	2.3146753	DOWN
HMX3	Dr.10448.1.S1_at	2.0356157	UP
HSD11B2	Dr.12359.1.A1_at	14.363574	UP
ADCYAP1	Dr.10739.2.S1_a_at	2.0281092	UP
GSN	Dr.4727.1.A1_at	2.2533439	DOWN
Cellular Growth and Proliferation			
KIF23	Dr.8295.1.S1_at	2.2917949	DOWN
TYMS	Dr.1047.1.S1_at	2.0492052	DOWN
SOCS3	Dr.6431.1.S1_at	2.0352392	UP
ANGPT2	Dr.12620.1.S1_at	2.4642771	UP
SLC4A2	Dr.1658.1.A1_at	2.0370382	DOWN
TDGF1	Dr.581.1.S1_at	8.5301637	UP
PLK1	Dr.20131.4.S1_at	2.0847763	DOWN
XIAP	Dr.12645.1.S1_at	2.4127052	UP
DUSP1	Dr.2413.1.S1_at	3.8725208	UP
DKK3	Dr.19049.1.A1_at	4.325465	DOWN
anxa1b	Dr.1190.1.S1_at	6.4396889	DOWN
anxa1c	Dr.4833.1.S1_at	2.3146753	DOWN
HSD11B2	Dr.12359.1.A1_at	14.363574	UP
FKBP5	Dr.2675.1.A1_at	6.3346811	UP
ADCYAP1	Dr.10739.2.S1 a at	2.0281092	UP
Cell Signaling			
SOCS3	Dr.6431.1.S1_at	2.0352392	UP
SYT4	Dr.13868.1.S1_at	2.5230733	UP
ANGPT2	Dr.12620.1.S1_at	2.4642771	UP
UCP2	Dr.21244.1.S1_at	2.5751274	UP
DUSP1	Dr.2413.1.S1_at	3.8725208	UP
CPLX2	Dr.3989.1.A1_at	3.4392884	UP
anxa1b	Dr.1190.1.S1_at	6.4396889	DOWN
anxa1c	Dr.4833.1.S1_at	2.3146753	DOWN
GSN	Dr.4727.1.A1_at	2.2533439	DOWN
ADCYAP1	Dr.10739.2.S1_a_at	2.0281092	UP
XIAP	Dr.12645.1.S1_at	2.4127052	UP
Organismal Survival			
CYP17A1	Dr.25390.1.A1_s_at	2.2035047	DOWN

SOCS3	Dr.6431.1.S1_at	2.0352392	UP
ANGPT2	Dr.12620.1.S1_at	2.4642771	UP
SLC4A2	Dr.1658.1.A1_at	2.0370382	DOWN
DUSP1	Dr.2413.1.S1_at	3.8725208	UP
anxa1b	Dr.1190.1.S1_at	6.4396889	DOWN
anxa1c	Dr.4833.1.S1_at	2.3146753	DOWN
EGLN3	Dr.9457.1.A1_at	4.8330303	UP
HSD11B2	Dr.12359.1.A1_at	14.363574	UP
GSN	Dr.4727.1.A1_at	2.2533439	DOWN
ADCYAP1	Dr.10739.2.S1_a_at	2.0281092	UP
Behavior			
CPLX2	Dr.3989.1.A1_at	3.4392884	UP
ADCYAP1	Dr.10739.2.S1_a_at	2.0281092	UP
Tumor Morphology			
SOCS3	Dr.6431.1.S1_at	2.0352392	UP
GFAP	Dr.14127.1.S1_at	2.0415683	UP
PLK1	Dr.20131.4.S1_at	2.0847763	DOWN
ADCYAP1	Dr.10739.2.S1_a_at	2.0281092	UP
KIF11	Dr.1557.1.S1_at	2.2506299	DOWN
Auditory and Vestibular System Development and Function			
HMX3	Dr.10448.1.S1_at	2.0356157	UP
Carbohydrate Metabolism			
SOCS3	Dr.6431.1.S1_at	2.0352392	UP
PTGES3 (includes EG:10728)	Dr.5031.1.S1_at	2.0355733	UP
GSN	Dr.4727.1.A1_at	2.2533439	DOWN
Cardiovascular System Development and Function			
ATP1A1	Dr.10343.1.S1_at	2.5449067	UP
ANGPT2	Dr.12620.1.S1_at	2.4642771	UP
HCN2	Dr.22826.1.A1_at	2.6670146	UP
DUSP1	Dr.2413.1.S1_at	3.8725208	UP
HSD11B2	Dr.12359.1.A1_at	14.363574	UP
Cell Morphology			
KIF23	Dr.8295.1.S1_at	2.2917949	DOWN
ANGPT2	Dr.12620.1.S1_at	2.4642771	UP
SLC4A2	Dr.1658.1.A1_at	2.0370382	DOWN
anxa1b	Dr.1190.1.S1_at	6.4396889	DOWN
anxa1c	Dr.4833.1.S1_at	2.3146753	DOWN
RRM2	Dr.1691.1.S1_at	2.0947138	DOWN
ADCYAP1	Dr.10739.2.S1_a_at	2.0281092	UP
GSN	Dr.4727.1.A1_at	2.2533439	DOWN
Cellular Compromise			
KIF23	Dr.8295.1.S1_at	2.2917949	DOWN

SOCS3	Dr.6431.1.S1_at	2.0352392	UP
ANGPT2	Dr.12620.1.S1_at	2.4642771	UP
DUSP1	Dr.2413.1.S1_at	3.8725208	UP
GSN	Dr.4727.1.A1_at	2.2533439	DOWN
ADCYAP1	Dr.10739.2.S1_a_at	2.0281092	UP
XIAP	Dr.12645.1.S1_at	2.4127052	UP
KIF11	Dr.1557.1.S1_at	2.2506299	DOWN
HMGB2	Dr.9746.12.S1_at	2.1815386	DOWN
Cellular Development			
SOCS3	Dr.6431.1.S1_at	2.0352392	UP
CA2	Dr.10405.1.S1_at	2.5744109	DOWN
SLC4A2	Dr.1658.1.A1_at	2.0370382	DOWN
TDGF1	Dr.581.1.S1_at	8.5301637	UP
GSN	Dr.4727.1.A1_at	2.2533439	DOWN
INSM1			
EVPL	Dr.5577.1.A1_at	3.0126001	DOWN
PDLIM7	Dr.16051.1.S1_at	2.2162526	UP
DKK3	Dr.19049.1.A1_at	4.325465	DOWN
DUSP1	Dr.2413.1.S1_at	3.8725208	UP
ASPM	Dr.19463.1.S1_at	2.0901034	DOWN
anxa1b	Dr.1190.1.S1_at	6.4396889	DOWN
anxa1c	Dr.4833.1.S1_at	2.3146753	DOWN
EGLN3	Dr.9457.1.A1_at	4.8330303	UP
ADCYAP1	Dr.10739.2.S1_a_at	2.0281092	UP
Cellular Function and Maintenance			
SLC26A5	Dr.4948.1.A1_at	2.1235644	UP
CA2	Dr.10405.1.S1_at	2.5744109	DOWN
SOCS3	Dr.6431.1.S1_at	2.0352392	UP
SYT4	Dr.13868.1.S1_at	2.5230733	UP
UCP2	Dr.21244.1.S1_at	2.5751274	UP
HCN2	Dr.22826.1.A1_at	2.6670146	UP
CPLX2	Dr.3989.1.A1_at	3.4392884	UP
GSN	Dr.4727.1.A1_at	2.2533439	DOWN
KIF11	Dr.1557.1.S1_at	2.2506299	DOWN
Connective Tissue Disorders			
SOCS3	Dr.6431.1.S1_at	2.0352392	UP
SLC4A2	Dr.1658.1.A1_at	2.0370382	DOWN
Dermatological Diseases and Conditions			
CYP17A1	Dr.25390.1.A1_s_at	2.2035047	DOWN
TYMS	Dr.1047.1.S1_at	2.0492052	DOWN
SOCS3	Dr.6431.1.S1_at	2.0352392	UP
PTGES3 (includes EG:10728)	Dr.5031.1.S1_at	2.0355733	UP
DUSP1	Dr.2413.1.S1_at	3.8725208	UP
PLK1	Dr.20131.4.S1_at	2.0847763	DOWN
MUS81	Dr.977.2.A1_at	2.0307253	DOWN

XIAP	Dr.12645.1.S1_at	2.4127052	UP
ESCO2	Dr.3337.1.S1_at	2.0632125	DOWN
PFKM	Dr.13621.1.A1_at	2.4286138	UP
Developmental Disorder			
CA2	Dr.10405.1.S1_at	2.5744109	DOWN
SLC4A2	Dr.1658.1.A1_at	2.0370382	DOWN
PTGES3 (includes EG:10728)	Dr.5031.1.S1_at	2.0355733	UP
HSD11B2	Dr.12359.1.A1_at	14.363574	UP
PLK1	Dr.20131.4.S1_at	2.0847763	DOWN
GFAP	Dr.14127.1.S1_at	2.0415683	UP
MUS81	Dr.977.2.A1_at	2.0307253	DOWN
XIAP	Dr.12645.1.S1_at	2.4127052	UP
PFKM	Dr.13621.1.A1_at	2.4286138	UP
Embryonic Development			
CA2	Dr.10405.1.S1_at	2.5744109	DOWN
SOCS3	Dr.6431.1.S1_at	2.0352392	UP
ANGPT2	Dr.12620.1.S1_at	2.4642771	UP
ASPM	Dr.19463.1.S1_at	2.0901034	DOWN
TDGF1	Dr.581.1.S1_at	8.5301637	UP
PLK1	Dr.20131.4.S1_at	2.0847763	DOWN
GSN	Dr.4727.1.A1_at	2.2533439	DOWN
XIAP	Dr.12645.1.S1_at	2.4127052	UP
Gene Expression			
SOCS3	Dr.6431.1.S1_at	2.0352392	UP
PTGES3 (includes EG:10728)	Dr.5031.1.S1_at	2.0355733	UP
SMC2	Dr.20402.1.A1_at	2.4920971	DOWN
DLX4	Dr.153.1.S1_at	2.0558797	DOWN
ADCYAP1	Dr.10739.2.S1_a_at	2.0281092	UP
HMGB2	Dr.9746.12.S1_at	2.1815386	DOWN
Infection Mechanism			
HSD11B2	Dr.12359.1.A1_at	14.363574	UP
Hematopoiesis			
SOCS3	Dr.6431.1.S1_at	2.0352392	UP
Metabolic Disease			
SOCS3	Dr.6431.1.S1_at	2.0352392	UP
UCP2	Dr.21244.1.S1_at	2.5751274	UP
DUSP1	Dr.2413.1.S1_at	3.8725208	UP
anxa1b	Dr.1190.1.S1_at	6.4396889	DOWN
anxa1c	Dr.4833.1.S1_at	2.3146753	DOWN
GLUL	Dr.4147.1.S1_at	2.8466879	UP
HSD11B2	Dr.12359.1.A1_at	14.363574	UP
GFAP	Dr.14127.1.S1_at	2.0415683	UP
GSN	Dr.4727.1.A1_at	2.2533439	DOWN

ADCYAP1	Dr.10739.2.S1_a_at	2.0281092	UP
GLDC	Dr.24995.4.S1_at	4.9345554	UP
PFKM	Dr.13621.1.A1_at	2.4286138	UP
Organ Development			
SOCS3	Dr.6431.1.S1_at	2.0352392	UP
HMX3	Dr.10448.1.S1_at	2.0356157	UP
Organ Morphology			
EVPL	Dr.5577.1.A1_at	3.0126001	DOWN
anxa1b	Dr.1190.1.S1_at	6.4396889	DOWN
anxa1c	Dr.4833.1.S1_at	2.3146753	DOWN
TDGF1	Dr.581.1.S1_at	8.5301637	UP
DCT	Dr.10336.1.S1_at	2.0475848	UP
ADCYAP1	Dr.10739.2.S1_a_at	2.0281092	UP
Organismal Development			
ADCYAP1	Dr.10739.2.S1_a_at	2.0281092	UP
SNCB	Dr.7855.1.A1_at	2.1825081	UP
XIAP	Dr.12645.1.S1_at	2.4127052	UP
Organismal Injury and Abnormalities			
SOCS3	Dr.6431.1.S1_at	2.0352392	UP
ANGPT2	Dr.12620.1.S1_at	2.4642771	UP
DUSP1	Dr.2413.1.S1_at	3.8725208	UP
TDGF1	Dr.581.1.S1_at	8.5301637	UP
RRM2	Dr.1691.1.S1_at	2.0947138	DOWN
XIAP	Dr.12645.1.S1_at	2.4127052	UP
KIF11	Dr.1557.1.S1_at	2.2506299	DOWN
Reproductive System Development and Function			
SOCS3	Dr.6431.1.S1_at	2.0352392	UP
SLC4A2	Dr.1658.1.A1_at	2.0370382	DOWN
DUSP1	Dr.2413.1.S1_at	3.8725208	UP
TDGF1	Dr.581.1.S1_at	8.5301637	UP
ADCYAP1	Dr.10739.2.S1_a_at	2.0281092	UP
Tissue Development			
SOCS3	Dr.6431.1.S1_at	2.0352392	UP
CA2	Dr.10405.1.S1_at	2.5744109	DOWN
ANGPT2	Dr.12620.1.S1_at	2.4642771	UP
DKK3	Dr.19049.1.A1_at	4.325465	DOWN
TDGF1	Dr.581.1.S1_at	8.5301637	UP
HMX3	Dr.10448.1.S1_at	2.0356157	UP
PLK1	Dr.20131.4.S1_at	2.0847763	DOWN
GSN	Dr.4727.1.A1_at	2.2533439	DOWN
ADCYAP1	Dr.10739.2.S1_a_at	2.0281092	UP

Tissue Morphology			
TYMS	Dr.1047.1.S1_at	2.0492052	DOWN
SOCS3	Dr.6431.1.S1_at	2.0352392	UP
CA2	Dr.10405.1.S1_at	2.5744109	DOWN
ANGPT2	Dr.12620.1.S1_at	2.4642771	UP
SLC4A2	Dr.1658.1.A1_at	2.0370382	DOWN
TDGF1	Dr.581.1.S1_at	8.5301637	UP
GSN	Dr.4727.1.A1_at	2.2533439	DOWN
XIAP	Dr.12645.1.S1_at	2.4127052	UP
DKK3	Dr.19049.1.A1_at	4.325465	DOWN
anxa1b	Dr.1190.1.S1_at	6.4396889	DOWN
anxa1c	Dr.4833.1.S1_at	2.3146753	DOWN
HSD11B2	Dr.12359.1.A1_at	14.363574	UP
GFAP	Dr.14127.1.S1_at	2.0415683	UP
ADCYAP1	Dr.10739.2.S1_a_at	2.0281092	UP
Visual System Development and Function			
HSD11B2	Dr.12359.1.A1_at	14.363574	UP
Hematological Disease			
SOCS3	Dr.6431.1.S1_at	2.0352392	UP
ANGPT2	Dr.12620.1.S1_at	2.4642771	UP
ATP1A1	Dr.10343.1.S1_at	2.5449067	UP
CDC20	Dr.26337.1.A1_at	2.1234569	DOWN
RRM2	Dr.1691.1.S1_at	2.0947138	DOWN
ANXA4	Dr.7269.1.A1_at	3.126881	UP
GFAP	Dr.14127.1.S1_at	2.0415683	UP
ADCYAP1	Dr.10739.2.S1_a_at	2.0281092	UP
GSN	Dr.4727.1.A1_at	2.2533439	DOWN
XIAP	Dr.12645.1.S1_at	2.4127052	UP
RRM1 (includes EG:6240)	Dr.1691.1.S1_at	2.0947138	DOWN
Endocrine System Disorders			
UCP2	Dr.21244.1.S1_at	2.5751274	UP
DUSP1	Dr.2413.1.S1_at	3.8725208	UP
anxa1b	Dr.1190.1.S1_at	6.4396889	DOWN
anxa1c	Dr.4833.1.S1_at	2.3146753	DOWN
GFAP	Dr.14127.1.S1_at	2.0415683	UP
Immunological Disease			
TYMS	Dr.1047.1.S1_at	2.0492052	DOWN
SOCS3	Dr.6431.1.S1_at	2.0352392	UP
UCP2	Dr.21244.1.S1_at	2.5751274	UP
DUSP1	Dr.2413.1.S1_at	3.8725208	UP
RRM2	Dr.1691.1.S1_at	2.0947138	DOWN
XIAP	Dr.12645.1.S1_at	2.4127052	UP
RRM1 (includes EG:6240)	Dr.1691.1.S1_at	2.0947138	DOWN

Psychological Disorders			
SYT4	Dr.13868.1.S1_at	2.5230733	UP
CA2	Dr.10405.1.S1_at	2.5744109	DOWN
UCP2	Dr.21244.1.S1_at	2.5751274	UP
SQRDL (includes EG:58472)			
PLK1	Dr.20131.4.S1_at	2.0847763	DOWN
GSN	Dr.4727.1.A1_at	2.2533439	DOWN
ATP1A1	Dr.10343.1.S1_at	2.5449067	UP
CPLX2	Dr.3989.1.A1_at	3.4392884	UP
DKK3	Dr.19049.1.A1_at	4.325465	DOWN
GFAP	Dr.14127.1.S1_at	2.0415683	UP
GLDC	Dr.24995.4.S1_at	4.9345554	UP
SNCB	Dr.7855.1.A1_at	2.1825081	UP
FKBP5	Dr.2675.1.A1_at	6.3346811	UP
ADCYAP1	Dr.10739.2.S1_a_at	2.0281092	UP
GATM	Dr.1064.1.S1_at	2.7011572	UP
Renal and Urological System Development and Function			
ANGPT2	Dr.12620.1.S1_at	2.4642771	UP
DUSP1	Dr.2413.1.S1_at	3.8725208	UP
PLK1	Dr.20131.4.S1_at	2.0847763	DOWN
Digestive System Development and Function			
SOCS3	Dr.6431.1.S1_at	2.0352392	UP
SLC4A2	Dr.1658.1.A1_at	2.0370382	DOWN
Free Radical Scavenging			
GSN	Dr.4727.1.A1_at	2.2533439	DOWN
Hair and Skin Development and Function			
EVPL	Dr.5577.1.A1_at	3.0126001	DOWN
PLK1	Dr.20131.4.S1_at	2.0847763	DOWN
DCT	Dr.10336.1.S1_at	2.0475848	UP
Nutritional Disease			
CA2	Dr.10405.1.S1_at	2.5744109	DOWN
SOCS3	Dr.6431.1.S1_at	2.0352392	UP
UCP2	Dr.21244.1.S1_at	2.5751274	UP
SLC4A2	Dr.1658.1.A1_at	2.0370382	DOWN
ADCYAP1	Dr.10739.2.S1_a_at	2.0281092	UP
Ophthalmic Disease			
TYMS	Dr.1047.1.S1_at	2.0492052	DOWN
CA2	Dr.10405.1.S1_at	2.5744109	DOWN
ANGPT2	Dr.12620.1.S1_at	2.4642771	UP
Cell-mediated Immune Response			
SOCS3	Dr.6431.1.S1_at	2.0352392	UP

Organismal Functions			
ADCYAP1	Dr.10739.2.S1_a_at	2.0281092	UP
Hepatic System Disease			
TYMS	Dr.1047.1.S1_at	2.0492052	DOWN
CA2	Dr.10405.1.S1_at	2.5744109	DOWN
SOCS3	Dr.6431.1.S1_at	2.0352392	UP
DUSP1	Dr.2413.1.S1_at	3.8725208	UP
Humoral Immune Response			
Cellular Response to Therapeutics			
XIAP	Dr.12645.1.S1_at	2.4127052	UP
Hepatic System Development and Function			
SOCS3	Dr.6431.1.S1_at	2.0352392	UP

Table 3S- 2.Oligonucleotides used for qRT-PCR.
List of gene specific primers used for qRT-PCR and cloning of *Cripto-1* for probe synthesis

Target gene	Sequence 5' to 3'	Affymetrix probe set number
F β-actin	AAGCAGGAGTACGATGAGTC	Dr.1109.1.S1_at
R β-actin	TGGAGTCCTCAGATGCATTG	Dr.1109.1.S1_at
F FKBP506	CACGTTCACAAACACACTGC	Dr.2675.1.A1_at
R FKBP506	ATCAAACGAACAAGCGGGTC	Dr.2675.1.A1_at
F GILZ	CGACTTGTTTATATGGGCTG	Dr.12437.1.A1_at
R GILZ	TCTTCAGACACCAACATGCC	Dr.12437.1.A1_at
F Glutamine synthase a	AAGGGTGGTTCTAACATGGC	Dr.4147.1.S1_at
R Glutamine synthase a	TGGACTGCGACTTTGTACCG	Dr.4147.1.S1_at
F One-eyed pinhead	ATTGTGTGTGTGTGTCAGTGCG	Dr.581.1.S1_at
R One-eyed pinhead	TCTCCATTAACAAGCACGGC	Dr.581.1.S1_at
F One-eyed pinhead	CACAACTTTCATTTGCCGTG	Dr.581.1.S1_at
R One-eyed pinhead	CTGGGTTTTTGATGCGAGTT	Dr.581.1.S1_at

Figure 3S- 1.Pathway analysis reveal interaction between *Cripto-1* and Activin signaling pathway.
Analysis of human orthologues of transcripts altered greater than 2fold by BDP exposure by Ingenuity software reveal reported interactions between TDGF1 and members of Activin signaling.

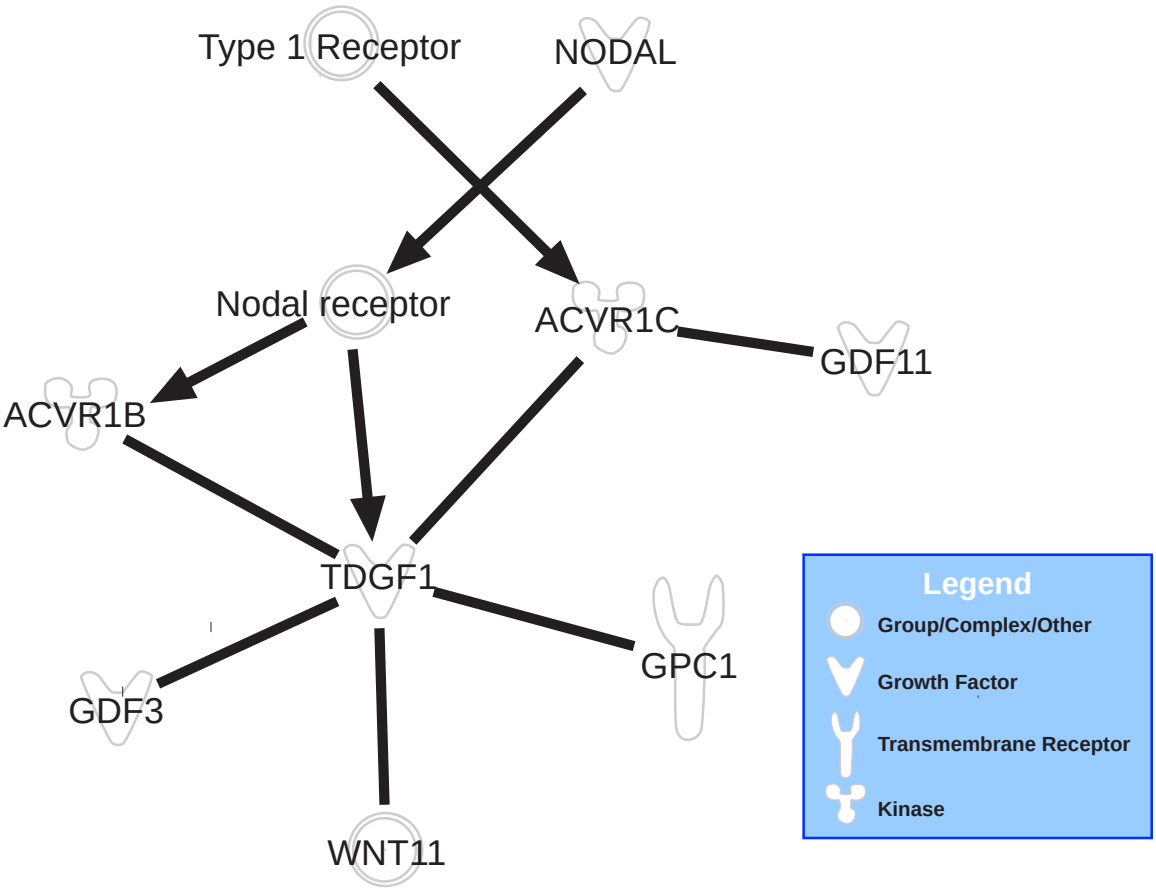

CHAPTER 4 – The Regenerative Activity of Glucocorticoids is Dictated by Alternate Ligand Structures

Sumitra Sengupta[1], William Bisson[3], Siva Kolluri[1], and Robert L Tanguay[1,2].

Department of Environmental and Molecular Toxicology[1], Environmental Health Sciences Center[2], Oregon State University, Corvallis, OR, 97331.Department of Pharmaceutical Biochemistry, University of Geneva, Switzerland 11211[3]

Formatted for Publication in Journal of Biological Chemistry

Abstract

Regenerative medicine aims to restore lost tissues and organs by inducing a regenerative response in mammals. We utilized an early life stage model of zebrafish caudal fin regeneration to identify the signaling pathways that facilitate regeneration response in vertebrates with an aim to therapeutically manipulate these pathways in the future to enable regeneration in mammals.

We have previously demonstrated that glucocorticoids inhibit tissue regeneration in a GR-dependent manner. In this study, we have investigated the differential regenerative response evoked by selected members of the GR ligand family. For example, though dexamethasone and beclomethasone dipropionate both activate GR, becloemthaosne dipropionate inhibits regeneration while dexamethasone doesnot. Molecular docking studies with the human GR illustrated the difference in GR conformation induced by the ligands and further explained the importance of the C17 substitutions moiety. We confirmed this observation by investigating ligands from two different chemical libraries based on their C17 substitution in our caudal fin regeneration model. Our results demonstrate that structural preference plays a critical role in determining the influence of GCs on tissue regeneration. Collectively these results indicate that inappropriate activation of the GR by GCs with specific ligand chemistry dictates the observed impacts on regeneration.

Introduction

The desire of humans to live a long and morbidity-free life drives the field of regenerative medicine to develop therapeutic strategies that can promote optimal healing and replacement of tissue damaged by trauma, disease, or congenital defects. In the last few years, the field of stem cell biology has made significant contributions by devising treatments to restore individual cell types known as “cell replacement therapy or stem cell therapy”. To date stem cell therapy has been able to replace specific cell types, but cannot recreate functional organs or appendages that requires reconstitution of numerous cells types and establishment of interactions between them. This process is known as epimorphic tissue regeneration, and requires the formation of a special structure called blastema and the reconstitution of complex tissue with multiple cell types. Mammals have a limited capacity for epimorphic regeneration of complex structures, which is demonstrated by few vertebrates such as salamander, newt and zebrafish. An aletrnative approach to stem cell therapy in the field of regenerative medicine is the concept of inducing regeneration in mammals. Identifying the cellular and molecular differences that dictate regenerative response in vertebrates has the potential to enable regeneration in mammals. We utilize the early life stage regeneration model of zebrafish to reveal these differences.

A two-day post fertilization (dpf) zebrafish can completely regenerate its caudal fin in three days post amputation (dpa). We combined this early life stage regeneration model with a chemical genetic approach and developed an *in vivo* larval regeneration assay to identify modulators of regeneration. A key concept to this approach is that a

chemical inhibitor of regeneratio affects a critical molecular target for the regeneration process. Identification of such chemical targets will allow better understanding of regenerative biology eventually enabling enhanced regeneration in mammals. As a proof of concept, we screened a 2000 member library of FDA approved drugs. The library comprised of thirty-three glucocorticoids (GCs), seven of which inhibit regeneration and render a characteristic 'V' shaped architecture to the caudal fin upon exposure. We pursued further studies with beclomethasone dipropionate as a representative GC, and revealed that activation of the glucocorticoid receptor (GR) is necessary for inhibition of regeneration.

Glucocorticoids are four-ring steroid compounds that elicit response by activating cytoplasmic GRs, which function as ligand dependent transcriptional regulators. GCs control a wide range of biological processes that regulate numerous physiological systems. Since the discovery of the anti-inflammatory property of cortisone in 1949, this class of steroids has enjoyed a remarkable career. GCs have captured the interest of virtually every leading pharmaceutical company, and an unprecedented number of structural modifications of the cortisol backbone have resulted in a myriad of synthetic corticosteroids. Approximately 40 new topically active anti-inflammatory corticosteroids have been introduced into therapy since 1952. A majority of the structural modifications are targeted to eliminate side effects associated with most of the GR ligands. This has led to the recent development of non-steroidal dissociated ligands such as AL438 [1-3], suggesting that ligand activities are strongly context dependent.

While GCs are mostly used as anti-inflammatory agents the newly identified role of GCs as modulators of tissue regeneration has opened a new paradigm in the field of regenerative medicine. This study attempts to explain the SARs of the known GR

ligands in the context of tissue regeneration in order to identify a pharmacophore backbone that dictates regenerative response. Our strategy was to first investigate whether the available known GR ligands demonstrate ligand selectivity for inhibition of tissue regeneration. We then determined whether these ligands induced different structural conformations upon GR binding, and further supported our observations with the identification of novel GR ligands that affect tissue regeneration.

Materials and Methods

Zebrafish Embryos

Zebrafish embryos (5D strain) were obtained from a breeding colony raised using standard husbandry procedures for all the experiments [4, 5]. Caudal fins of 2 days post fertilization (2 dpf) larvae were amputated as previously described [6-8] and chemical screening was performed based on our previously described in vivo larval regeneration assay protocol [9]. All experimental groups consisted of sample size n =12.

Chemical Exposures

2 dpf amputated larvae were exposed to 1 µM Dexamethasone (DEX) (D1756, Sigma), Beclomethasone diproprionate (BDP) B3022, Sigma), Beclomethasone (Beclo) (B0385, Sigma), or Hydrocortisone (HC) (H4001, Sigma). R198897 (21-Cl-9-α-F-17-α-HO-16-β-me-pregna-1,4-diene-3,11,20-trione butanoate) and R20220 (9-α,11-β-di-Cl-17-α,21-di-HO-16-α-me-pregna-1,4-diene-3,20-dione) were purchased from Sigma and ST075178 (2S,10S,11S,13S,15S,17S,1R,14R)-1-fluoro-17-hydroxy-14-(2-hydroxyacetyl)-2,13, 15-trimethyl-5-oxotetracyclo[8.7.0.0<2,7>.0<11,15>]heptadeca-3,6-dien-14-yl pentanoate, and ST075183(2-((2S,10S,11S,15S,17S,1R,13R,14R)-1-fluoro-

14,17-dihydroxy-2,13,15-trimethyl-5-oxotetracyclo[8.7.0.0<2,7>.0<11,15>]heptadeca-3,6-dien-14-yl)-2-oxoethyl acetate) were purchased from TimTec.

Sequence Alignment and Homology Modeling

The GR ligand binding domain (LBD) sequences in FASTA format for human and zebrafish were retrieved from the NCBI database. Sequence alignment was performed on line with the LALIGN program [http://www.ch.embnet.org/software/LALIGN_form.html]. We used the X-Ray crystal structure of the human GR-LBD bound to dexamethasone (DEX) in the agonist conformation available in the Protein Data Bank (PDB) 1P93 [10] as the 3D coordinate template for the homology modeling of the zebrafish isoform 2 GR-LBD. The model was energetically refined using the internal coordinate space with Molsoft ICM v3.5-1p. [4, 11]

Molecular Docking

The energy terms were based on the all-atom vacuum force field ECEPP/3 with appended terms from the Merck Molecular Force Field to account for solvation free energy and entropic contribution [4]. Modified intermolecular terms such as soft van der Waals and hydrogen-bonding as well as a hydrophobic term were added. Conformational sampling was based on the biased probability Monte Carlo (BPMC) procedure, which randomly selects a conformation in the internal coordinate space and then makes a step to a new random position independent of the previous one according to a predefined continuous probability distribution. It also has been shown that after each random step, full local minimization improves the efficiency of the iterative docking procedure. In the ICM-VLS (Molsoft ICM v3.5-1p) screening procedure, the ligand

scoring was optimized to obtain maximal separation between binders and non binders [5,12] Each steroidal GR agonist was assigned a score according to its fit within the receptor, which accounted for continuum and discreet electrostatics, hydrophobicity and entropy parameters [4, 5, 12].

The 3D coordinates of human GR-LBD-DEX complex in the agonist conformation was taken from crystal structures 1P93 [10]. BDP was manually inserted into the GR-LBD binding pocket by matching the orientation of the 3-C=O keton oxygen from the A-ring of DEX in the crystal structure involved in HB interactions with residues Gln570 (α3) and Arg611 (α7) [10].

Molecular Dynamics simulations

The prep files of DEX and BDP were performed using the program ANTECHAMBER and LEAP. DEX-GR-LBD and BDP-GR-LBD complex models were immersed in a box of water molecules and Na+ counterions were added to the solvent bulk of the protein/water complexes to maintain neutrality of the system using program AMBER10 [7]. Periodic boundary conditions were applied. The AMBER force field [7] all atom parameters (parm03) were used for the protein and the Na+ ions. The minimization protocol consisted of 1000 cycles of steepest descent followed by conjugate gradient method until the root-mean square deviation (rmsd) of the Cartesian elements of the gradient reached a value smaller than 0.15 Å. The dynamic protocol consisted of three steps: MD1, MD2 and MD3. The initial temperature for MD1, MD2 and MD3 were set at 0, 150, and 300 °K respectively. During all dynamic steps the reference temperature of the system was fixed at 300 °K according to Berendsen's coupling algorithms [13]. The time step for all three dynamic procedures was 0.002

picosec (ps). For minimization and molecular dynamics, the primary cutoff distance for non bonded interaction was set at 9 Å. Regarding the molecular dynamics protocol used, the first (MD1) aimed the equilibration of water molecules and ions of the water boxed and charge neutralized model. An initial velocity was given to the system and trajectories were allowed to evolve in time according to Newtonian laws keeping the model protein fixed. The number of dynamics steps was 7500 corresponding to 15 ps. Next, 15 ps of constant volume dynamic (MD2) was performed on the entire system to adjust density to a value of one. In the third step, a 500 ps constant pressure dynamic (MD3) at 1 atm was applied without any constraint to assess conformational stability. The energy minimization, molecular dynamics and the corresponding analyses were performed using program AMBER10. Geometrical quality assessments of the models, were performed at different time points using PROCHECK [9].

RNA isolation

The caudal fins of 2 dpf embryos were amputated, and embryos were placed individually in wells of 96-well plates with exposure solutions of dimethyl sulfoxide (DMSO, vehicle control) or chemical. Twelve embryos were pooled for each of the three replicates per treatment and RNA was isolated using Tri Reagent.

Quantitative real time reverse transcriptase polymerase chain reaction (qRT-PCR)

Total RNA was isolated from whole embryos. Each treatment comprised three replicates with an n of 12 expbryos per replicate and cDNA was synthesized from 1 µg of total RNA isolated from each group using Superscript II (Life Technologies) with oligo(dT) primers. QRT-PCR was performed on the Opticon 2 real time PCR detection

system (MJ Research) using SYBR green qPCR detection kits (Finnzymes). Gene specific primers are listed in supplemental table 1. Each sample was normalized to endogenous β-actin quantity. Agarose gel electrophoresis and melt curve analysis confirmed expected PCR product formation. Statistical significance of differences in mRNA abundance was determined by One way ANOVA on log10 transformed data with a post test using Tukeys method ($p<0.05$) (Sigmastat Software).

Oligonucleotides

The oligonucleotide primers used for qRT-PCR were synthesized by MWG-Biotech (High Point). Oligotech and Primer blast programs were used to design the primers ilisted in supplemental table 1. Forward and antisense reverse primers are prefixed with F and R accordingly.

Morpholinos

Fluorescein tagged zebrafish GR (zf GR) morpholino (5' - CGGAACCCTAAAATACATGAAGCAG - 3') designed to target the splicing of exons 7 and 8 was used to knockdown GR expression. Standard control morpholino (Gene Tools) (5' CTCTTACCTCAGTTACAATTTATA 3') was injected at matching concentration. The morpholinos were diluted to a stock concentration of 3mM in 1x Danieau's solution (58 mM NaCl, 0.7 mM KCl, 0.4 mM MgSO4, 0.6 mM Ca(NO3)2, 5 mM HEPES, pH 7.6) [14] and approximately 2nl of control and zf GR morpholino was injected in 1- 2 cell stage embryos. The injected embryos were screened for uniform fluorescence at 24 hpf to confirm uniform distribution of the morpholino. At 2 dpf, caudal fin or morphants were amputated, followed by exposure to chemical.

Results

Glucocorticoids elicit differential regenerative responses

We screened a 2000 member library comprised of FDA approved drugs for novel modulators of regeneration using an *in vivo* larval regeneration assay. A total of thirty three glucocorticoids comprised the library, out of which seven glucocorticoids inhibited regeneration while twenty-one glucocorticoids from the library had no effect on regeneration at the screening concentration of 25 µM (Fig. 1). We followed this screen with a dose response analysis, and pursued mechanistic studies with BDP. Since BDP can inhibit regeneration even at low nanomolar concentrations, we performed further experiments at a screening concentration of 1 µM [9]. We further validated the results of DEX, HC and beclo by purchasing these chemicals from a commercial source and repeating the regeneration assay. This confirmed that the chemicals did not inhibit regeneration at the screening concentration. Mechanistic data revealed that overexpression of *Cripto-1* mediates BDP impaired tissue regeneration (manuscript in preparation). Our qRT-PCR results demonstrating lack of *Cripto-1* differential expression following DEX, HC and beclo (Fig. 2) exposure confirmed that, unlike BDP, these chemicals did not influence tissue regeneration. We performed further studies to explain the differential response elicited by DEX, HC, Beclo and BDP.

Inappropriate activation of GR is requisite for inhibiting tissue regeneration

All of the chemicals selected for the study are well known GR ligands. Annexin a1b (*anxa1b*) is one of the transcripts repressed by activated GR. In order to evaluate whether these ligands were activating GR in our system, we performed qRT-PCR to evaluate *anxa1b* expression upon exposure to the ligands. DEX, HC, Beclo and BDP exposure suppressed *anxa1b* expression at 1µM indicating activation of GR (Fig. 3).

These data combined with the larval fin regeneration assay results showed that GR activation by DEX, HC or Beclo did not impact regeneration. However, GR activation by BDP did inhibit regeneration. These differential responses suggest that there is a difference in GR activation by BDP as compared to DEX, HC or Beclo.

Molecular docking studies revealed a conformational difference induced by ligand binding

To explain the difference in activated GR we performed molecular dynamic simulation studies with human GR, as the crystallographic structure of zebrafish GR is not available. The human and zebrafish isoform 2 GR-LBD share 72% sequence identity and majority of the residues directly involved in the binding to DEX such as Gln 570 (α3), Arg 611 (α7), Gln 642 (α8) and Thr 739 (α11) are conserved between the two species (Fig. 4). The homology model of zebrafish GR-LBD was then built using the 3D coordinate of the human GR-LBD bound to DEX available in the PDB 1P93 and energetically refined as described in the Methods section.

Molecular Docking.

Selected steroidal GR agonists from the 2000 member library that evoked differential impact on regeneration were docked into the human and zebrafish GR-LBD models (Table 1). Docking results were similar for both species. Most of the active GR agonists that inhibit regeneration didnot dock or docked with poor energy scores into the GR-LBD binding pocket while most of the inactive GR agonists that did not inhibit regeneration did dock into GR-LBD. This suggests that docked steroidal GR agonists are stable in GR-LBD-DEX agonist conformation, while steroidal GR agonists like BDP do not fit into the binding pocket and become unstable. In order to bind and stabilize the

agonist 3D tertiary structure of the GR-LBD, active compounds induce conformational changes involving either residue side chains or secondary structure portions of the protein. Similar cases are reported in literature with strong steroidal GR agonists deacylcortivazol (DAC) and fluticasone furoate (FF), which were co-crystallized into the human GR-LBD (PDB: 3BQD and 3CLD, respectively).

To identify the conformational changes of the GR-LBD upon active compounds binding , we ran 1.15ns Molecular Dynamic (MD) simulations with the human GR-LBD complexed with ligands DEX and BDP. DEX is a known inactive compound and for this reason the X-Ray crystal structure 1P93 was considered as the 3D structure reference for steroidal GR agonists unable to inhibit regeneration. BDP was instead manually inserted into the human GR-LBD binding pocket as described in the Methods section.

Molecular Dynamics simulations.

By looking at the RMSD as a function of time of all models, the GR-LBD-DEX complex reached a plateau during 1.15 ns MD (Fig. 5A), representing stable conformation over time. On the other hand, GR-LBD-BDP complex was not able to reach that stability, and this is mainly due to the instability of BDP in the binding pocket during the simulation time (Fig. 5B). DEX crystallographic orientation with the HB network remained stable over time with a low RMSD of 0.75 Å, while BDP revealed considerable instability especially in the range between 0.3-0.5 ns MD (Fig. 5B). Overall, the low RMSD of both GR-LBD complexes around 2.25 Å and structural comparison along the simulation time indicates that the starting X-Ray structure represents a stable conformation and the MD protocol is suited to assess the stability of the models.

Distances (Å) between atoms of specific residues were calculated and analyzed over 1.15 ns MD. The stability of the crystallographic orientation of dex in the GR-LBD over time was confirmed. (Fig. 5C-E). The HB network involving the side chains of residues Gln 570 (Fig. 5C), Arg 611 (Fig. 5D) and Gln 642 (Fig. 5E) and DEX is critical for the stability of the ligand in the GR-LBD agonist conformation with an average calculated distance of 3Å. This was not the case for BDP. (Fig. 5D-F) The stability of the human GR-LBD-DEX complex during simulation time is well described by looking at the superimposition of DEX and residues Gln 570, Arg 611, Gln 642 and Thr 739 from the pdb structure of the complex at initial (t=0 ns) and final (t=1.15 ns) MD time (Fig. 6a). No 3D significant differences were detected for the residues and the ligand over time (Fig. 6a). During 1.15ns MD the GR-LBD-BDP complex was instead very unstable (Fig. 5A,B) and the calculated inter-atomic distances between BDP and key residue side chains atoms showed that conformational changes are occurring over time to accommodate the ligand into the binding pocket and thus stabilize the GR-LBD agonist conformation (Fig. 5F-H).

BDP was inserted inserted manually into the GR-LBD binding pocket by positioning the 3-C=O keton oxygen in the vicinity of the side chains of Gln 570 and Arg 611 to maintain the energetically favorable HB network observed with DEX. and other GR agonists. During the simulation however these HB interactions were unstable due to residue side chain conformation changes, which produced significant fluctuations in the calculated inter-atomic distances (Fig.5F-H). For a better understanding of these fluctuations we superimposed similarly BDP and amino acids Gln 570, Arg 611 and Gln 642 from the PDB structure of the complex at initial (t=0 ns) and final (t=1.15 ns) MD time (Fig. 6b,c). During 1.15 ns MD (Fig. 5F, 6b) the side chain of Gln 570 rotated and

HB interaction was lost. In the case of Arg 611, there was only a change in the orientation between the two N-H atoms of the primary amino group of the side chain of Arg 611. Hence, that HB interaction with BDP remained stable with an inter-atomic distance between the two functional groups of about 3Å for the entire period of simulation (Fig. 5G, 6b). The analysis of the inter-atomic distances over time between BDP and the side chain of Gln 642 produced the most interesting results (Fig. 5H). Significant conformational changes involving this residue and the ligand are taking place. We calculated the inter-atomic distance between the side chain of Gln 642 and the two carbonyl oxygen atoms C-2=O (C-17-*endo*-propionate ester) and C-4=O (C-17-*exo*-propionate ester) of BDP (Fig. 1). From the graphic shown in Figure 5H we observed that the distance during simulation time between the side chain of Gln 642 and C-2=O of BDP remains more or less stable around 3.5 Å, whereas the distance between Gln 642 and C-4=O of BDP is unstable proving the C-17-*exo*-propionate ester moiety of BDP is moving in a considerable way. We then analyzed the superimposition of residue Gln 642 and BDP from the pdb structure of the complex at initial (t=0 ns) and final (t=1.15 ns) MD time (Fig. 6c). The side chain of Gln 642 shifts towards the binding cavity to stabilize BDP in the binding pocket. As a consequence, the C-17-*exo*-propionate ester moiety of BDP [Figure 1] is moving towards a hydrophobic pocket surrounded by residues Trp 600, Leu 732, Leu 733 and Ile 757 (Fig. 6c). To further validate the effect of the C17-substitution on *in vivo* regeneration inhibition we selected and bought several steroidal compounds commercially available at Sigma (Diflorasone diacetate (DFDA), R198897 and R200220) and TimTec (ST 075183 and ST 075178).

Novel ligands identified based on molecular docking results confirm the importance of C17 substitution

Dose dependent *in vivo* larval regeneration analysis revealed that a suite of ligands that inhibit regeneration at 1μM concentration. Based on the results of the docking studies, we identified novel GR ligands that maintained the cortisol backbone, but varied in C17 substitution size (Fig.7). QRT-PCR studies revealed induced *fkbp5* expression in embryos exposed to the novel ligands compared to the control. In the absence of GR, this induction was not observed. These results suggest GR activation by the ligands. Regeneration assays performed in the presence of the ligands indicate inhibition of regeneration by the ligands in a GR dependent manner that is further confirmed by the induced *Cripto -1* expression (Fig.8).

Discussion

Regenerative medicine is an emerging field of medical therapy. While major contributions in terms of therapeutic approach have been made by stem cell biology, recently established larval regeneration model of zebrafish has the potential to significantly advance the field. One approach is by revealing the underlying signaling pathways that determine tissue regeneration. This will explain why mammals cannot regenerate as well as provide opportunity to manipulate the pathways to trigger regenerative responses. Another approach is identifying targets that can activate tissue regeneration thus benefiting many human diseases. So far chemical genetics approach has identified numerous modulators of stem cell differentiation and stem cell fate. While the *in vivo* model approach is still in its early days we utilized chemical genetics and identified GCs as modulators of regeneration in the early life stage larval regeneration model of zebrafish. Our study revealed that not all members of the GC family elicit similar regenerative response.

The genre of GCs in the drug development field is an excellent example of how structural modifications can dictate biological response. Since the discovery of the anti-inflammatory property of cortisol, this pharmacophore has been manipulated to modify the effects induced by the ligands. HC, the 11β-hydroxy analogue of cortisone, was the first structurally modified cortisone introduced as a drug. DEX introduced by Merck has been the principle anti-inflammatory drug used for diverse range of treatment because of its reduced side effects and longer bioavailability. While most of the structural modifications are dedicated to reduce the side effects of GC administration thus improving the therapeutic index, the implication of SAR in the newly identified role of GCs as modulators of regeneration remains unexplored [14]. So far, chemical genetics approach has identified numerous modulators of stem cell differentiation and stem cell fate. The recent identification of fluorinated GCs as modulators of stem cell activity underlines the requirement for better understanding of structure function relationship amongst the GR ligands. Since there are numerous commercially available structural analogues of cortisol, we utilized the existing drugs. This allowed us to bypass the requirement of synthesizing new analogues to modulate regeneration. We adopted chemical genetics approach utilizing the early life stage larval regeneration model that identified GCs as modulators of regeneration to dissect the correlation of structural preference with impact on regeneration by GCs.

Our previous results demonstrate that GR activation is necessary for inhibition of regeneration. However, the results demonstrate that not all ligands that activate GR inhibit regeneration. Previous studies have shown that ligand chemistry dictates biological response by the activated receptor. The best examples are the estrogen receptor ligands estradiol and tamoxifen that invoke different gene expression profile as

well as different function in different cell type [45, 46]. The striking difference in ligand structures suggest complicated correlation between chemical structures and biological response.

It has been reported that differences in ligand chemistry can give rise to a host of functionally distinct GR-containing regulatory complexes [47] and hence impact different set of genes. Absence of *Cripto-1* induction by DEX, HC or Beclo supports previous reports confirming that the hosts of genes affected by these ligands are different and not critical for inhibition of tissue regeneration.

In order to initiate a SAR study we performed docking studies against human and zebrafish GR-LBD models with the database of known steroidal GR agonists previously tested in the regeneration assay (Table 1). The docking results revealed a correlation between the stability of the GR-LBD-ligand complex and the *in vivo* activity upon ligand binding. Molecular Dynamics simulation on GR-LBD-DEX and BDP complexes for 1.15ns were utilized to investigate the change of GR agonist conformation induced by a ligand over time. MD data showed that in order to stabilize BDP into the human GR-LBD, Gln 570 (α3), Arg 611 (α7) and Gln 642 (α8) demonstrate remarkable shift. Previous studies suggest difference in conformational changes of GR-LBD upon DAc and FF binding compared to DEX. The difference is highlighted by 3D movements taking place to accommodate a large ligand in order to achieve a stable agonist conformation.

The conformational changes of residues observed with BDP during 1.15ns MD are similar to the reported data. These residues in the GR-LBD influence ligand binding directly and are flexible enough to expand the binding pocket volume to accommodate large ligands. This allows the helical tertiary structure of the GR-LBD agonist

conformation to stay intact. This also suggests that these residues might play a role in the thermodynamic equilibrium between the inactive (no effect on regeneration) and the active (inhibit regeneration) GR-LBD conformation. Active ligands have sterically hindered substitutions at C-17 position. Molecular Docking runs showed that active GR agonists are unable to dock into the human GR-LBD-DEX binding pocket (inactive conformation) (Table 1) and this is primarily due to the size of ligands.

To further validate the rationality behind our SAR analysis we selected several commercially available steroidal compounds. All steroidal derivatives possess high *in vivo* activity similarly to BDP (Fig.7). At concentrations less than 1μM, all selected ligands inhibited regeneration in a GR dependent manner confirming that C-17 substitution is critical for affecting regeneration by GCs.

Since we have utilized an *in vivo* system for our study, metabolism and uptake might play a role in differential response. Metabolism of BDP involves hydrolysis to beclomethasone monopropionate (17-BMP) and finally beclomethasone (Beclo). Docking studies revealed comparable results for 17-BMP and BDP (Table 1). Suppression of anxa1b by the ligands confirms the intake and activation of GR by the ligands as well.

In summary, our results explore the new potential of GCs to explain regenerative biology. This study also demonstrates the power of early life stage larval regeneration model in not only elucidating signaling molecules involved in regeneration, but also in correlating ligand structure with functional preference. This study has the potential to advance regenerative medicine as well as GR biology. It is expected that in upcoming years novel synthetic steroidal and non-steroidal glucocorticoid molecules will provide a new promise to more successful regenerative medicine.

References

1. Xu, Y., T. Zhang, and M. Chen, Combining 3D-QSAR, docking, molecular dynamics and MM/PBSA methods to predict binding modes for nonsteroidal selective modulator to glucocorticoid receptor. Bioorg Med Chem Lett, 2009. 19(2): p. 393-6.

2. Einstein, M., et al., Selective glucocorticoid receptor nonsteroidal ligands completely antagonize the dexamethasone mediated induction of enzymes involved in gluconeogenesis and glutamine metabolism. J Steroid Biochem Mol Biol, 2004. 92(5): p. 345-56.

3. Schacke, H., et al., Selective glucocorticoid receptor agonists (SEGRAs): novel ligands with an improved therapeutic index. Mol Cell Endocrinol, 2007. 275(1-2): p. 109-17.

4. Westerfield, M., The zebrafish book : a guide for the laboratory use of zebrafish (Danio rerio). Ed. 4. ed. 2000, [Eugene, Or.]: M. Westerfield. 1 v. (unpaged).

5. Westerfield, M., The zebrafish book a guide for the laboratory use of zebrafish Danio (Brachydanio) rerio. 1993, Institute of Neuroscience, University of Oregon: [Eugene, OR.

6. Poss, K.D., et al., Mps1 defines a proximal blastemal proliferative compartment essential for zebrafish fin regeneration. Development, 2002. 129(22): p. 5141-9.

7. Mathew, L.K., E.A. Andreasen, and R.L. Tanguay, Aryl hydrocarbon receptor activation inhibits regenerative growth. Mol Pharmacol, 2006. 69(1): p. 257-65.

8. Andreasen, E.A., L.K. Mathew, and R.L. Tanguay, Regenerative growth is impacted by TCDD: gene expression analysis reveals extracellular matrix modulation. Toxicol Sci, 2006. 92(1): p. 254-69.

9. Mathew, L.K., et al., Unraveling tissue regeneration pathways using chemical genetics. J Biol Chem, 2007. 282(48): p. 35202-10.

10. Kauppi, B., et al., The three-dimensional structures of antagonistic and agonistic forms of the glucocorticoid receptor ligand-binding domain: RU-486 induces a transconformation that leads to active antagonism. J Biol Chem, 2003. 278(25): p. 22748-54.

11. Cardozo, T., M. Totrov, and R. Abagyan, Homology modeling by the ICM method. Proteins, 1995. 23(3): p. 403-14.

12. Totrov, M. and R. Abagyan, Flexible protein-ligand docking by global energy optimization in internal coordinates. Proteins, 1997. Suppl 1: p. 215-20.

13. Di Nola, A., D. Roccatano, and H.J. Berendsen, Molecular dynamics simulation of the docking of substrates to proteins. Proteins, 1994. 19(3): p. 174-82.

14. Nasevicius, A. and S.C. Ekker, Effective targeted gene 'knockdown' in zebrafish. Nat Genet, 2000. 26(2): p. 216-20.

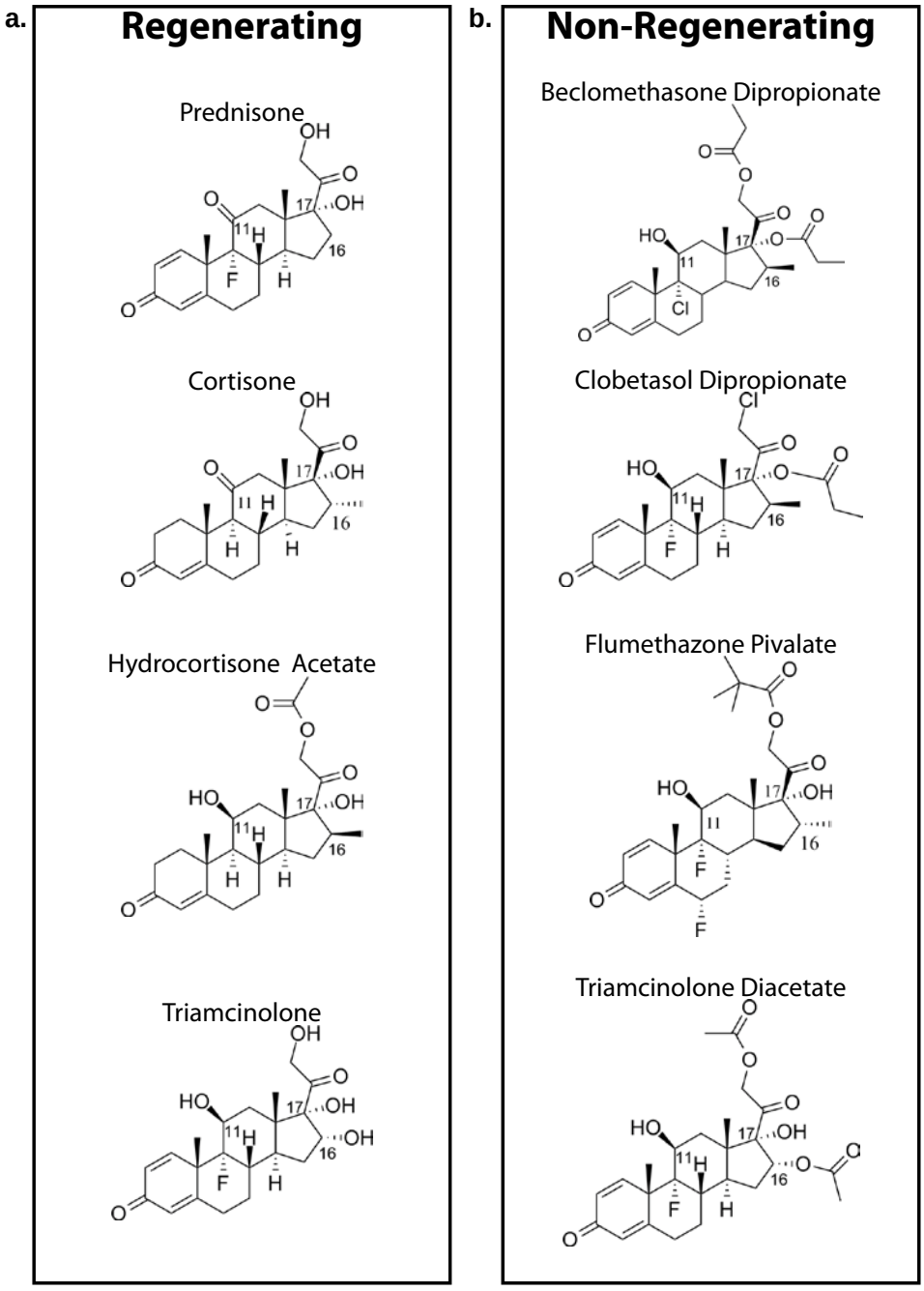

Figure 4- 1.Select chemical structure from FDA Library.
Chemical structure of selected chemicals from the 2000 member FDA approved library that induced regeneration **(A)** [Cortisol, Prednisone, Hydrocortisone acetate, Triamcinolone] or inhibit regeneration **(B)** [Beclomethasone dipropionate, Clobetasol dipropionate, Flumethazone pivalate, Triamcinolone diacetate] response.

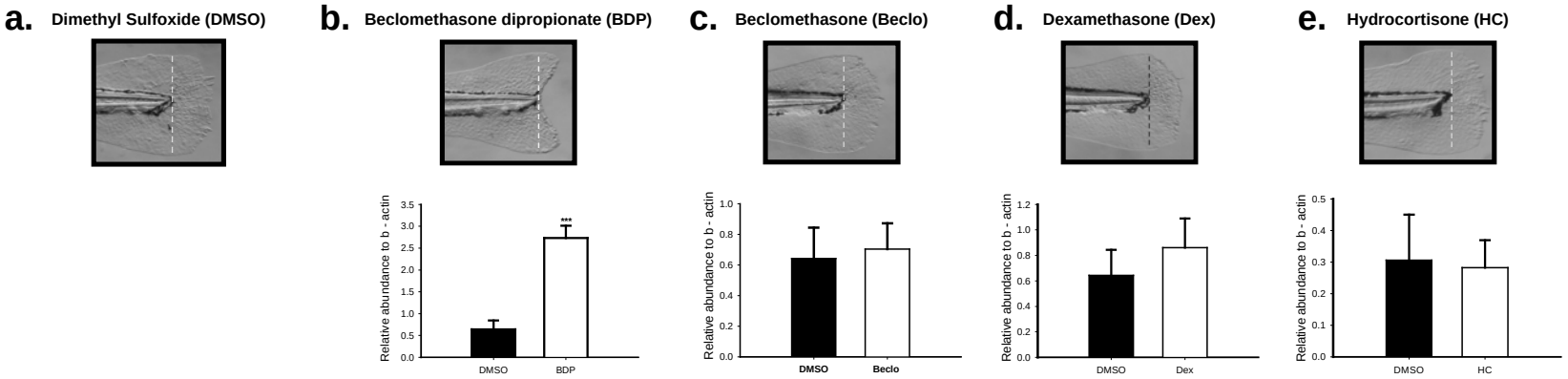

Figure 4- 2. *Cripto-1* expression in larval tissue.
Caudal fin of 2dpf larvae were amputated (dotted lines mark the plane of amputation) and continuously exposed to **a)** dimethyl sulfoxide (DMSO), b)Beclomethasone dipropionate (BDP), **c)** Beclomethasone (Beclo), **d)** Dexamethasone (DEX), **e)** Hydrocortisone (HC) at 1 µM concentration for three days for regeneration assay. Pictures were taken at 3dpa and RNA was collected at 1dpa from whole embryos for cDNA synthesis and qRT-PCR for *Cripto-1* expression. The abundance of *Cripto-1* transcript at 1dpa is elevated on BDP exposure. However, there was no difference in expression on dex, beclo or HC treatment. The respective values represent the mean ± SEM and the asterisks indicate statistical significance (One way ANOVA, n=3).

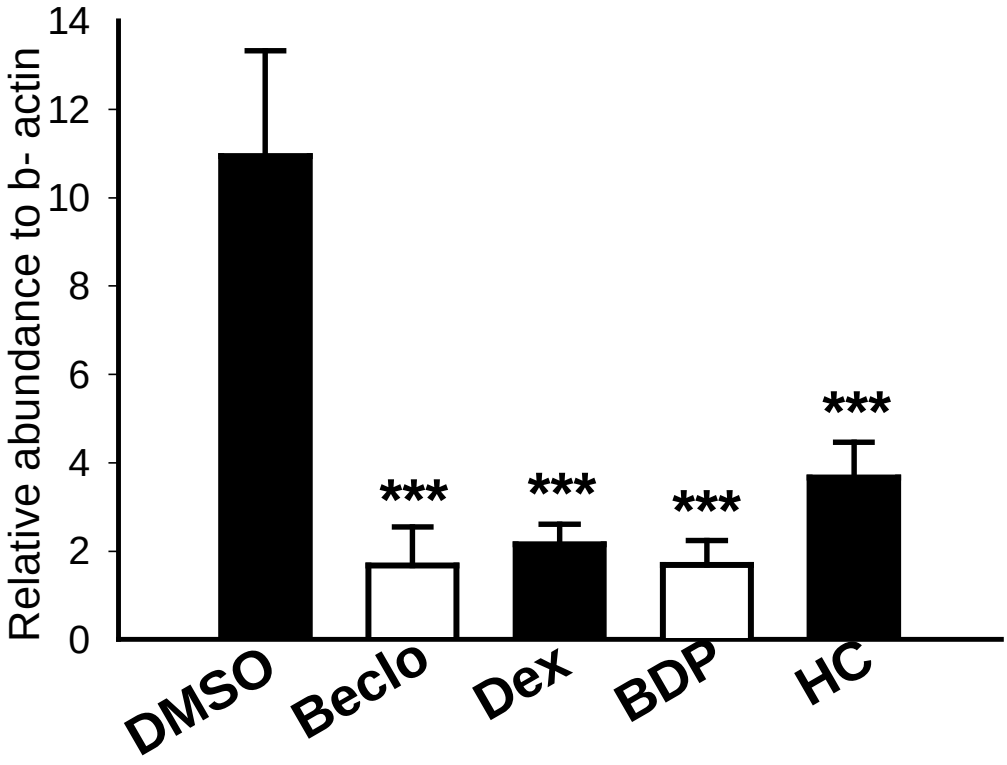

Figure 4- 3.Expression of *anxa1b* transcript in larval tissue.
2dpf larvae were exposed to 1 µM dex, beclo, HC, BDP and DMSO following amputation. The abundance of *anxa1b* transcript estimated by qRT-PCR at 1dpa in the whole embryo indicate significantly reduced expression in the exposed larvae indicating GR activtaion. The respective values represent the mean ± SEM and the asterisks indicate statistical significance (One way ANOVA, n=3).

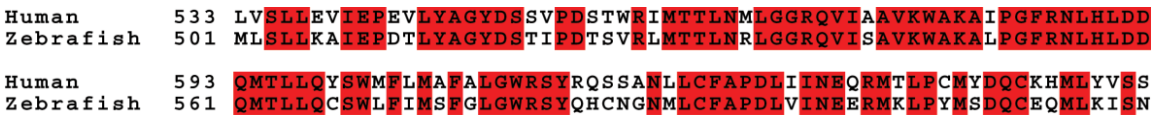

Figure 4- 4. Aligned ZF and Human GR.
Snapshot of aligned zebrafish GR with human GR demonstrate conserved glutamine (Q), Arginine (R), and threonine (T) at positions 570, 642,611 and 739 respectively.

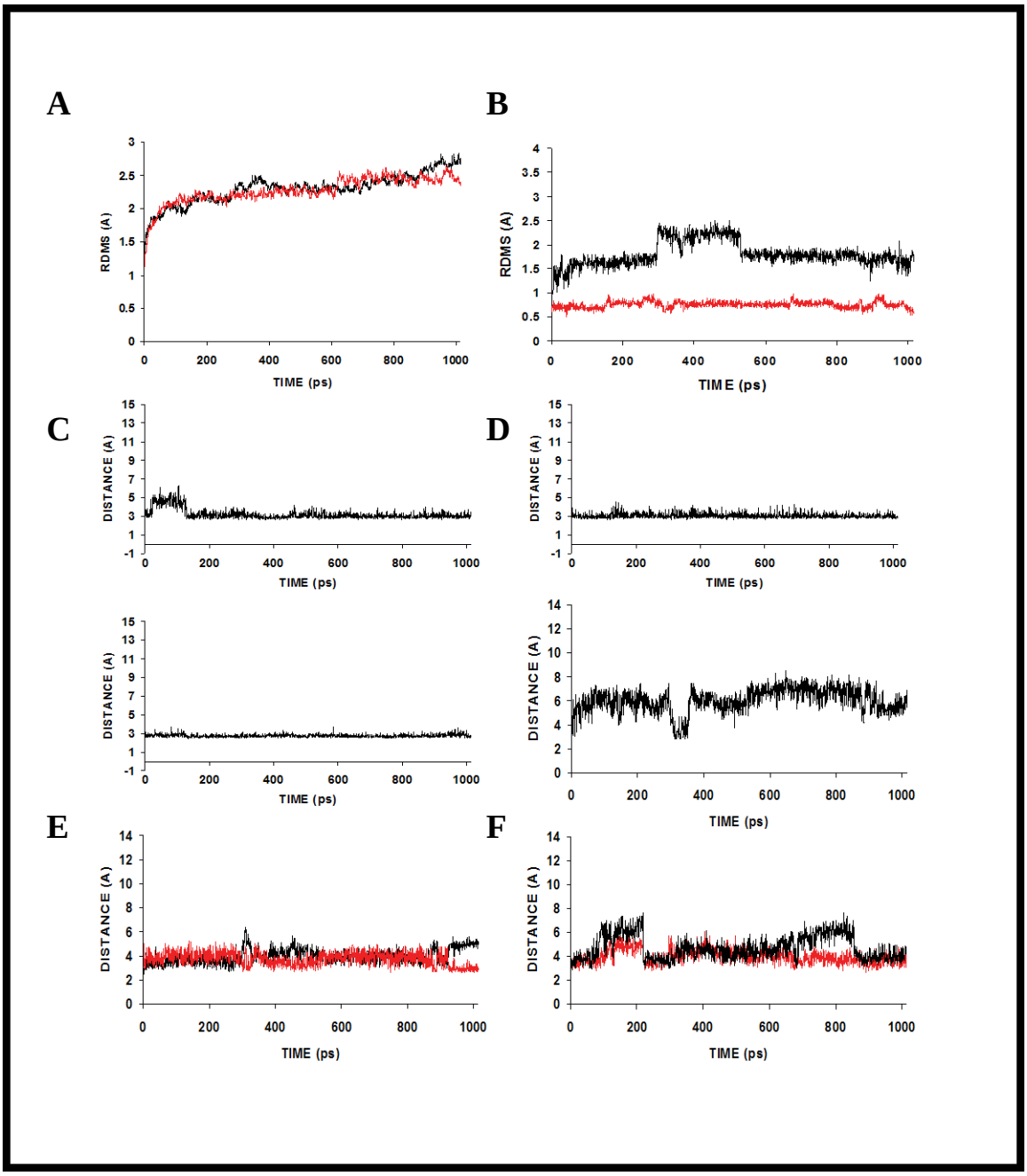

Figure 4- 5. RMSD graphics.
RMSD graphics (all atoms plotted) versus time (picoseconds) during 1.15 ns of MD of **A)** GR-LBD from X-ray crystal structure (pdb 1p93) in complex with Dexamethasone, Dex (black) and docked Beclomethasone di-propionate, BDP (red) and **B)** Dex (black) from X-ray crystal structure (pdb 1p93) and docked BDP (red). Evolution of interatomic intramolecular distance during 1.15 ns of MD in the complex between **C,D,E)** Dex and **F,G,H)** and BDP and GR-LBD, respectively. Initial time (t = 0 ps) is measured after

minimization stage (see Methods). Color code: C) black, NH_2 R611—$\underline{O}_1$=C Dex; D) black, NE_2 Q570—$\underline{O}_1$=C Dex; E) black OE_1 Q642—H$\underline{O}_3$-C Dex; F) black, NE_2 Q570—$\underline{O}_6$=C BDP; G) black, NH_1 R611—$\underline{O}_6$=C BDP, red, NH_2 R611—$\underline{O}_6$=C BDP; H) black, OE_1 Q642— $\underline{O}_4$=C BDP, red, OE_1 Q642— $\underline{O}_2$=C BDP.

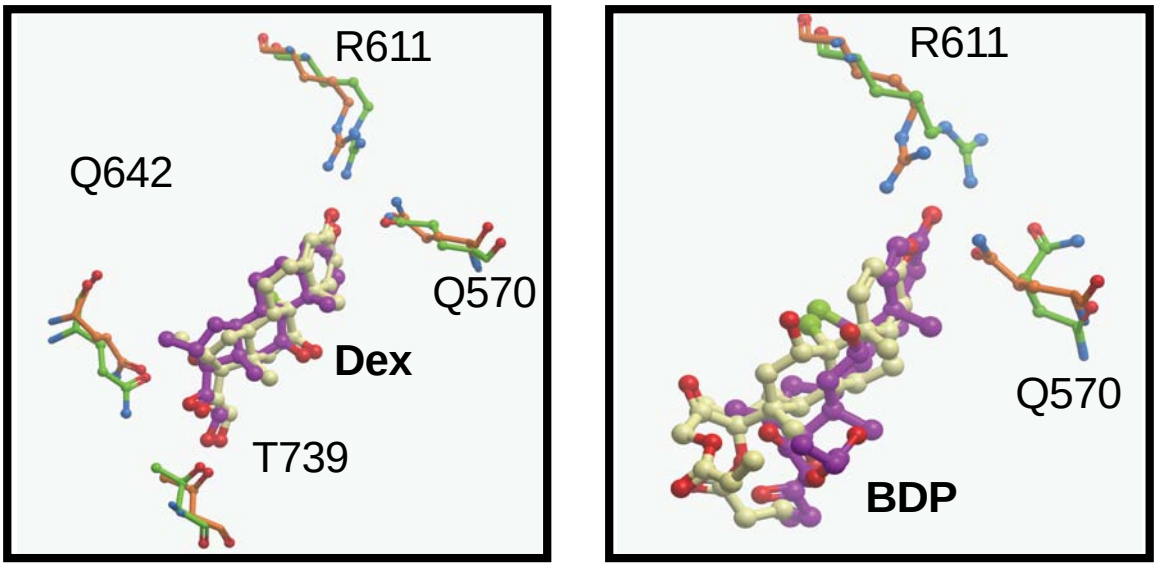

Figure 4- 6A. X-ray Crystal Structure.
Residual side chain and ligand shift during 1.15 ns of MD of GR-LBD from X-ray crystal structure (pdb 1p93) in the complex between **A)** Dex and **B,C)** docked BDP. The ligands are colored by atom type with carbon atoms in white (0 ps of MD) and magenta (1015 ps of MD) and displayed as ball and stick. Residues are colored in orange (0 ps of MD) and green (1015 ps of MD) and displayed as ball and stick (ICM v3.5-1p).

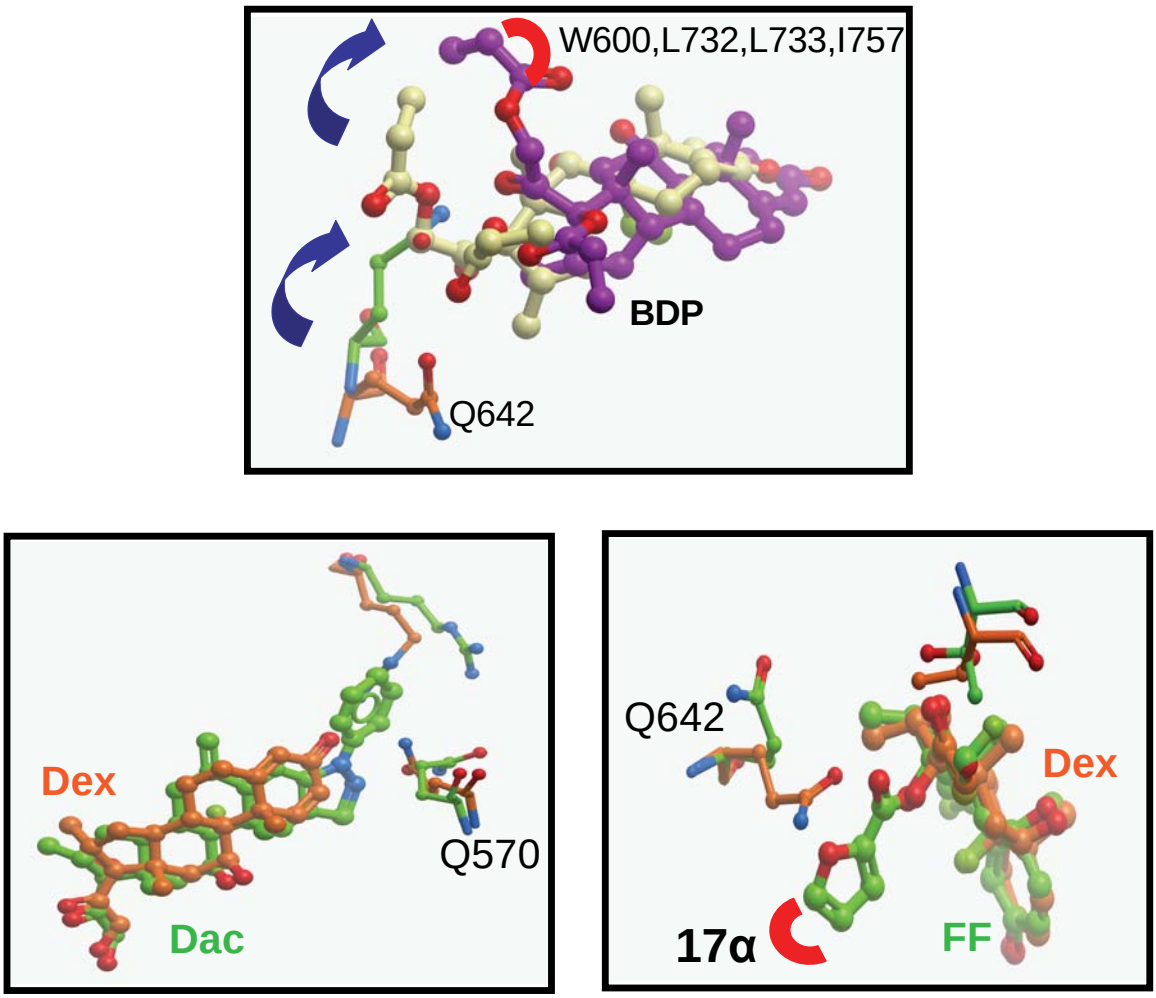

Figure 4- 6B. X-ray Crystal Structure.
Superimposition of the X-Ray crystal structure of GR-LBD complexed with A) Dex (pdb 1p93) and DAC (pdb 3bqd) and B) Dex (pdb 1p93) and FF (pdb 3cld). The ligands and the residues are colored by atom type with carbon atoms in orange A,B: Dex) and green (A: DAC, B: FF) and displayed as ball and stick (ICM v3.5-1p).

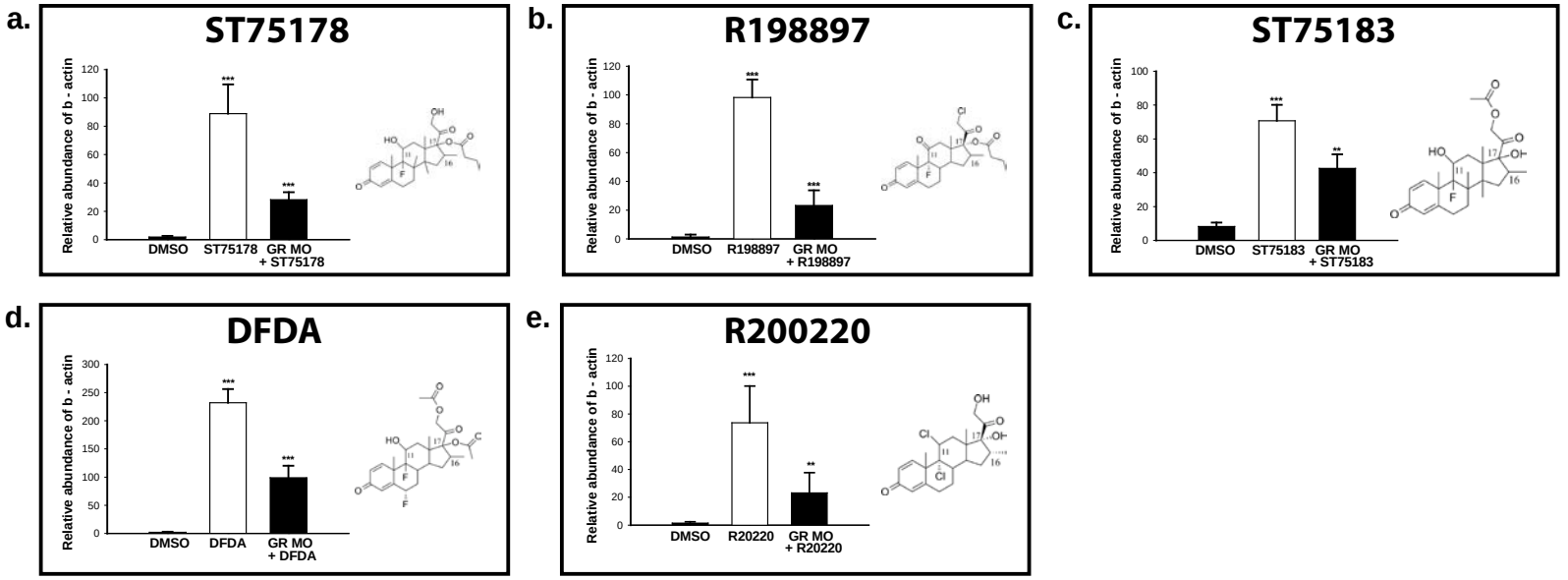

Figure 4- 7. Chemicals identified based on cortisol backbone and C17 substitution activate GR
Structures of novel GR ligands **a)** ST75178, **b)** R198897, **c)** ST75183, **d)** DFDA and **e)** R200220 identified based on cortisol backbone and C17 substitution. GR splice variant MO transiently knocked down GR compared to standard control morpholino injected embryos. The amputated control and *GR* morphants were exposed to DMSO or the novel GR ligands. The abundance of FKBP506 estimated by qRT-PCR at 1dpa in the whole embryo indicates significantly reduced expression in the GR ligand exposed morphants. The respective values represent the mean ±SEM and the asterisks indicate statistical significance (One way ANOVA, n=3).

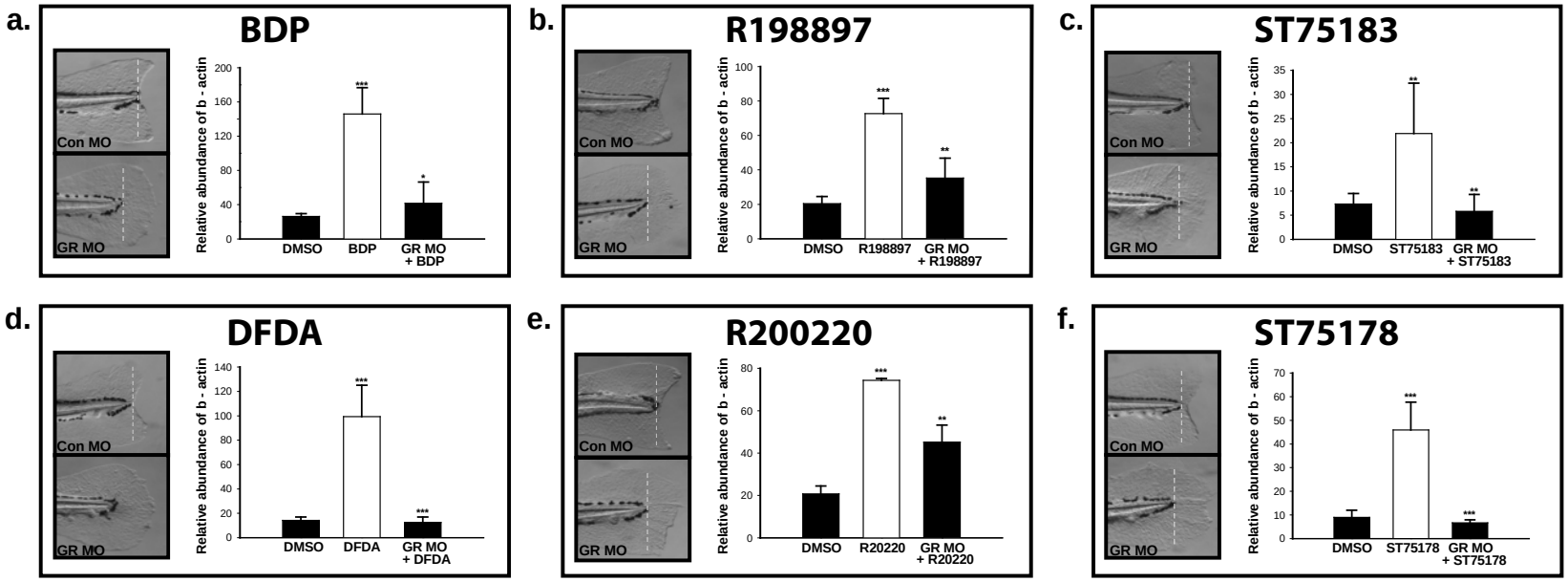

Figure 4- 8. Transient knock down of GR.
Splice blocking GR MO was used to transiently knocked down GR. GR and control morphants were amputated at 2dpf and exposed to the GR ligands. Regenerative progression was assessed and pictures taken after three days of exposure. RNA was isolated from GR morphants and control morpholino exposed embryos 24 hours after exposure. QRT-PCR evaluated the expression of *Cripto-1* that was significantly elevated in the control morphants and suppressed in the GR morphants exposed to the GR ligands.

Table 4S- 1. Data on Molecular Docking in human and zebrafish GR-LBD in agnoist conformation (pdb 1p93).

Compound	Human	Zebrafish
Hydrocortisone *	nd	nd
Fluocinonide *	nd	nd
Flumethazone pivalate *	nd	nd
Triamcinolone diacetate *	nd	nd
Betamethasone valerate *	nd	d
Halcinonide *	nd	nd
Clobetasol propionate *	d	d
Beclomethasone diproprionate *	nd	nd
Beclomethasone*	nd	nd
17 Beclomethasone monopropionate	nd	nd
R200220 *	nd	nd
R198897 *	nd	nd
Betamethasone **	d	d
Amcinonide	nd	nd
Prednisone	d	d
Prednisolone	d	d
Prednisoloe acetate	d	nd
Cortisone	d	d
Me-prednisolone	d	d
Fluorometholone	d	d
Dexamethasone acetate	d	d
Fluocinolone acetonide	d	d
Hydrocortisone acetate	d	d
Hydrocortisone butyrate	d	d
Triamcinolone acetonide	d	d
Triamcinolone	d	d
Dexamethasone	d	d

d: docked; nd: not docked; *:no ; **: partial regeneration;

CHAPTER 5 –Conclusions

Zebrafish caudal fin regeneration is an exceptional platform to dissect molecular signaling pathways responsible for inducing regeneration in vertebrates. While adult caudal fin regeneration is an established model to study tissue regeneration, we utilized the short regeneration time and genetic tractability to develop an early life stage regeneration model. We took a comparative approach to identify the differentially expressed transcripts common to regenerating adult caudal fin, heart and larval caudal fin tissue. This approach identified raldh2, a rate-limiting enzyme for the synthesis of retinoic acid (RA) as a critical gene required for the early stages of regeneration. RA signaling also plays an important role in patterning during regeneration. Through the identification of raldh2 we established the role of RA during early stages of regeneration. We also confirmed the role of Wnt and Fgf in the larval regeneration model. Additionally we established the early life stage regeneration model as an exceptional platform to understand regeneration biology.

Next, we utilized the early life stage model and adopted chemical genetic approach to identify novel modulators of regeneration. The underlying concept is if a chemical modulates a molecular pathway critical for regeneration, exposure to the chemical will perturb regenerative progression. We developed an *in vivo* larval regeneration assay and screened a 2000 member library of FDA approved drugs. The library comprised of thirty-three glucocorticoids (GCs) out of which seven of them inhibit regeneration. We pursued further studies with beclomethasone dipropionate (BDP) and revealed that GR activation was critical for inhibition of regeneration. In order to elucidate the molecular

signaling molecules downstream of GR that are necessary to inhibit regeneration we performed a global genomic expression analysis on BDP exposed fin regenerates. Cripto-1, an inhibitor of activin signaling was one of the highly induced transcripts. Initially we confirmed the role of activin signaling in larval regeneration model using a chemical inhibitor of activin signaling. We performed further experiments to confirm the role of Cripto-1 in GR mediated inhibition of tissue regeneration by suppressing Cripto-1 expression using antisense repression technique and retinoic acid. Rescue of BDP impaired tissue regeneration in absence of Cripto-1 induced expression and revealed that GR activation influenced Cripto-1 expression leading to inhibition of activin signaling. Taken together these results demonstrate an inhibition of tissue regeneration. Further studies are necessary to understand how activated GR induce Cripto-1 expression. The results of this study has the potential to improve the development of GCs, as well as understand GR biology.

The 2000 member library was also comprised of GCs that did not impact regeneration such as dexamethasone. Members of the GC family are known GR ligands and we demonstrated that even though these ligands activated GR they could not inhibit regeneration. This was contrary to our prior observation that activation of GR was important for influencing regeneration. Since the biological response evoked by an activated receptor depends on ligand chemistry we further analyzed the structure of the ligands and the GR confirmation induced. Molecular docking studies revealed that BDP was unstable in the dex induced conformation. BDP activated stable GR conformation was different than dex induced GR conformation and this difference in conformation was results of bulky C17 substitution in BDP. We identified analogues of the cortisol backbone with bulky C17 substitution and confirmed the above observation. This study

was the first report of a possible pharmacophore backbone revealed by an *in vivo* regeneration model and has further implications for the development of therapeutics that can induce regeneration in mammals. However, future studies are required to explain the details of structural dependence amongst GR ligands that dictates regenerative response. Screening of an analogue library with different substitution at a single position will further help to reveal the intricacies of structure dependent response by GR in impacting regeneration.

In summary this thesis attempts to establish early life stage zebrafish regeneration model as a powerful platform to study tissue regeneration as demonstrated by the identification of GCs as modulators of regeneration and establishment of a pharmacophore backbone that dictates regenerative response among the GR ligand family.